

Spring 2020

Exploring the Precursors of Disinfection Byproducts and CDOM Fluorescence Monitoring

Victoria Choy
Bard College

Follow this and additional works at: https://digitalcommons.bard.edu/senproj_s2020

 Part of the [Environmental Health and Protection Commons](#), [Environmental Indicators and Impact Assessment Commons](#), and the [Environmental Monitoring Commons](#)



This work is licensed under a [Creative Commons Attribution-NonCommercial-No Derivative Works 4.0 License](#).

Recommended Citation

Choy, Victoria, "Exploring the Precursors of Disinfection Byproducts and CDOM Fluorescence Monitoring" (2020). *Senior Projects Spring 2020*. 104.
https://digitalcommons.bard.edu/senproj_s2020/104

This Open Access work is protected by copyright and/or related rights. It has been provided to you by Bard College's Stevenson Library with permission from the rights-holder(s). You are free to use this work in any way that is permitted by the copyright and related rights. For other uses you need to obtain permission from the rights-holder(s) directly, unless additional rights are indicated by a Creative Commons license in the record and/or on the work itself. For more information, please contact digitalcommons@bard.edu.

Engaging the Saw Kill Watershed Community:
An Exploration of the Precursors of Disinfection Byproducts and CDOM Fluorescence
Monitoring

Senior Project Submitted to
The Division of Social Studies
of Bard College

by
Victoria Choy

Annandale-on-Hudson, New York
May 2020

Acknowledgments

I am tremendously grateful for each and every person who has been a part of my journey for this project. I would like to thank Robyn Smyth for being a great professor, teacher, and mentor. You have continuously pushed me to reach my fullest potential. Not to mention, you have fostered my growth over my three years at Bard, and I am truly thankful for your influence on my academic career. This project would not have been possible without your guidance and help. Thank you for believing in me and inspiring me.

To Karen Moore and Dave Van Valkenburg, thank you for taking me on as a mentee. I have learned so much from the both of you, and I am constantly inspired by your depth of knowledge. Your expertise has undoubtedly advanced my project to a higher level of sophistication. I am extremely grateful for the effort and time the both of you have invested in me.

To Eli Dueker and Helen Epstein, thank you for adding valuable insight to my project and for being my teachers throughout my years at Bard.

To Emily White, Lindsey Drew, and Marco Spodek, thank you for contributing to the process of interpreting the Saw Kill data. Thank you to the Saw Kill Watershed Community for allowing me to be a part of a wonderful group of people who care about the watershed and for sparking my interest in water quality analysis.

To Arseny Khakhalin, thank you for opening your door to answering my spontaneous R Studio questions and for your love of squirrels.

To Lily O'Donnell thank you for being generous, kind, and big-hearted. To the good old days of getting up early together on Wednesday mornings. Lastly, thank you Emily Giangiulio, for peer reviewing my work and being so supportive.

*Dedicated to my immigrant father and grandmother.
Thank you for giving me a better life.*

Table of Contents

Abstract	1
Chapter 1: Introduction to Disinfection Byproducts	2
Chapter 2: Natural Organic Matter in the Saw Kill	6
Chapter 3: Investigating Temperature Effects on CDOM Measurements	27
Chapter 4: Recommendations for the Saw Kill Monitoring Program	49
Appendix	52
Bibliography	113

Abstract

Disinfection byproducts (DBPs) are formed when chlorine, or any other disinfectant, is added to drinking water and reacts to a small fraction of natural organic matter (NOM) present in the water supply. DBPs may be carcinogenic when exposed for a long term at high concentrations. However, the usage of chlorine or other disinfectants on the water supply must not be compromised. The precursors of DBPs are studied in the Saw Kill by acquiring data from 2017 to 2019 from the Saw Kill Monitoring Program. This includes colored dissolved organic matter (CDOM), chlorophyll a, and turbidity, which are indicative of NOM behavior in the river. Three figures of each parameter are created in relation to land usage (forested, developed, and MCA) and seasonality, while distribution plots and natural log-transformed plots are created to test for normality via the Shapiro-Wilks test. Correlations between the parameters are plotted and tested via Kendall Tau and Spearman Rho's test. In addition, stream inflows to the reservoirs of Neversink and Cannonsville are studied by evaluating its grab samples for temperature fluorescence quenching of CDOM and sample degradation via two Handheld AquaFluor Fluorometers (of the same model, but different calibration methods), and microbial activity via an ATP (adenine triphosphate) assay. The CDOM data is corrected for temperature effects by using the equation provided by Watras et al. (2011), $CDOM_r = CDOM_m / [1 + \rho(T_m - T_r)]$, and then correlated with dissolved organic carbon (DOC). Results from the Saw Kill plots indicate that parameters are not normally distributed, and there is a weak correlation between them. From the limited dataset, there is no indication of seasonality or land usage affecting the concentration of the investigated parameters. Furthermore, preliminary results from the laboratory experiments of Neversink and Cannonsville samples reveal that CDOM fluorescence emission intensity decreases by ~1% per temperature (°C) increase. The corrected CDOM values are highly correlated with DOC ($r=0.97$). From the results of the limited ATP assays, Cannonsville has greater microbial activity. Samples with 72 and 58 holding days have a sample degradation of ~2 RFU and may be considered negligible in comparison to RFU changes between samples of different months. Saw Kill data suggest that DBP formation potential associated with CDOM and turbidity are highest in the fall of 2018 and associated with chlorophyll a is highest in the spring and summer of 2019. Meanwhile, Neversink and Cannonsville data suggest that CDOM temperature correction varies based on sample collection in regard to river hydrology. Corrected CDOM data is indicative of a strong indicator for DOC; however, further research is needed. Despite the fluorometers having different calibration methods, there are negligible differences in the data analysis. Ultimately, the following are recommendations provided for the Saw Kill Monitoring Program: the Bard fluorometer should be calibrated using quinine sulfate, and CDOM values should be corrected by using the equation provided by Watras et al. (2011). From the equation, the temperature coefficient, ρ , should be determined by conducting temperature quenching experiments and taking account of influences such as storms and river hydrology.

Chapter 1: Introduction to Disinfection Byproducts

Chlorine has been established as the conventional method for disinfecting drinking water since the 20th century and is widely regarded as a major achievement in the public health sector. This reformation greatly reduced waterborne diseases contracted from the drinking supply. Although the application of chlorine is essential for a sanitary water supply, there are negative consequences in using this chemical. When chlorine is added to the supply, it reacts with water and forms hypochlorous acid. Likewise, when bromine, an alternate disinfectant to chlorine, is added to the drinking supply, it forms hypobromous acid. In 1974, Johannes J. Rook discovered that the reactions of hypochlorous and hypobromous acid with natural organic matter in bodies of water forms disinfection byproducts (DBPs) (CDC 2016). All types of disinfectants, such as ozone, chlorine dioxide, chloramines, and UV-radiation, react to organic matter to form DBPs (Matilainen et al. 2011). Since Rook's discovery, there have been over 600 DPBs that have been identified (CDC 2016), and the EPA regulates bromate, with the standard of 10 $\mu\text{g/L}$, chlorite, with the standard of 1000 $\mu\text{g/L}$, total trihalomethanes (THMs), with the standard of 80 $\mu\text{g/L}$, and total haloacetic acids (HAAs), with the standard of 60 $\mu\text{g/L}$. The four regulated THMs are chloroform, bromoform, bromodichloromethane, and dibromochloromethane, and the five regulated HAAs are monochloroacetic acid, monobromoacetic acid, dichloroacetic acid, dibromoacetic acid, and trichloroacetic acid (US EPA 2020).

DBPs are regulated because research has shown that they can be harmful to human health when exposed to high concentrations via inhalation, ingestion, and dermal contact through showering or swimming in disinfected waters (Chaves et al. 2019). For instance, epidemiological studies suggest the consistent association with bladder cancer (Freeman et al. 2017; Regli et al.

2015), rectal cancer (Bove, Rogerson, and Vena 2007; Jones et al. 2019), and adverse reproductive outcomes. Notably, researchers evaluated the effects of high exposure of DBPs on pregnant women and found an increased risk for cardiac effects (Cedergren et al. 2002), intrauterine growth retardation (Kramer et al. 1992), and small for gestational age (SGA) (Levallois et al. 2012). Evidence for the harmful effects of DBPs is apparent in toxicological studies as well. These studies revealed that high concentrations of DBPs in laboratory animals resulted in smaller body weights, a reduced chance in offspring survival, deformed neurological, and cardiovascular systems. Exposure through inhalation has shown pregnancy loss and growth retardation (Nieuwenhuijsen et al. 2000).

Researchers have attempted to better understand DBP formation by analyzing various factors such as the origins and safety thresholds of DBP precursors. This allows watershed management to predict the presence of DBPs and to make well-informed decisions about the selection of higher quality water for distribution (Moore et al. 2019a). Precursors of DBPs include anthropogenic contaminants such as sewage, fertilizers, herbicides, pesticides, fabric dyes, personal care products, pharmaceutical products, and hormones (Chaves et al. 2019). However, the major precursors are not anthropogenic sources, but are natural organic matter (NOM), which can be in the form of particulate organic matter or dissolved organic matter. The biggest contributors to NOM are humic substances (Matilainen, Vepsäläinen, and Sillanpää 2010), which are mainly composed of soil humus and plants and are ubiquitous throughout the environment (Tang et al. 2014). Humic substances are significant, as they also contribute to more than 50% of the total organic carbon in water bodies (Matilainen, Vepsäläinen, and Sillanpää 2010).

NOM is commonly found in groundwater and more so in surface water. Thus, surface water is typically more concentrated with DBPs (Nieuwenhuijsen et al. 2000). The emergence of NOM results from various biological, hydrological, and geological activities. More specifically, biological activities include algal or bacterial growth, which primarily contributes to the internal generation of NOM, also known as autochthonous NOM. The external generation of NOM, known as allochthonous NOM, can be introduced into the water body through the drainage basin carrying the decomposition of terrestrial organisms (Sillanpää et al. 2018). The concentration and composition of NOM differs in various bodies of water, including fresh and marine (Moreno-Andrés and Peperzak 2019), and even in the same watershed due to seasonal changes such as droughts, floods, and rainfalls (Sillanpää et al. 2018). Varying NOM compositions will result in distinct DBP formations (Matilainen, Vepsäläinen, and Sillanpää 2010), and only a small fraction of NOM will react to disinfectants like chlorine (Moore et al. 2019a). To be clear, NOM is not innately toxic; however, it is viewed as a nuisance in our water supply because not only does it contribute to the formation of DBPs, but it also degrades the quality of the water by unfavorably altering the color, taste, and odor. In addition, NOM can be a carrier of toxic pollutants such as pesticides (Sillanpää et al. 2018).

The formation of DBP is dependent on the physical and chemical attributes of the water quality (Chaves et al. 2019), as well as the operational conditions of the water treatment plant. NOM is typically removed in treatment plants by the following processes: coagulation, flocculation, sedimentation and sand filtration (Matilainen, Vepsäläinen, and Sillanpää 2010). Fortunately, coagulation has been regarded as a very efficient process in preventing the formation of DBPs. However, there have been global reports of NOM growth throughout many bodies of water. This is problematic as higher concentrations of NOM increases formation

potential of DBP and the need to strengthen disinfectant and coagulant doses, which then results in higher DBP concentrations (Matilainen et al. 2011). Temperature conditions also play a role in DBP formation potential, as warmer water temperature encourages DBP formation (Serrano et al. 2015). Moreover, pH is also a relevant factor. For example, Hung et. al (2017) finds that the formation of chloroform and THM decreases as the pH becomes more acidic.

There are several methods to measure the precursors of DBPs. One method involves the measurement UV_{254} , which measures the organic compound's absorbance of light at a wavelength of 254 nm. Another option involves detecting colored dissolved organic matter (CDOM), which is the measurement of dissolved organic matter that fluoresces. Additionally, monitoring organic carbon and DBP formation potential via a laboratory test can be a proxy for DBPs (Moore et al. 2019b).

The objectives of this paper are to a) investigate the seasonal trends of the precursors of DBPs, as measured by CDOM and chlorophyll fluorescence and turbidity in relation to land usage in the Saw Kill, b) evaluate the effects of temperature on CDOM fluorescence intensity on the stream inflows to the reservoirs of NYC's drinking supply through laboratory experiments, and c) provide recommendations for the Saw Kill Monitoring Program on improving CDOM monitoring via fluorometry.

Chapter 2: Natural Organic Matter in the Saw Kill

Introduction

The Saw Kill Watershed Community (SKWC) was formed in 2015 with the help of Bard College, uniting community members with the mission of protecting the Saw Kill watershed by means of education, science, and advocacy. Community members are from nearby towns (including Red Hook, Rhinebeck, Milan, and Bard College), representatives from several programs and nonprofits, and officials from the state, local, and county level. Since then, the following four teams were established to protect the watershed: science, education, stewardship, and municipal (Saw Kill Watershed Community, “About”, n.d.). The science team has a water quality monitoring program, called Saw Kill Monitoring Program (SKMP), which is a citizen science program aimed to create a baseline of data about the condition of the Saw Kill. The monitoring program emerged in 1975, monitoring 20 sites along the Saw Kill, but discontinued in 1982 (Saw Kill Watershed Community, “Science”, n.d.). The monitoring program was restarted in 2016 and is stationed in the Bard Water Lab at Bard College. The SKMP now monitors 14 sites along the Saw Kill (Bard Water Lab, n.d.) (Figure 2.1).

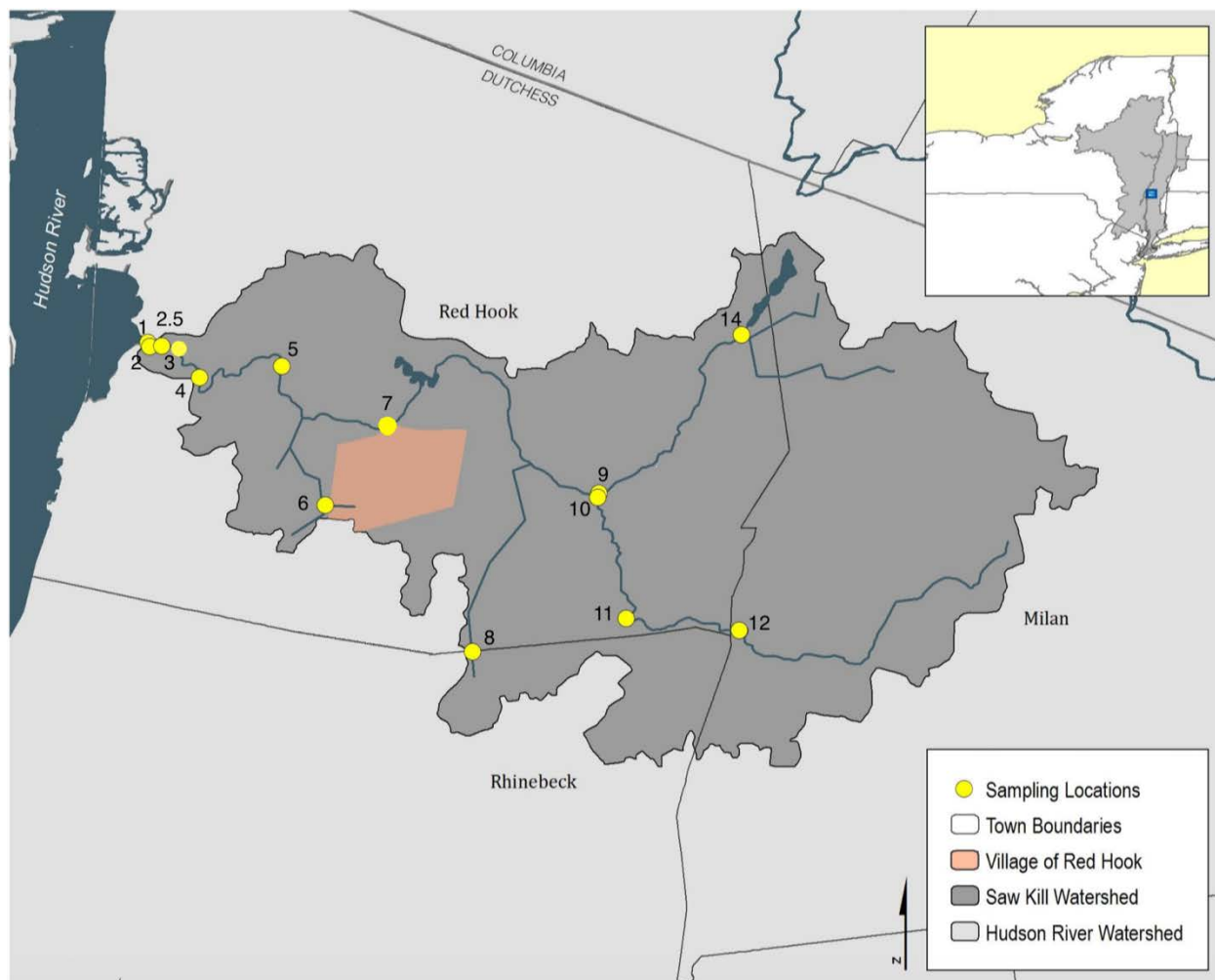


Figure 2.1. Map of Sample Sites Along the Saw Kill. The yellow circles represent sampling points along the Saw Kill. Map modified from (Riverkeeper, n.d.).

The site that this study will be evaluating is the Saw Kill, which is a tributary of the Hudson River. It is 14.3 miles long and it runs through Red Hook, Milan, Rhinebeck, and the Bard campus. The Saw Kill watershed is 26.2 mi², located on the eastern edge of the Hudson River and in the northwestern area of Dutchess County, New York (42°00'N, 73°53'W). The watershed is divided by the following land usages: 51.4% forested, 23.4% agricultural, 14% developed, and 11.2% other. It is a subwatershed of the Hudson River basin (Spodek 2017). The Saw Kill is of interest to study because it is a source of drinking water for Bard, as well as an area where treated water is discharged. It also serves multiple ecological benefits for community

members, including sightseeing, swimming, fishing, and boating (Saw Kill Watershed Community 2019). Therefore, looking at the source of DBPs in this river is significant because of the potential health risks to the large local population (CDC 2009).

Grab samples from each monitored site along the Saw Kill are collected the second Friday of every month using sterile technique (Appendix A). A dipper is used to collect water from the stream and then poured into a 1L bottle. Once the bottles are filled, they are placed in backpacks with ice packs, and transported to the Bard Water Lab. At the laboratory, various water quality parameters are tested on the collected samples by trained community members, along with running blank samples using autoclave deionized water for quality control purposes. The tested parameters include sewage indicating bacteria (enterococci, total coliforms, and *E. coli*), turbidity (see Appendix B for the turbidity protocol), conductivity, and fluorescence (see Appendix C for the fluorometry protocol) to indicate chlorophyll a, colored dissolved organic matter, optical brighteners, and phycocyanin.

For purposes of analyzing the sources of disinfection byproducts, data from the monitoring program was acquired from December 2017 to December 2019 of the following parameters: colored dissolved organic matter (CDOM), chlorophyll a, and turbidity. Analysis of CDOM gives an estimation for total organic carbon and organic matter, while chlorophyll a provides a measure of the concentration of phytoplankton in a body of water. In addition, turbidity measures the relative transparency of a water sample; more turbid waters have more suspended particles such as clay, silt, and organic matter (USGS, n.d.). These parameters are crucial for evaluation because they are indicative of the NOM dynamics in the Saw Kill.

I hypothesize that

1. Seasonality will have an impact on CDOM, chlorophyll a, and turbidity concentrations. I predict that summer is when these parameters would peak.
2. Land cover will affect the variables tested. I predict that sites that are forested will have higher concentrations of CDOM while developed and MCA regions have higher concentrations of chlorophyll a and turbidity.

Methods

Turbidity in water samples were measured using a Portable Turbidimeter by Hach, Model # 2100Q. The turbidimeter hits the sample with light and measures the scattered light at a 90-degree angle. Values are reported in the Nephelometric Turbidity Unit (NTU). The Hach Turbidimeter has the range of 0-1000 NTU, and Hach StablCal® standards (20 NTU, 100 NTU, 800 NTU) are used for a full range calibration. The turbidimeter is calibrated every month, just before a SKWC sampling event.

CDOM and chlorophyll a were measured with two AquaFluor Handheld Fluorometers from Turner Designs, Model # 8000-010. The specifications for these fluorometers are reported in Chapter 3 (see page 33). On both fluorometers, CDOM and chlorophyll a is measured on Channel B. These two fluorometers were calibrated on September 11, 2019, using Red Fluorescence Water Tracing Dye. CDOM and chlorophyll a values are reported in relative fluorescence units (RFU), relative to standards made by diluting this tracing dye to a solution concentration of 2-375 ppm. The tracing dye contains the chemical compound, Rhodamine WT; however, the exact concentration of Rhodamine WT in the dye is unknown. Along with the calibration, both instrument settings were adjusted to give readings on a scale of 0 to 1. For the CDOM channel, the 375 ppm solution standard was used to set the reading to 1, while the

chlorophyll a channel used the 160 ppm solution standard. Prior to the scale adjustment, the CDOM and chlorophyll a channels were on a scale of 0 to 100 and 0 to 400, respectively, and the method and date of previous calibration is unknown. As a result of scale adjustment, data after calibration, September 2019 to December 2019, was corrected to match the scale of the old data, December 2017 to August 2019. This was achieved by multiplying post September CDOM and chlorophyll a data by correction factors of 470 and 576, respectively. In addition to correcting for the scale change, these correction factors account for differences in the standard values, which were measured immediately before and after the instrument was calibrated. Thus, the corrected data reported in this chapter are directly comparable to the data prior to September 2019. Since the September 2019 calibration, both fluorometers have been checked for monthly drift within two days prior to each SKWC sampling event (White 2020).

The three parameters, CDOM, chlorophyll a, and turbidity, are examined in relation to land usage because NOM sources in the Saw Kill may be heavily influenced by the activities of the surrounding land. However, Sites 6, 8, and 14 were removed from analysis because those sites are outliers; they are all tributaries of the Saw Kill and have shown consistently abnormal values of CDOM, chlorophyll a, and turbidity. In particular, Site 6 has irregular high and low values of the three parameters, while Site 8 is below a landfill, near an airport, and has an unusually high concentration of the three parameters. Lastly, Site 14 has abnormally low values of all three parameters. Therefore, only a total of 11 sites are analyzed.

In order to examine the relationship between land usage and the sites along the Saw Kill, sites had to be categorized by their predominant land cover. Spodek (2017) calculated the areas of the new and old sampling sites upstream along the Saw Kill by a 500m x 500m drainage scale for each of the following categories: upland forest, developed, MCA

(meadow/cultural/agricultural) and other (open water, barren land, vegetated wetland, and shrubland). The “other” category was omitted from analysis as well because the definition was too broad and thus; would be not be appropriate for data interpretation. Using these drainage calculations, a table was formulated to represent data of only the new sample sites (Table 2.1), which was then used to determine each site’s dominant land usage (Table 2.2). Sites 1, 2, 2.5, 3, 4, 5, 11, and 12 were established as an “upland forest” dominated region, whereas Site 7 was established as a “developed” dominated area. Lastly, sites 9 and 10 are grouped as “MCA”.

After classifying each site, three plots were created to each illustrate the concentration of CDOM, chlorophyll a, and turbidity, throughout December 2017 and December 2019 in three categories: upland forest, MCA, and developed. Heat maps of CDOM and chlorophyll a in the Saw Kill were also created in a flip book format to analyze the seasonal patterns from a geographical perspective (Appendix D and E). To evaluate the normality of the three parameters, distribution plots were made. However, they failed the Shapiro-Wilks normality test, and were natural log-transformed to evaluate the correlation between log-transformed chlorophyll and turbidity and log-transformed CDOM and turbidity. The correlation tests, Kendall Tau and Spearman Rho, were applied. All graphs were created in R Studio, using ‘ggplot2’, ‘dplyr’ and the base package.

Table 2.1. Areas of Upland Forest, Developed, MCA, and Total Area calculated from a 500m x 500m drainage for sites along the Saw Kill. Note: “MCA” includes meadow, cultural, and agriculture. Modified from (Spodek 2017).

Site ID	Upland Forest (m ²)	Developed (m ²)	MCA (m ²)	Total Area (m ²)
1	258694	25963	9599	294319
2	229805	36418	34968	304776
2.5	233078	48003	37509	325433
3	228329	51140	37545	324073
4	180681	53504	36343	283869
5	280140	40474	0	321446
7	67650	178513	75266	384283
9	2268	27979	871284	129003
10	45468	39822	102686	314323
11	168347	67353	43085	290033
12	168145	88281	126823	393051

Table 2.2. Dominant Land Use of Each Site. Note: “MCA” includes meadow, cultural, and agriculture.

Site ID	Dominant Land Use
1	Upland Forest
2	Upland Forest
2.5	Upland Forest
3	Upland Forest
4	Upland Forest
5	Upland Forest
7	Developed
9	MCA
10	MCA
11	Upland Forest
12	Upland Forest

Results

CDOM, chlorophyll a, and turbidity do not have normally distributed samples ($p < 2.2e-16$). Thus, these variables were natural log-transformed to reduce the skewness in the variables (Figure 2.2). Unfortunately, the log-transformed plots still did not pass the Shapiro-Wilks normality test (CDOM $p=0.006$, chlorophyll a $p=8.42e-11$, and turbidity $p=1.45e-13$), meaning that these samples are not normally distributed. Therefore, analysis for these variables must be evaluated with non-parametric tests. Furthermore, there is a weak to insignificant correlative relationship between CDOM and turbidity (Kendall=0.083, Spearman=0.115), and chlorophyll a and turbidity (Kendall=0.073, Spearman=0.09) (Figure 2.3).

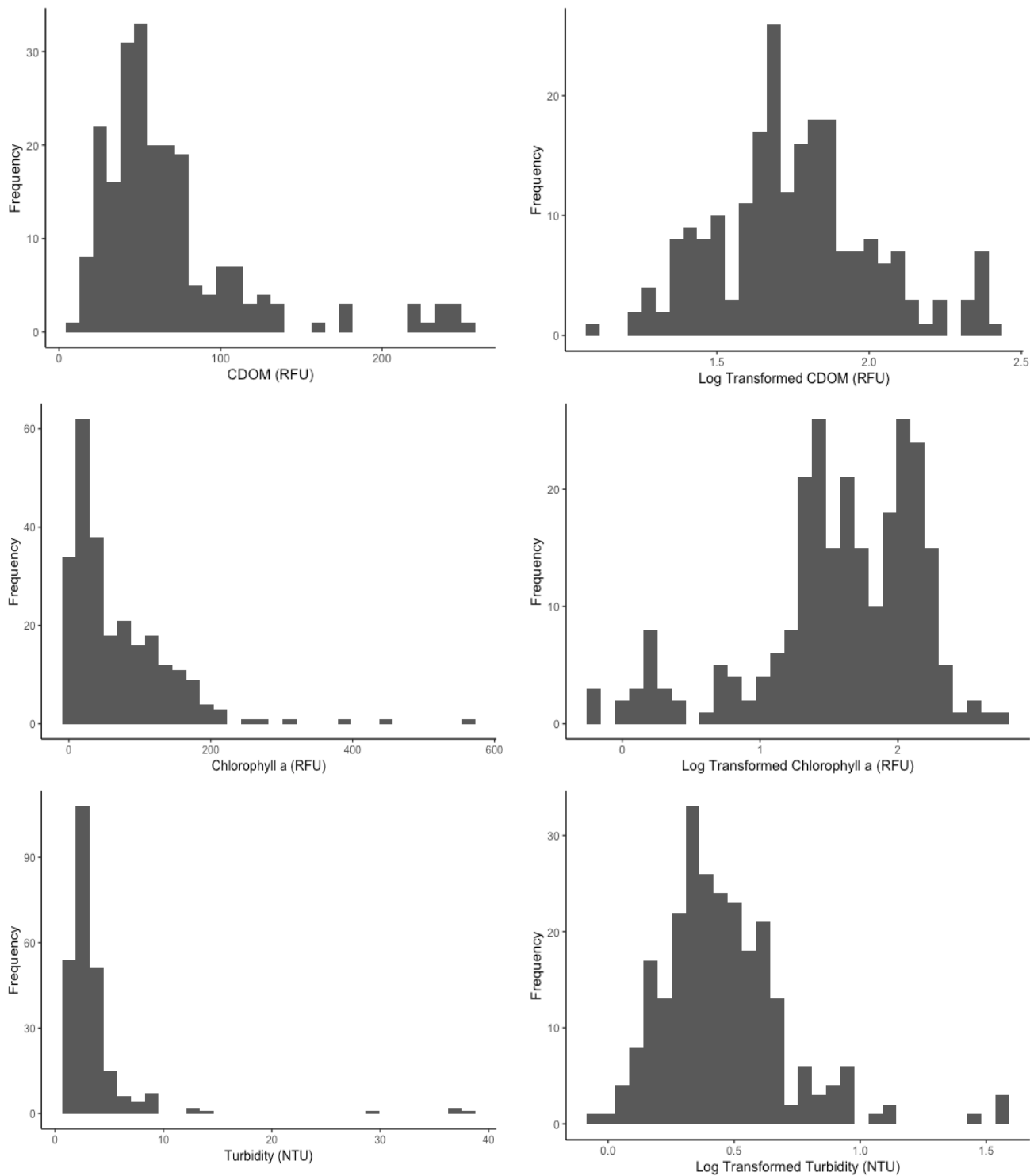


Figure 2.2. Distribution and Natural Log-Transformed Plots of CDOM, Chlorophyll a, and Turbidity. The left shows distribution frequency plots of CDOM ($p < 2.2e-16$), chlorophyll a ($p < 2.2e-16$), and turbidity ($p < 2.2e-16$). The right depicts natural log-transformed graphs of CDOM ($p = 0.005572$), chlorophyll a ($p = 8.42e-11$), and turbidity ($p = 1.452e-13$).

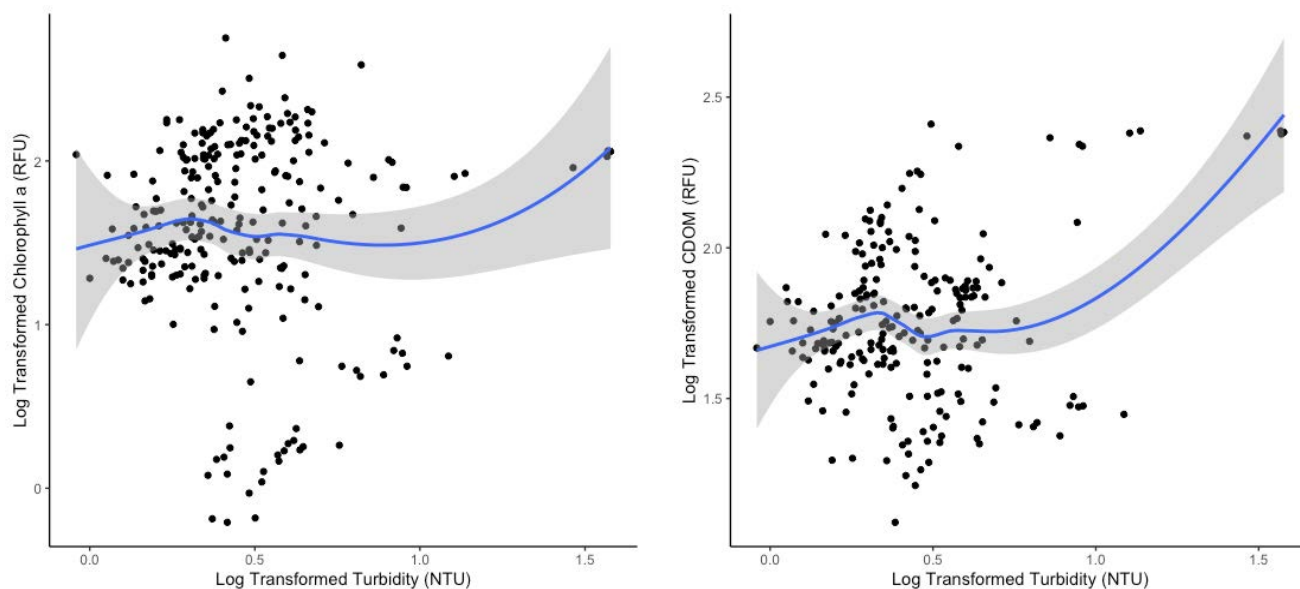


Figure 2.3. Correlation Plots. The left depicts correlation between log-transformed chlorophyll a v.s. log-transformed turbidity (Kendall = 0.07301335, Spearman: 0.09045148), while the right depicts correlation between log-transformed CDOM and log-transformed turbidity (Kendall = 0.082804, Spearman: 0.115495).

There are no seasonal trends of CDOM in the Saw Kill from 2017 to 2019 (Figure 2.4).

The general observation, apparent in developed, MCA, and forested regions, is that the concentration of CDOM slowly increases from late fall 2017 into fall 2018, and peaks during the month of October. Concentrations then decrease into winter 2019, and eventually levels off during spring and summer 2019. There is a slight increase in concentrations in the fall of 2019. Outliers to this behavior include site 2.5, a predominantly forested area on the Bard campus, and a location where the wastewater treatment plant discharges its water. During the late fall of 2017 to spring of 2018, CDOM values are much higher in site 2.5 compared to all other sites, and the concentrations drastically decrease during this period. Concentration levels peak during October, but begin to decrease during the winter of 2019, then slowly increase from spring 2019 to fall 2019. All sites in forested, developed and MCA region exhibit the same pattern in CDOM levels. CDOM is higher in forested areas (with a mean concentration of 74.69 ± 49.88 RFU), by 12.34% than in developed locations (66.01 ± 51.33 RFU), and 46.1% greater than MCA regions, (46.71

± 40.1 RFU) (Table 2.3). Unfortunately, data for CDOM in the Saw Kill was not collected during the summer of 2019, which includes the months of June, July, and August.

There are also no seasonal trends of chlorophyll a or variations in chlorophyll a behavior throughout different land covers in the Saw Kill (Figure 2.5). During the late fall of 2017 to fall of 2018, chlorophyll levels are consistently low at < 100 RFU. From winter of 2018 to summer of 2019, chlorophyll a concentrations increase, then slowly decreases in fall of 2019. Chlorophyll a is slightly higher in developed regions (with a mean concentration of 82.87 ± 95.76 RFU), by 12.51% compared to forested regions (73.114 ± 73.08 RFU), and 42.45% greater than MCA regions (53.853 ± 61.12 RFU). Lastly, there are also no seasonal trends of turbidity in the Saw Kill or varying turbidity behaviors in different land covers (Figure 2.6). Turbidity levels at all sites and all land usages are generally low in concentration, at < 10 NTU, except for the month of October in 2018, which drives the small peak in some sites. Turbidity levels are very similar throughout all land covers: 3.955 ± 5.11 NTU in forested areas, 3.14 ± 2.35 NTU in developed regions, and 2.810 ± 1.59 NTU in MCA areas. For all parameters, data was not collected in January, except for site 2, most likely due to unsafe sampling weather conditions.

Table 2.3. Mean, standard deviation, and number of samples were calculated for the following parameters: CDOM, chlorophyll a, and turbidity.

Variable	Land Use	Average Concentration \pm SD	Units	N (number of samples)
CDOM	Forested	74.69 \pm 49.88	RFU	159
	MCA	46.71 \pm 40.1	RFU	40
	Developed	66.01 \pm 51.33	RFU	19
Chlorophyll a	Forested	73.11 \pm 73.08	RFU	183
	MCA	53.85 \pm 61.12	RFU	46
	Developed	82.87 \pm 95.76	RFU	23
Turbidity	Forested	3.96 \pm 5.11	NTU	183
	MCA	2.81 \pm 1.59	NTU	46
	Developed	3.14 \pm 2.35	NTU	23

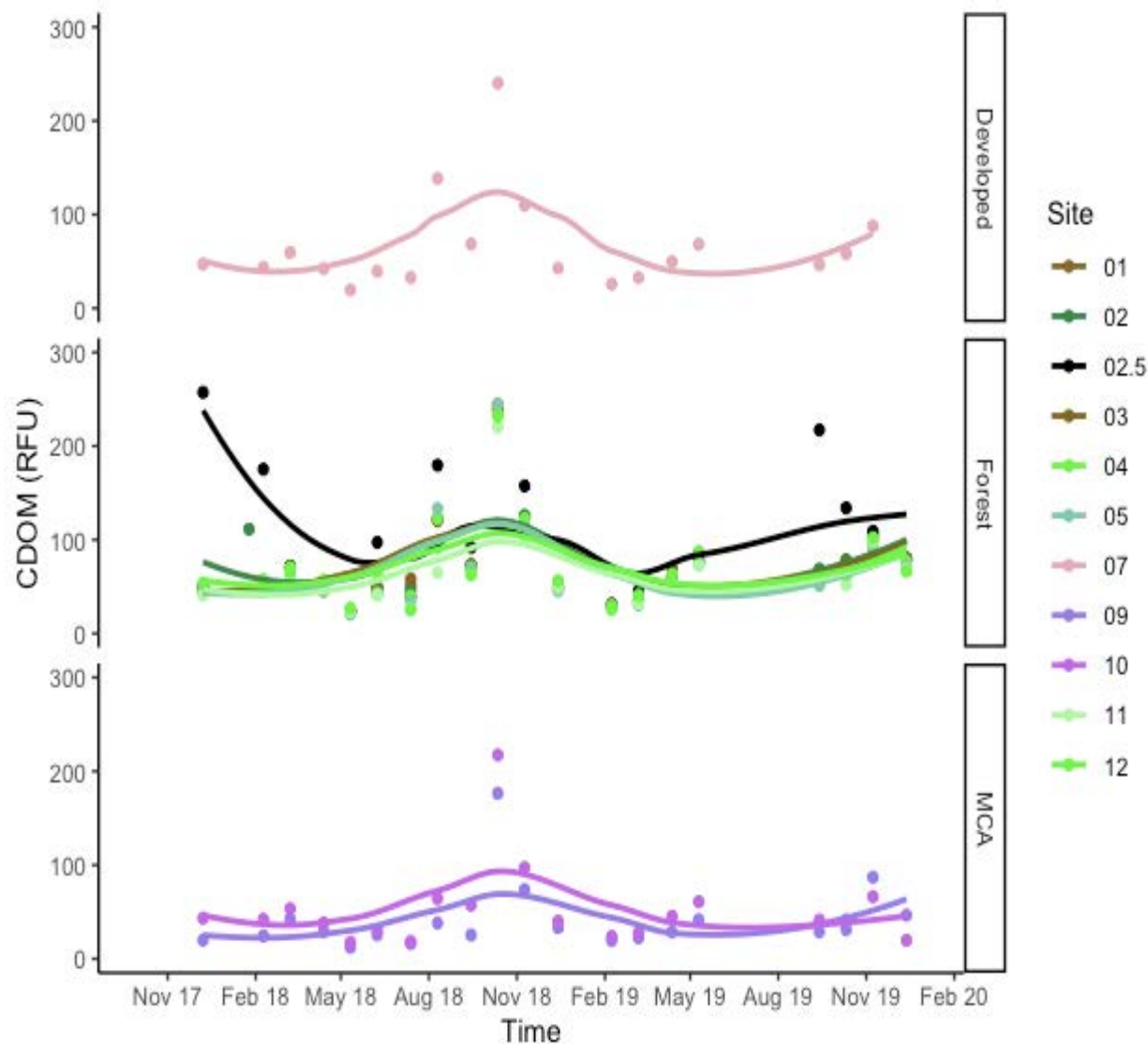


Figure 2.4. Concentration of CDOM (RFU) Over Time. Each colored line on the graph represents a distinct sample site in Saw Kill, revealing the concentration of CDOM (RFU) throughout December 2017 to December 2019. The top section depicts a site in a primarily developed land cover, the middle section illustrates sites from a predominantly MCA area, and the bottom graph displays sites in a substantially forested location.

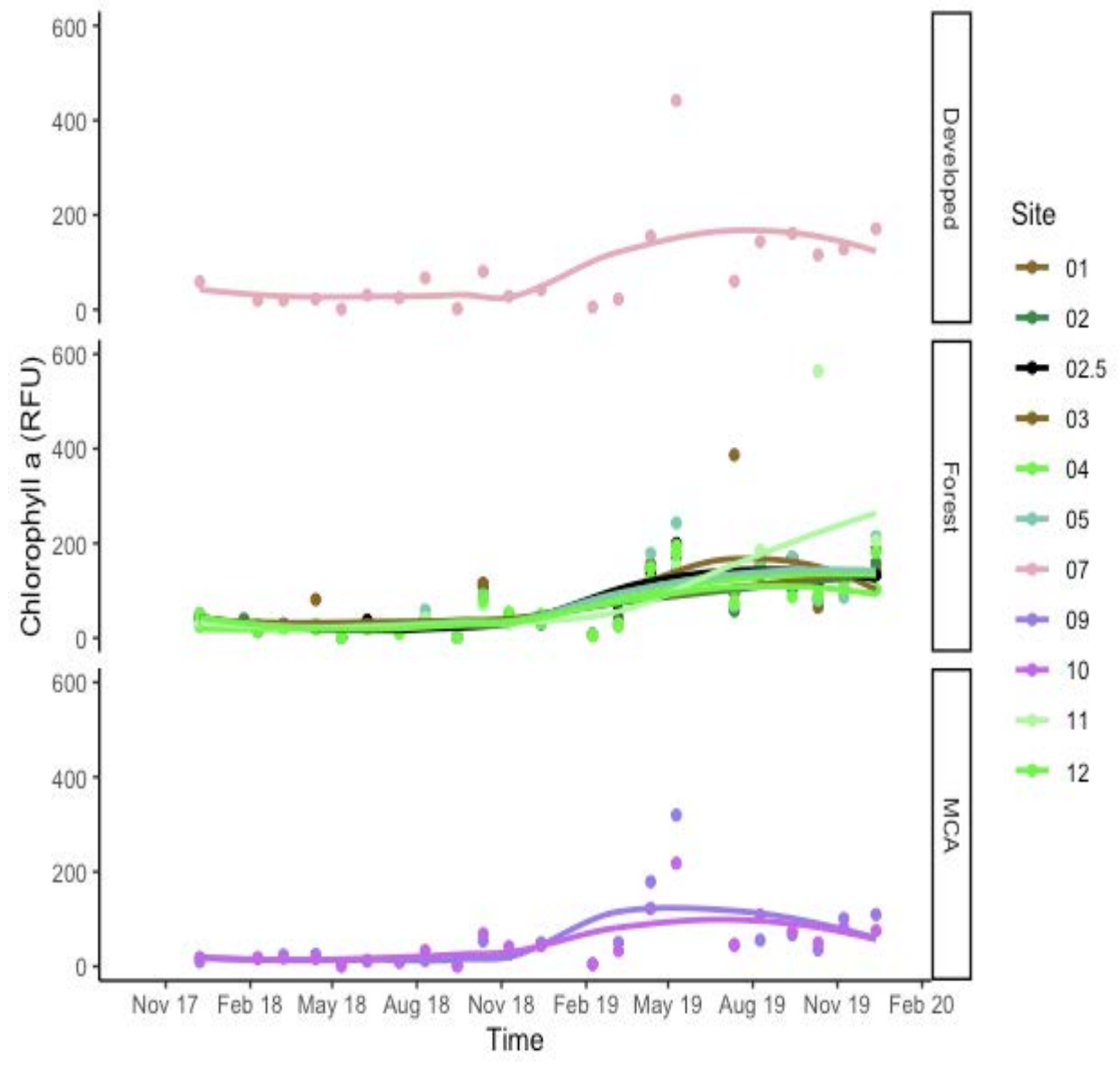


Figure 2.5. Concentration of Chlorophyll A (RFU) Over Time. Each colored line on the graph represents a distinct sample site in Saw Kill, revealing the concentration of chlorophyll a (RFU) throughout December 2017 to December 2019. The top section depicts a site in a primarily developed land cover, the middle section illustrates sites from a predominantly MCA area, and the bottom graph displays sites in a substantially forested location.

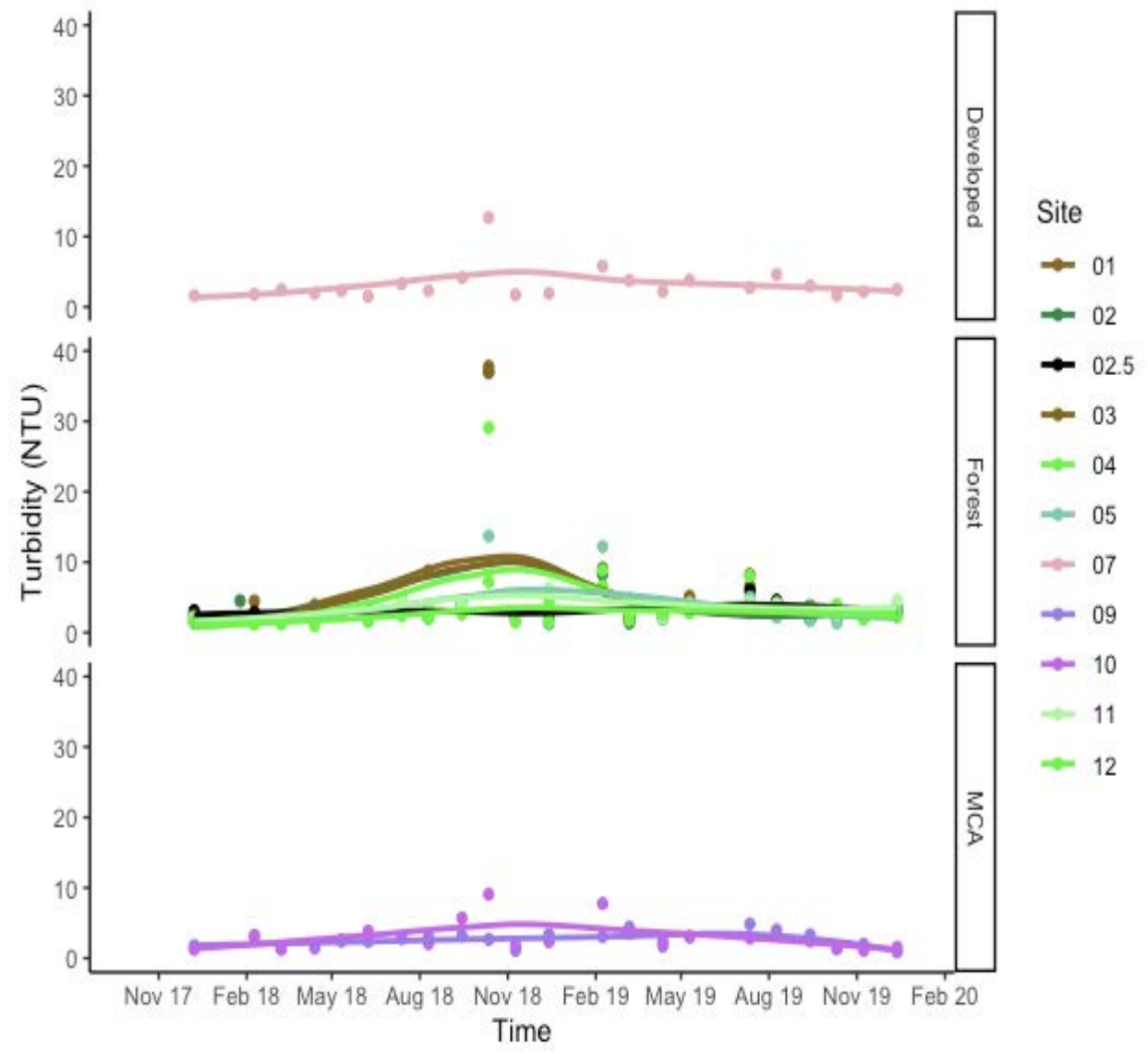


Figure 2.6. Concentration of Turbidity Over Time. Each colored line on the graph represents a distinct sample site in Saw Kill, revealing the concentration of turbidity (NTU) throughout December 2017 to December 2019. The top section depicts a site in a primarily developed land cover, the middle section illustrates sites from a predominantly MCA area, and the bottom graph displays sites in a substantially forested location.

Discussion

Influences of Land Use

Forested land use is often associated with better quality of water because there is typically less erosion and fewer pollutant inputs of sediment, fertilizers, and pesticides (Cunha, Sabogal-Paz, and Dodds 2016). Forest and riparian areas also protect water quality by serving as a filter or buffer area to contaminants (Ernst, Gullick, and Nixon 2004). Furthermore, Ernst, Gullick, and Nixon (2004) report that an increase in forest cover decreases the operating treatment plant costs for water from surface sources. On the other hand, the primary source of water pollution comes from runoff from agricultural lands (Hascic and Wu 2006) and pollutants include pesticides, nutrients, sediments, and organic substances (Camara, Jamil, and Abdullah 2019). Due to poor water qualities from agricultural areas, Abildtrup, Garcia, and Stenger (2013) finds an increase in water costs. Similarly, urban land covers are associated with a decline in water quality (Cunha, Sabogal-Paz, and Dodds 2016) and urban runoff consists of suspended solids, bacteria, nutrients, fats, and metals (Camara, Jamil, and Abdullah 2019). A risk associated with both agriculture and urban areas is excessive eutrophication (Hascic and Wu 2006).

Although it is hypothesized that land use would influence the tested variables, from observing Figures 2.4, 2.5, and 2.6, there is not a clear relationship between land cover and the investigated parameters because all land uses reflect similar concentrations and patterns. However, there are some slight variations in the concentrations of CDOM, chlorophyll a, and turbidity throughout each land cover. For example, forested areas in the Saw Kill have slightly higher concentrations of CDOM, 12.34% greater than developed areas and 46.1% greater than MCA. This is expected as sources of CDOM mainly emerge from the decomposition of terrestrial and aquatic vegetations, and to a lesser extent, production from aquatic plants and

phytoplankton (Griffin et al. 2018). Turbidity is also higher in forested sites, but the differences across varying land uses are negligible. It is interesting that turbidity levels in MCA and developed regions aren't higher than in forested sites because those regions are expected to have anthropogenic contaminants flowing into the Saw Kill. In addition, developed regions in the Saw Kill have slightly higher concentrations of chlorophyll a; 12.51% greater than forested regions, and 42.45% greater than MCA regions. It is also interesting that MCA sites have lower concentrations of chlorophyll a, since eutrophication is often associated with agricultural areas. Despite these variations across land usage, there is not a clear pattern of the impacts of land uses. Therefore, the relationship between land usage and CDOM, chlorophyll a, and turbidity can't be concluded.

The impacts of land use may be hard to detect on the account of limitations to this dataset. Forested sites have a lot more samples than developed and MCA areas. For reference, there is only one site that is in the developed category, two sites in the MCA category, and eight sites from the forested region. Moreover, due to time constraints, statistical analysis was not performed to determine the significance in the relationship between land use and the measured parameters. Thus, further research, such as collecting more data and running statistical analyses, is recommended to have a better grasp of this relationship.

Influences of Seasonality

It is hypothesized that seasonality will have an impact on concentrations of CDOM, chlorophyll a, and turbidity, and more specifically, warmer seasons like spring and summer are expected to have an effect on the measured parameters. This is because organic carbon and turbidity are generally found to be higher in warmer seasons (Cunha, Sabogal-Paz, and Dodds 2016) and phytoplankton typically blooms in the spring and summer when there is greater

sunlight (Lindsey and Scott 2010). However, seasonality in the Saw Kill, from 2017 to 2019, was not observed to play a role in the concentration of the investigated parameters in Figures 2.4, 2.5, and 2.6. This is because the parameters do not reflect any cyclical behavior and only peak for one season throughout two years. In particular, CDOM only peaks in the fall of 2018, which most likely reflects the decay of organic matter from terrestrial sources such as plant matter, leaves, and woody debris (Vannote et al. 1980). Likewise, turbidity only peaks during the fall of 2018, and has extremely low concentrations of < 10 NTU throughout the rest of the years. Additionally, chlorophyll a peaks during the spring and summer of 2019, which indicates a high concentration of algae, corresponding with the EPA (2019) as they report that algae typically blooms during the summer or with warmer water conditions. Ultimately, this suggests that the Saw Kill is at the highest risk of formation potential of dissolved organic matter and turbidity associated DBP in the fall of 2018, and of chlorophyll a associated DBP in the spring and summer of 2019.

Unfortunately, Saw Kill samples were not analyzed for CDOM during the summer of 2019, because the fluorometer was borrowed from the Bard Water Lab. The missing data is critical to understanding the seasonality of CDOM because in many water bodies, CDOM tends to peak in the summer. Hence, the interpretation of CDOM seasonality may be misled. Another reason that seasonal trends are not apparent is that there needs to be more data collected. Further research over years could be more revealing of seasonal trends. A speculation of the drivers of the CDOM and turbidity peaks in October 2018, may be due to an extreme weather event such as intense precipitation or flood as Cunha, Sabogal-Paz, and Dodds (2016) find that turbidity, total organic carbon, and total THM formation potential are higher during rainy seasons.

Relationship between NOM and DBP

Although there are peak moments when the Saw Kill is at the highest risk of formation potential of specific associated organic matter during fall 2018 and spring/summer 2019, the increased likelihood of DBP exposure to the Bard community is uncertain. To have a better understanding of this dynamic, more information is needed about the operational conditions of Bard's water treatment plant (WTP). As mentioned previously, operational factors of WTP have a great influence on DBP formation, such as the effectiveness of removing NOM and the disinfectant and coagulant doses. For instance, Serrano et al. (2015) finds high contents of organic carbon in raw water; however, after undergoing treatment, organic carbon contents had been removed by almost half. With regards to the water treatment at Bard, the Annual Drinking Water Quality Report for 2018 reveals that the WTP has been effective in minimizing DBP formation and concentration, as concentrations of total THMs and HAAs are in compliance with federal standards, 31.85 $\mu\text{g/L}$ and 30.05 $\mu\text{g/L}$, respectively.

In attempts to comprehend the complex relationship of NOM and DBP concentrations in the Saw Kill and finished drinking water, raw monthly data of THMs and HAAs were attempted to be acquired; however, it was not successful. Although access to the Annual Drinking Water Quality Reports for 2014, 2017, and 2018 were gained, they only report the annual mean of total HAAs and THMs. Unfortunately, the annual means do not provide enough information of DBPs on a seasonal scale, and as a result, conclusions of the relationship between NOM and DBP levels cannot be drawn. If monthly data of THMs and HAAs on raw and finished waters could be attained, further research would help understand the association between NOM in the Saw Kill and DBP concentrations in treated waters from WTP. In addition, analyzing CDOM, chlorophyll a, and turbidity in filtered water samples of the Saw Kill would be more revealing of this

relationship because they are more reflective of the operational processes of the water treatment plant.

Conclusion

The hypothesis predicted that land usage and seasonality would have an impact on the investigated parameters of CDOM, chlorophyll a, and turbidity; however, results reject this hypothesis. From the gathered data, seasonality does not have a significant impact on CDOM, chlorophyll a, and turbidity, and there isn't a clear effect from land usage (forested, developed, and MCA). Data suggests that the fall of 2018 is when the formation potential of DBPs associated with CDOM and turbidity are the highest and the summer of 2019 is when formation potential of DBPs associated with chlorophyll a are the highest in the Saw Kill. An approach for this chapter that wasn't taken due to time constraints was to explore the variables in relation to dry and wet seasons in order to take the effects of precipitation into consideration. Ultimately, extended research on this topic is recommended to better understand the effects of seasonality and land cover, and the link between NOM and DBPs in the Saw Kill.

Limitations

There are several limitations to this chapter. First and foremost, the nature of a citizen science program has some constraints, such as the inconsistency in data analysis. CDOM was unable to be analyzed during the summer season, which is a very important piece of information that would greatly impact our comprehension of the results. Another limitation is the nature of using CDOM as an indication for organic matter in water bodies. The fluorometer only measures the fraction of CDOM that fluoresces, which is a small pool of total organic matter, revealing

only a small snippet of precursors to DBPs.

Chapter 3: Investigating Temperature Effects on CDOM Measurements

Introduction

There are various proxy measurements of disinfection byproducts. As mentioned, one method is to measure the fraction of colored dissolved organic matter (CDOM) that fluoresces, also known as fDOM, by using a fluorometer. Fluorometers use UV light to excite fluorophores (Watras et al. 2011), which raises the energy of electrons from a ground state to an excited state. During this state of excitation, the organic fluorophores emit blue light, which allows for the detection of CDOM and electrons to return to their ground state (Avantes BV 2019). The usage of fluorometers to measure CDOM is becoming an increasingly common proxy for dissolved organic carbon (DOC) in streams, because it is a relatively quick and inexpensive method to utilize. However, there are limitations to CDOM fluorescence readings due to the inverse relationship between temperature and CDOM emission intensity. This circumstance occurs when the rise in temperature increases the chance that electrons in their excited state will return to ground state without emitting electromagnetic radiation. As a result, this reduces CDOM emission intensity. In other words, CDOM values decrease as temperature increases.

Thus, when analyzing data with temperature variation, on a diel and seasonal time scale, raw fluorescence CDOM data may be misleading (Downing et al. 2012). A research group from the University of Wisconsin-Madison derived an equation to compensate CDOM for temperature effects:

$$\text{CDOM}_r = \text{CDOM}_m / [1 + \rho(T_m - T_r)].$$

In this equation, T is temperature ($^{\circ}\text{C}$), ρ is the temperature-specific coefficient of fluorescence ($^{\circ}\text{C}^{-1}$), and the subscripts r and m are the reference and measured values (Watras et al. 2011). Watras et al. (2011) encourages temperature compensation as a necessary and fundamental component to CDOM monitoring via fluorescence sensors.

This chapter analyzes the effects of temperature on CDOM values in collaboration with the New York City Department of Environmental Protection. The NYC DEP is a city agency that protects the public health and environment by supplying and monitoring drinking water and wastewater. The water supply system, which consists of aqueducts, reservoirs, tunnels, and pipes, drawing water from the suburban and rural hinterlands, serves approximately 5 billion liters of fresh water to about 9 million consumers in New York City and a few suburban regions on a daily basis. The upstate watersheds and reservoirs include the Croton system (12 reservoirs and 3 controlled lakes), the Catskill system (Ashokan and Schoharie reservoir), the Delaware system (Cannonsville, Neversink, Pepacton and Rondout reservoirs), and the Kensico, Hillview, and Jerome Park reservoirs (Figure 3.1). This water source is one of the few in the nation of its grand size that is both acquired from surface and groundwater. The water from the Catskill and Delaware reservoirs are unfiltered, but disinfected with chlorine and ultraviolet treatment (Pires 2004).

Methods

The two study sites are the primary river inflows to reservoirs of the Delaware system, Neversink (NCG) and Cannonsville (CBS) (Figure 3.2). Cannonsville Reservoir is located in the western region of Delaware County, bordering New York and Pennsylvania (NYC Environmental Protection, “Cannonsville”, n.d.) (42°N , -75°W) (Latitude, n.d.). The reservoir

was created by constructing a dam on the West Branch of the Delaware River. The river's new course flows south below the dam, eventually joining the lower Delaware River (NYC Environmental Protection, "Cannonsville", n.d.). The reservoir has been in service since 1964 and is the newest reservoir in the city's water supply system. The reservoir is 4,703 acres, 12 miles long, and has a maximum depth of 121 feet (NYC Department of Environmental Conservation, n.d.). It has a drainage area of 455 mi², which is the largest drainage basin of all the system's reservoirs and has a maximum capacity of 95.7 billion gallons (NYC Environmental Protection, "Cannonsville", n.d.) The state of Cannonsville ranges from mesotrophic to eutrophic in terms of its algal productivity, with an agricultural land use of 19%, and 63% forested land cover. Additionally, there are four wastewater treatment plants within the watershed (Moore et al. 2019b).

Neversink Reservoir is located in Sullivan County (41°N, -74°W) (USGS, n.d.). Similar to Cannonsville, the reservoir was formed with the construction of a dam on the Neversink River. The release below the dam flows into the continuation of the Neversink River, which joins the lower Delaware River further downstream. This reservoir has been in service since 1954. It is a smaller reservoir than Cannonsville (NYC Environmental Protection, "Neversink", n.d.); it covers 1539 acres (USGS, n.d.), with a drainage basin of 92 mi², and capacity of up to 34.9 billion gallons (NYC Environmental Protection, "Neversink", n.d.). Unlike Cannonsville, the reservoir is in an oligotrophic (lower productivity) state. It is heavily forested (91%) and has minimal agricultural activity (1.4%). There are no wastewater treatment plants within the watershed (Moore et al. 2019b).



Figure 3.1. Map of NYC's Water Supply System. (Pires 2004, Figure 1).

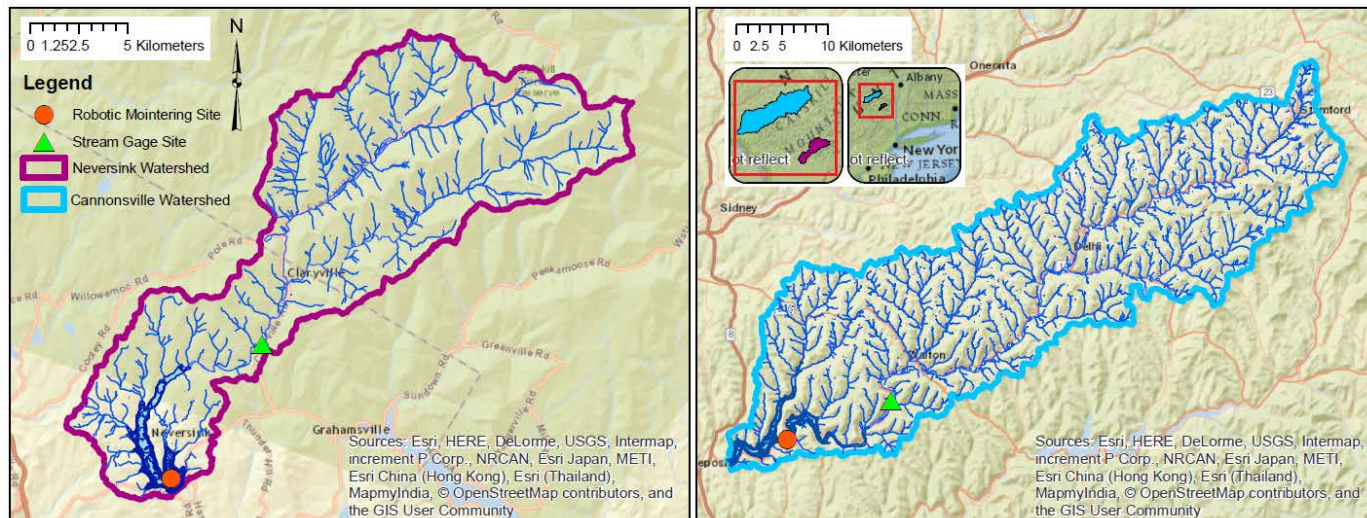


Figure 3.2. Map of Neversink and Cannonsville Reservoir Watershed. Neversink is on the left and Cannonsville is on the right. The Neversink sampling location is situated at the USGS stream gage site, #0143500, represented by the green triangle. The Cannonsville sampling location is positioned at the West Branch Delaware River, downstream from the USGS stream gage site, #01423000, which is also portrayed by the green triangle. Map created by Samantha Cash for the NYC DEP in 2016.

Grab samples from stream inflows into both reservoirs were taken by DEP's Grahamsville field staff. Samples were ideally collected mid-stream, and once the dark sample bottles were filled, they were placed in a cooler. In situ measurements of temperature, pH, and dissolved oxygen were conducted after sample collection, as well as site observations such as precipitation and time. Afterwards, the sample bottles were transported back to DEP's laboratory in Grahamsville and later transferred to DEP's Kingston laboratory on ice, and immediately placed in a refrigerator without added preservatives.

A total of 20 grab samples were collected throughout November 2019 to February 2020; 11 from CBS and 9 from NCG (Figures 3.3 and 3.4). From collected samples, both sites have generally low concentrations in dissolved organic carbon, with all samples measuring < 2 mg/L, and low in turbidity, with all samples < 11 NTU. Laboratory experiments were not always conducted immediately after sample collection. Some samples were in the refrigerator up to 51 days before they were analyzed, but on average, samples were analyzed within 15.6 days. Four

samples were re-analyzed twice, two from NCG and two from CBS, testing for sample stability over time. Moreover, each fluorometer did not test the same number of samples. DEP's fluorometer tested all samples from CBS and NCG, a total of 20 samples, while Bard's fluorometer tested a total of 6 samples, 3 from each reservoir.

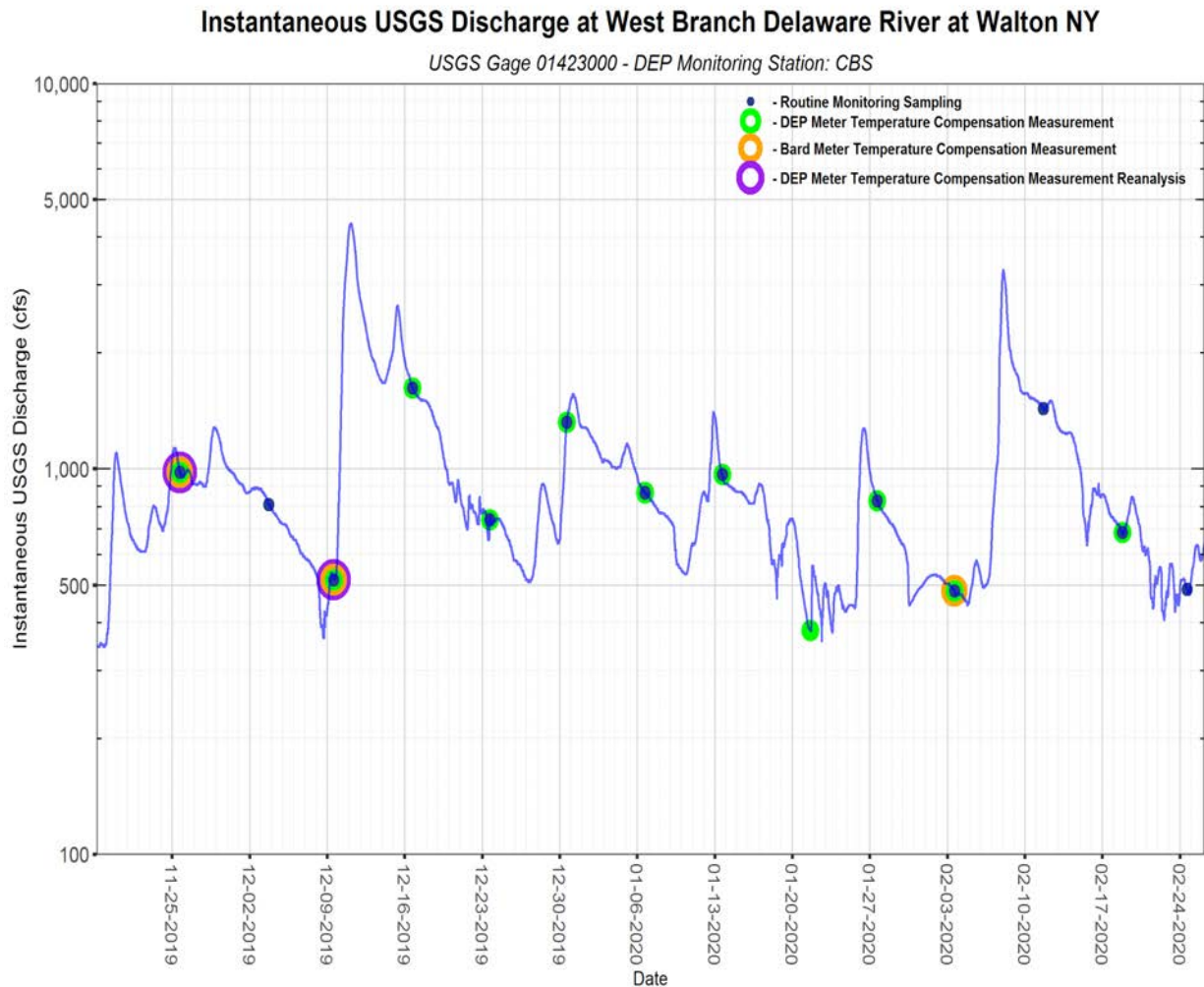


Figure 3.3. Discharge at Cannonsville Reservoir Throughout November 2019 to February 2020. Grab samples collected are represented by the blue dot, analysis of the samples with DEP's fluorometer are depicted by the green ring, samples analysis with Bard's fluorometer are represented by the orange ring, and sample re-analysis with DEP's fluorometer are portrayed by the purple ring. Figure created by Dave Van Valkenburg.

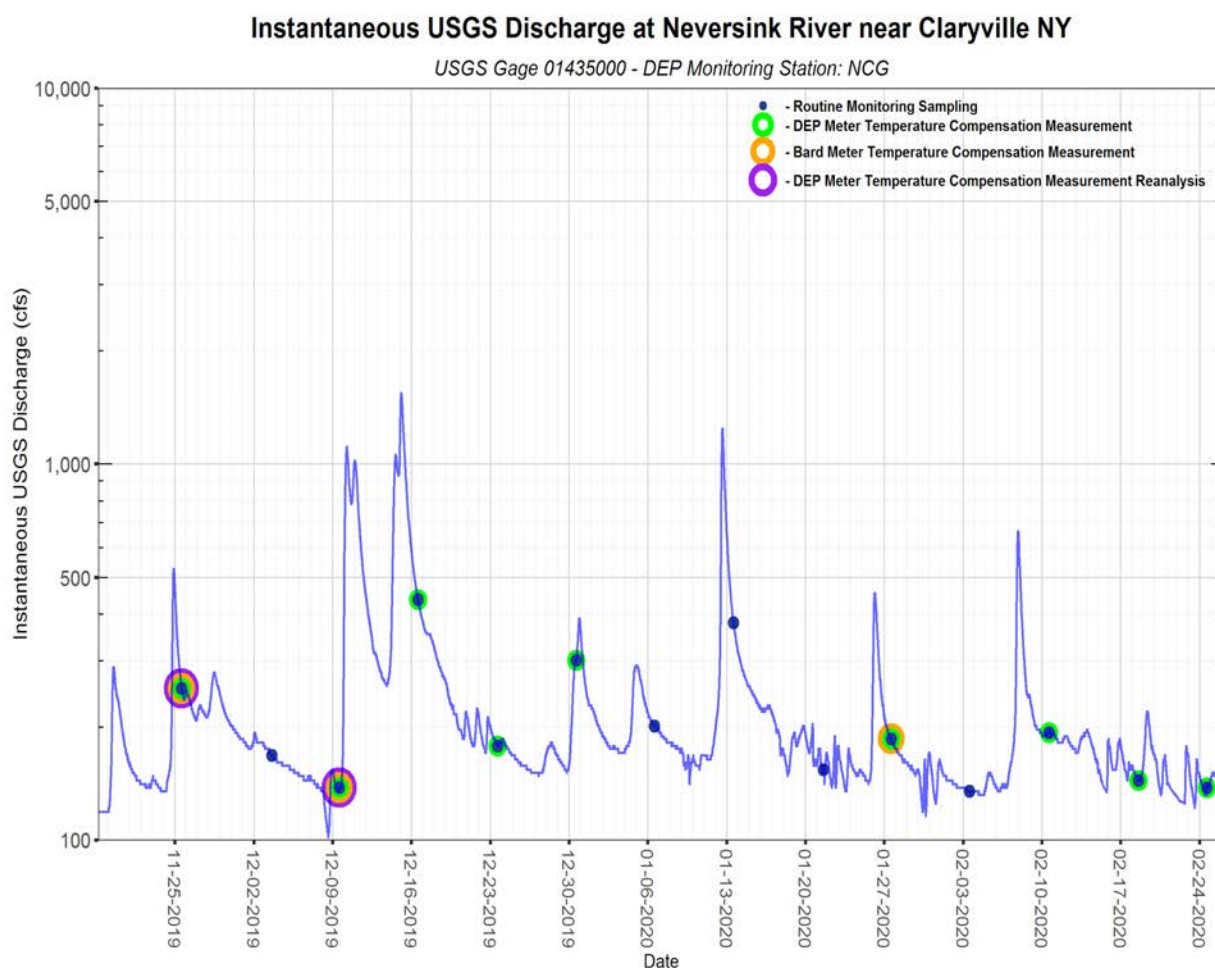


Figure 3.4. Discharge at Neversink Reservoir Throughout November 2019 to February 2020. Grab samples collected are represented by the blue dot, analysis of the samples with DEP’s fluorometer are depicted by the green ring, samples analysis with Bard’s fluorometer are represented by the orange ring, and sample re-analysis with DEP’s fluorometer are portrayed by the purple ring. Figure created by Dave Van Valkenburg.

Temperature quenching experiments were conducted using two AquaFluor HandHeld Fluorometers from Turner Designs. One instrument belongs to the DEP’s Grahamsville Laboratory and the other is from the Bard Water Lab at Bard College. Both instruments are the same model, Model # 8000-010, and use UV LED for colored dissolved organic matter fluorescence. The specification for both Turner Design fluorometers is 375 nm center wavelength, excitation 350 +/- 40 nm, emission ≥ 420 nm, 0.1 ppb method detection limit, and linear range of 0-1000 ppb (Turner Designs, n.d.). Although both instruments are essentially the

same (in consideration of the slight variation in the manufacturing of each fluorometer), there are notable differences in calibration. The CDOM parameter in Bard's fluorometer has been calibrated using rhodamine dye in September 2019, and since then has been checked for monthly drifts using rhodamine. However, Turner Designs does not recommend rhodamine as a standard to calibrate CDOM, and instead suggests using quinine sulfate (Henderson 2020). The scale for CDOM is set from 0 to 1 RFU (relative fluorescence units). On the other hand, DEP's fluorometer was last calibrated for CDOM in summer of 2019, using a quinine sulfate standard made from the Grahamsville laboratory. The fluorometer's scale for CDOM is at 0 to 100 RFU.

Laboratory experiments were conducted at the DEP laboratory in Kingston, NY. The method for temperature fluorescence quenching that supervisors Dave Van Valkenburg, Karen Moore, and I developed, involved the process of evaluating water samples for the effects of temperature on CDOM intensity. Stream samples flowing into Neversink and Cannonsville were measured for CDOM at a temperature range of approximately 3°C to 30°C, in ~5°C increments. The ideal temperature target ranges were:

- < 5°C
- 5°C - 10°C
- 10°C - 15°C
- 15°C - 20°C
- 20°C - 25°C
- 25°C - 30°C.

These ranges were chosen because 5-6 data points are sufficient to analyze the relationship between temperature and CDOM fluorescence intensity. Water samples were first cooled down in a walk-in cooler with an ice bath, in order to achieve the temperature ranges of < 5°C and 5°C

- 10°C. Samples were then transferred to the laboratory and heated with a hot water bath to achieve the rest of the target ranges. The temperature was continuously monitored with a NIST digital thermometer. The cuvettes and the digital thermometer were rinsed with deionized water and wiped dry with KimTech wipes. See (Appendix F) for more details.

To provide more insight about the procedure, temperature quenching experiments were only conducted in the laboratory during the period of method development. However, it was found to be extremely difficult to achieve temperature stabilization of the samples < 5°C, which resulted in the decision to conduct the low temperature portions of the experiments in the walk-in cooler. To ensure reliable data, data points with temperatures < 5°C were determined to be difficult to measure and therefore highly variable because of the constant temperature fluctuation. Thus, only samples analyzed during this experimental period with measurements at < 5°C were omitted from data analysis and graphical representation (Figures 3.5, 3.6, 3.7, and 3.8). This data removal includes CBS and NCG samples collected on November 25 and December 9, 2019, which were examined on both fluorometers.

To examine effects of temperature on CDOM fluorescence emission intensity, raw CDOM data were corrected by using the equation $CDOM_r = CDOM_m / [1 + \rho(T_m - T_r)]$, provided by Watras et al. (2011). These results are presented graphically. One figure represents raw and corrected CDOM from Cannonsville (Figure 3.5), while the other figure represents the same analysis, but from Neversink (Figure 3.6). The corrected CBS CDOM data, measured with the DEP's fluorometer, was then applied to assess the robustness of the CDOM-DOC relationship (Figure 3.7). In addition, sample degradation of CBS and NCG were analyzed over a graph, illustrating CDOM values originally detected and CDOM values detected when re-analyzed at a later date (Figure 3.8). Lastly, the results of exploratory ATP (adenine triphosphate) tests were

evaluated. All plots were created in R Studio using the ‘ggplot2’ package and the statistical analysis such as correlation was executed using ‘Pearson’s r’ test.

Results

Temperature effects on CDOM intensity

There is a linear decrease in CDOM intensity as temperature increases in both NCG and CBS samples, measured with both Bard and DEP fluorimeters (Figures 3.5 and 3.6). This effect of temperature on CDOM intensity was observed to be reversible during laboratory experiments. For example, when samples exceeded the temperature target range, CDOM values would be remeasured at a cooler temperature, which resulted in higher CDOM values. This reversible effect was also reported by Watras et al. (2011).

Over the temperature range of 3°C to 30°C, taking into account all samples from both fluorimeters and sites, CDOM intensity decreases at approximately $1\% \pm 0.2$ per degree temperature (°C) increase, which is consistent with the experimental work of Downing et al. (2012). When analyzing Cannonsville samples, DEP’s fluorometer measured CDOM values decreasing at an average of $0.84\% \pm 0.181$ per 1°C increase (range = -0.69% to -1.353%, n = 11 tests) (Table 3.1). Likewise, when using Bard’s fluorometer to analyze Cannonsville samples, measured CDOM values decreased at an average of $0.84\% \pm 0.0018$, per 1°C increase (range = -0.66% to -1.02%, n = 3 tests). When looking at water samples from Neversink, DEP’s fluorometer measured CDOM values decreasing at an average of $1.09\% \pm 0.0018$ per 1°C increase (range = -0.97% to -1.53%, n = 9). Similarly, Bard’s fluorometer measured Neversink CDOM values decreasing at an average of $1.05\% \pm 0.0015$ per 1°C increase (range = -0.88% to -1.18%, n = 3 tests). This data suggests that there are no major differences between fluorimeters

in the results for temperature quenching, despite calibration differences. However, there seems to be a difference between sample sites. On average, Neversink CDOM intensity decreases at 1.07%, while Cannonsville decreases at 0.85% per 1°C increase, which is approximately 23% slower rate than Neversink. This may be a reflection of the differences in organic matter composition between the two watersheds. Watras et al. (2011) tested samples from different sites with known compositional differences and found that different sites had different fluorescence quenching behavior.

The inverse relationship between CDOM and temperature, apparent in (Figures 3.5 and 3.6), indicates that data needs to be corrected for temperature, reported at a reference temperature. To correct CDOM values, the equation Watras et al. (2011) derived for temperature compensation was used:

$$\text{CDOM}_r = \text{CDOM}_m / [1 + \rho(T_m - T_r)].$$

Again, in this equation, T is temperature (°C), ρ is the temperature-specific coefficient of fluorescence (°C⁻¹), and the subscripts r and m are the reference and measured values. The temperature coefficient is derived by taking the “slope/ intercept” of each sample. There are no major differences in the coefficients in the samples between each fluorometer. NCG and CBS samples analyzed with using DEP’s fluorometer has an average temperature coefficient of -0.009 ± 0.002045 , and samples analyzed with using Bard’s fluorometer has an average temperature coefficient of -0.0092 ± 0.00169 . However, there are differences in the mean coefficient between both sites. The average temperature coefficient of CBS is -0.0083 ± 0.0017 and NCG is -0.0102 ± 0.0015 . The coefficient for each site and each fluorometer (Table 3.1) was applied to Watras’

equation, along with the chosen reference temperature of 20°C to correct CDOM values (Figures 3.5 and 3.6). These corrected values are highly correlated with dissolved organic carbon (DOC) ($r^2=0.97$) (Figure 3.7).

Table 3.1. Temperature Coefficient, Average Change of CDOM per Degree and the Range were calculated for two study sites, Cannonsville and Neversink Reservoir, by using two Turner Designs fluorometers.

CDOM Sensor	Matrix	Date Analyzed	N (number of samples)	Change of CDOM Per Degree (Average \pm SD)	Range of CDOM Change per Degree	Temperature Coefficient (ρ) (Average \pm SD)
Turner Designs; DEP	Cannonsville Reservoir	December January February	11	-0.84% \pm 0.181	-0.69% to - 1.353%	-0.008 \pm 0.0018
Turner Designs; DEP	Neversink Reservoir	December January February	9	-1.09% \pm 0.0018	-0.97% to - 1.53%	-0.0103 \pm 0.0016
Turner Designs; Bard	Cannonsville Reservoir	December February	3	-0.84% \pm 0.0018	-0.66% to - 1.02%	-0.0085 \pm 0.0019
Turner Designs; Bard	Neversink Reservoir	December	3	-1.05% \pm 0.0015	-0.88% to - 1.18%	-0.01 \pm 0.0014

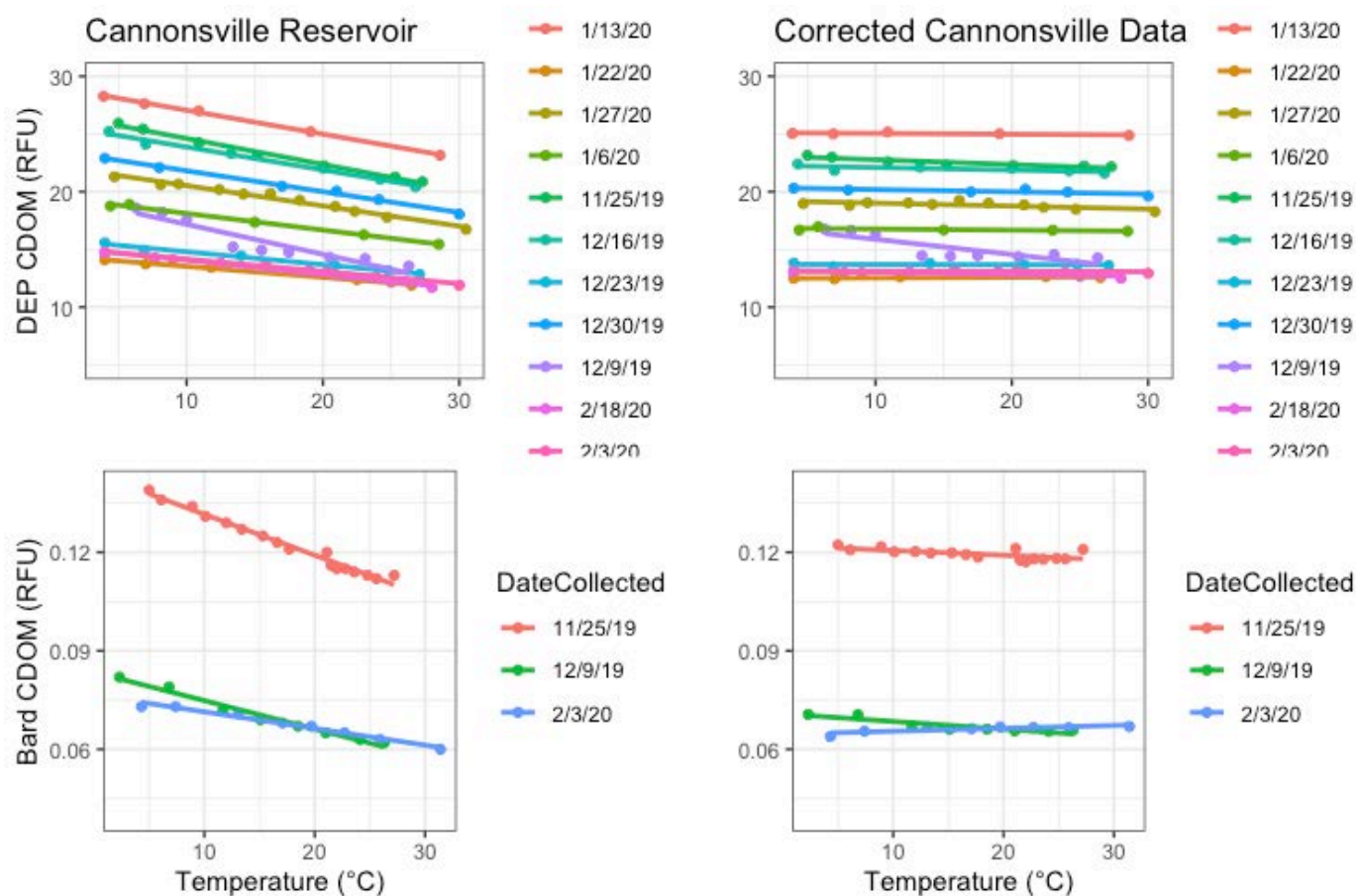


Figure 3.5. Cannonsville CDOM Values Over a Range of Temperature. Raw fluorescence CDOM data from Cannonsville Reservoir are represented over a temperature scale of 3°C - 30°C on the left side. The right side depicts corrected CDOM data by utilizing Watras' et al. (2011) equation, with the reference temperature of 20°C and the temperature coefficient of -0.008 (DEP's fluorometer) and -0.0085 (Bard's fluorometer). The top graphs are samples analyzed with DEP's fluorometer, while the bottom graphs are samples analyzed with Bard's fluorometer. Each colored line represents a distinct sample.

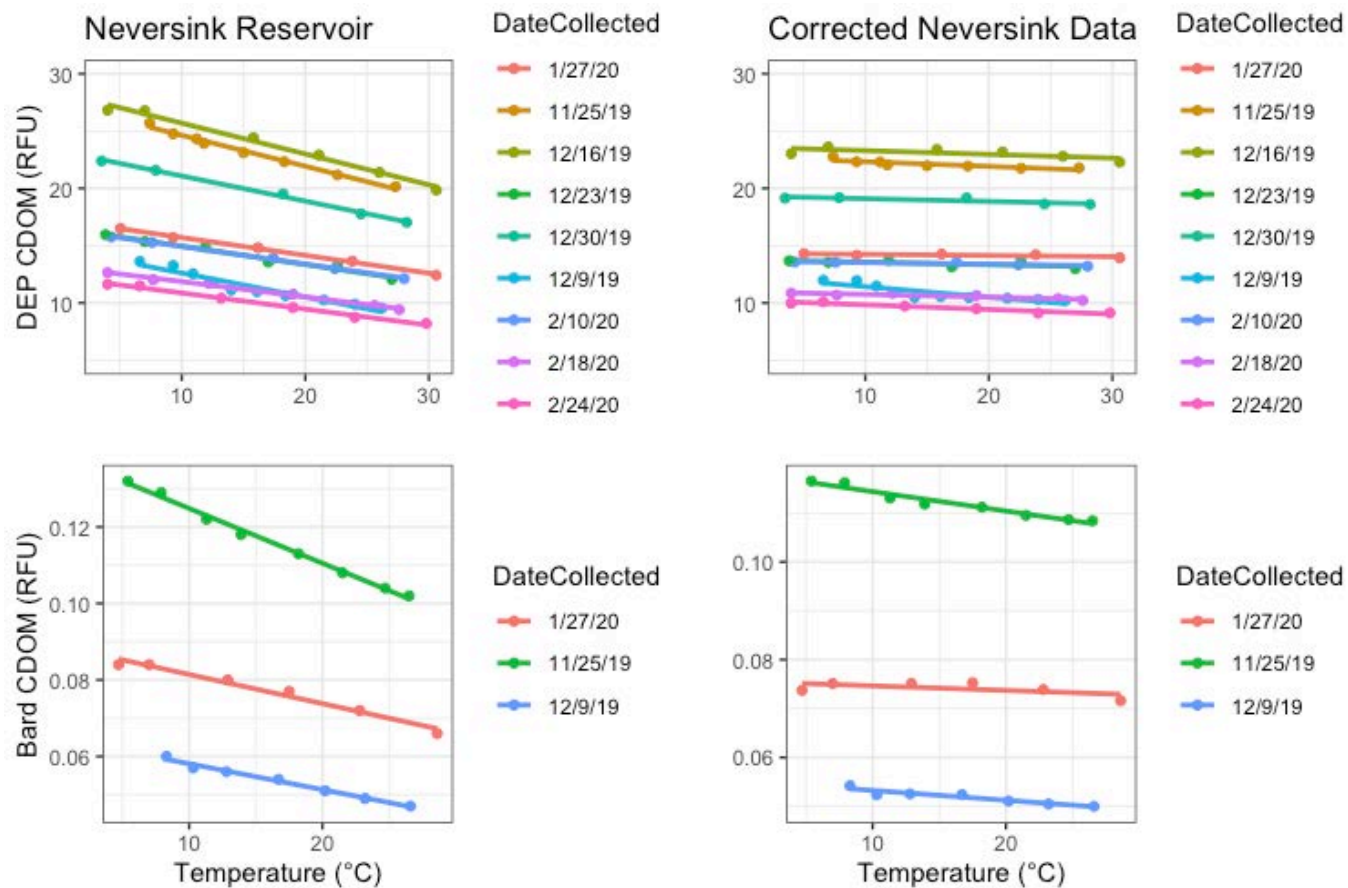


Figure 3.6. Neversink CDOM Values Over a Range of Temperature. Raw fluorescence CDOM data from Neversink Reservoir are represented over a temperature scale of 3°C - 30°C on the left side. The right side depicts corrected CDOM data by utilizing Watras' et al. (2011) equation, with the reference temperature of 20°C and the temperature coefficient of -0.0103 (DEP's fluorometer) and -0.01 (Bard's fluorometer). The top graphs are samples analyzed with DEP's fluorometer, while the bottom graphs are samples analyzed with Bard's fluorometer. Each colored line represents a distinct sample.

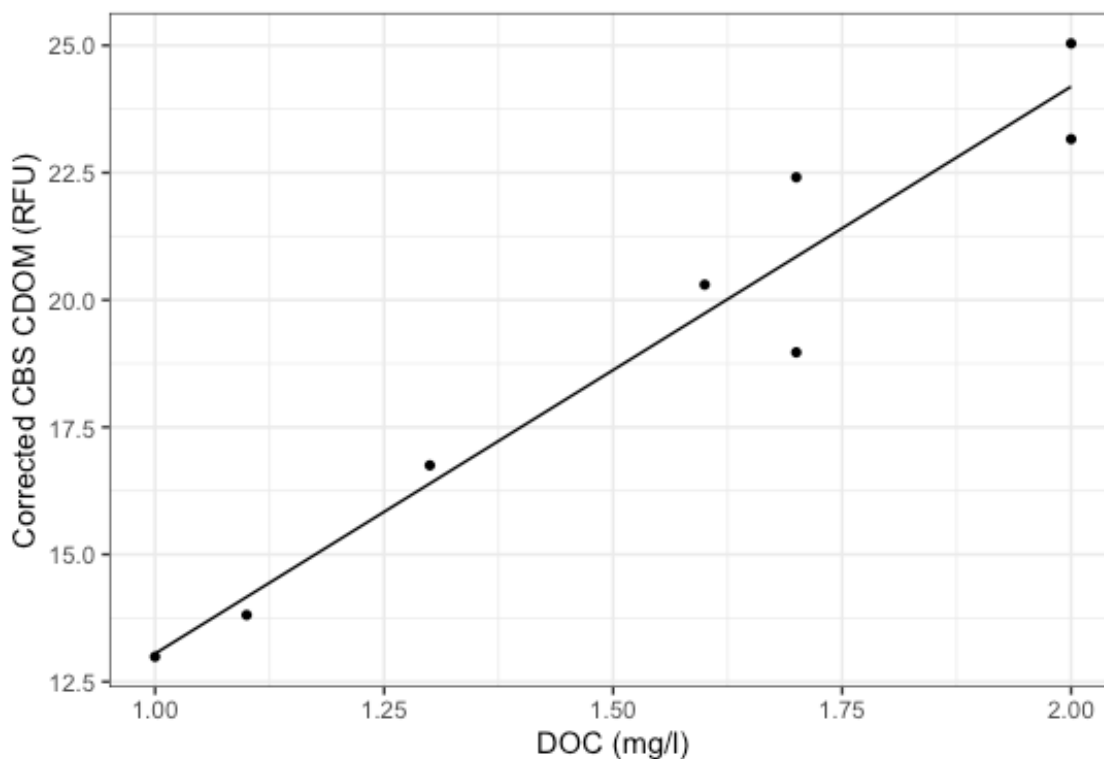


Figure 3.7. CDOM v.s. DOC. Corrected Cannonsville CDOM values, measured with the DEP's fluorometer, used as a proxy for dissolved organic carbon. $R^2= 0.97$.

Sample Degradation Over Time

Four samples were tested for shelf life; two from CBS and two from NCG. Each site had a grab sample collected on November 25 and December 9, 2019. They were first analyzed using DEP's fluorometer, on December 11, 2019, holding time of 16 and 2 days respectively, and then reanalyzed on February 5, 2020, holding time of 72 and 58 days respectively (Figure 3.8). The temperature coefficient of CBS collected in November and analyzed in December is, -0.008, and the reanalysis in February is -0.007. The coefficient of CBS collected in December and analyzed in December is -0.01, and the reanalysis in February is -0.007. The coefficient of the NCG sample collected in November and analyzed in December is -0.01, and the reanalysis is -0.009. Lastly, the coefficient of the NCG sample collected in December and analyzed in December is -

0.014 and reanalyzed in February is -0.009. These coefficients suggest that a holding period of 72 days show signs of degradation of water quality in the samples.

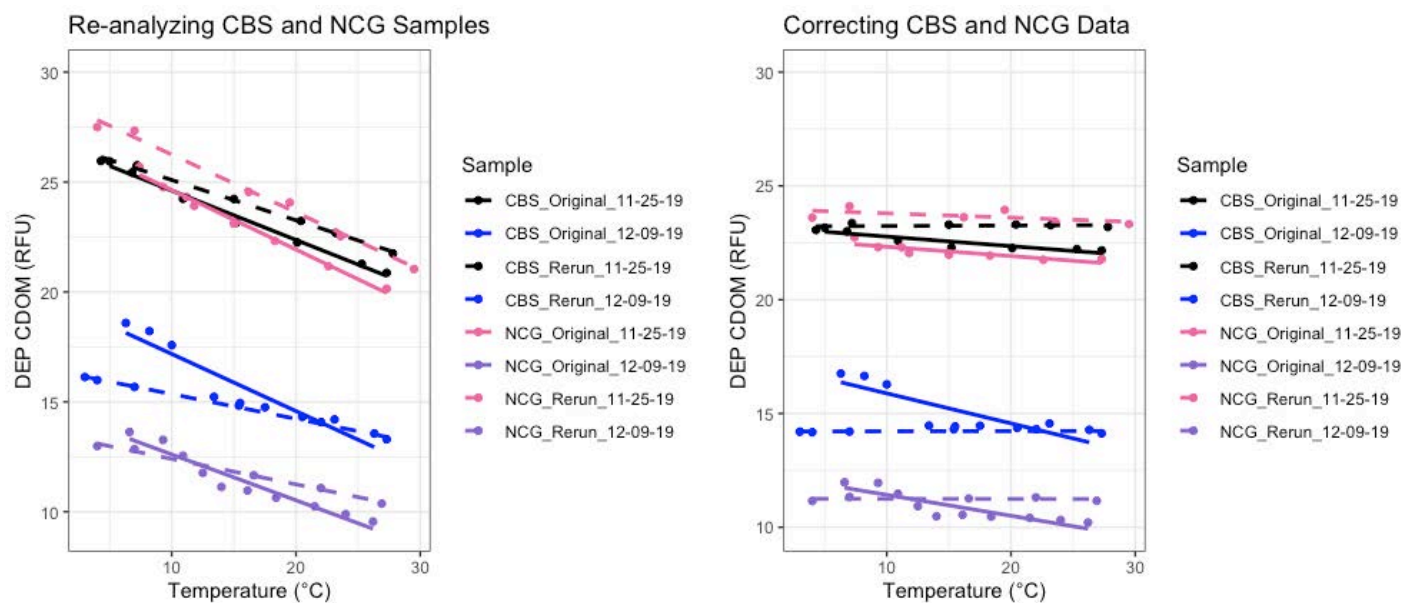


Figure 3.8. Re-analyzing NCG and CBS Samples with DEP’s Fluorometer. The left depicts Neversink and Cannonsville samples analyzed at an original date, and then re-analyzed at a later date. The right depicts these values corrected by utilizing Watras’ et al. (2011) equation, with the reference temperature of 20°C and the temperature coefficient of -0.008, and -0.0103 for CBS and NCG, respectively. Each colored line represents a distinct sample.

Discussion

Corrected CDOM values

All corrected CDOM values (in Figures 3.5, 3.6, and 3.8), should have a slope of zero due to the compensation for temperature effects on CDOM emission intensity. When looking at Cannonsville and Neversink data, (Figures 3.5 and 3.6), none of the samples have a zero slope, but for the most part have slopes that are generally close to zero. However, a noteworthy outlier to this is the CBS sample from December 9, 2019, analyzed with the DEP fluorometer. Corrected CDOM values range from 16.53 RFU at 6.3°C to 14.38 RFU at 26.3°C, decreasing by ~2 RFU

with a -13.01 percent change. Likewise, the December 9, 2019 sample from NCG, analyzed with the DEP's fluorometer, is an outlier as well. Corrected CDOM values range from 12.15 RFU at 6.6°C, to 10.13 RFU at 26.2°C, decreasing by ~2 RFU with a -16.63 percent change.

An explanation for these outliers may be that there is a need to correct CDOM values due to turbidity, in addition to correcting for temperature effects. Downing et al. (2012) explains that suspended particles may reduce the excitation signal from the fluorometer and the CDOM fluorescence intensity emission, an effect known as light attenuation. Thus, correcting for turbidity may adjust the slopes closer to zero and produce data with greater accuracy. However, a closer examination of turbidity in the CBS and NCG December samples reveals that turbidity values were quite low: 1.7 NTU and 0.5 NTU, respectively. It can be inferred that the need for correcting these outliers for turbidity effects is not critical because there may not be much of an impact from light attenuation. The same could apply to all the samples from both sites, as CBS samples have turbidity levels of < 11 NTU, while samples from NCG have turbidity levels of < 3 NTU. Future exploration on this relationship is beneficial to understanding effects turbidity on CDOM fluorescence emission intensity.

A more reasoned explanation of why some corrected data do not have a slope of zero is because an average temperature coefficient by site and fluorometer was applied rather than using specific coefficients of each sample. Perhaps by using sample-specific coefficients, the slopes can be closer to zero (Moore 2020). Another narrative for the skewed slopes may point to human error during the temperature quenching experiments. The outlier samples were analyzed when the process of method development for temperature fluorescence quenching was in progress. As mentioned previously, the minimization of human errors was attempted by omitting the data

points of these specific samples with temperatures $< 5^{\circ}\text{C}$. Other errors could possibly include smudging the cuvette or not wiping off the cuvette well enough.

Interestingly, corrected Cannonsville samples with higher CDOM concentrations, > 18 RFU, generally has a much higher discharge rate, > 900 csf (Figure 3.3), than the samples with lower CDOM concentrations. Samples of higher CDOM concentrations include November 25, December 16, December 30, January 13, and January 27, measured with both fluorometers (Figure 3.5). However, the January sample is an exception to the higher discharge rate observation. Its discharge rate is a little over 800 csf. Likewise, Neversink samples with higher CDOM concentrations, > 18 RFU, has the highest discharge rates compared to samples with lower CDOM concentrations, approximately > 250 cfs (Figure 3.4). These greater CDOM concentration samples are November 25, December 16, and December 30, which are measured with both fluorometers (Figure 3.6). It would be noteworthy to continue to assess more of this hydrological relationship with corrected CDOM concentrations, especially during a rising limb/storm event, as most samples were collected during a falling limb.

CDOM-DOC relationship

Nevertheless, corrected CDOM values strengthen the relationship between CDOM and dissolved organic carbon (DOC), as CDOM is often used as a predictor for DOC. A robust relationship can be indicative of the changes in the timing and the export of DOC during weather events and can provide information on the aquatic carbon cycle and budget. Fortunately, this relationship has been determined to be quite reliable (Spencer et al. 2012). However, as Spencer et al. (2012) observes, there are limitations to this relationship because in four atypical systems, there is a weak relationship between CDOM and DOC. These rivers experience substantial

impoundments or drain from the Great Lakes and are composed of photodegraded dissolved organic matter. Griffin et al. (2018) also finds that low-colored lakes have a weak CDOM-DOC relationship. Ultimately, these limitations should be taken into account when using CDOM as a proxy for DOC.

Although (Figure 3.7) reveals a highly correlated relationship with corrected CDOM data (from Cannonsville analyzed with the DEP fluorometer) and DOC, $r^2 = 0.97$, this is just the preliminary work because CDOM values were analyzed in the late fall/winter when CDOM values are typically at their lowest. In other words, the data in (Figure 3.7) is not reflective of the stream's annual organic matter concentration. Further research needs to be implemented to achieve a better understanding of the relationship in CBS and expand this work into NCG. It is recommended that research should further investigate seasonal changes by analyzing data in the spring, summer, and early fall season, as well as research over several years to get an understanding of the contrast between wet and dry years (Moore 2020).

Shelf life

CBS and NCG samples collected on November 25 and December 9, 2019 indicate sample degradation over a holding time of 72 and 58 days, respectively (Figure 3.7). However, the degradation of samples may be considered negligible, as most samples have approximately a maximum 2 RFU difference. For instance, corrected NCG November samples detected 21.75 RFU at $\sim 20^\circ\text{C}$ while the reanalysis detected 23.41 RFU. This is a difference of about 2 RFUs, with an increased CDOM signal of 7.63%. A more significant difference are the changes between the original November and December NCG samples. The November sample measured 21.75 RFU at $\sim 20^\circ\text{C}$, while the December sample measured 10.41 RFU, with a signal reduction

of 52.14%. Similarly, the original CBS November sample, measured 22.28 RFU at ~20°C and the CBS December sample measured 14.37 RFU, with a signal reduction of -35.5%. These drastic reductions in CDOM concentrations over a timeline of two weeks are of more interest to continue studying. It indicates how dynamic organic composition can be within a stream system, further stressing the appeal of using CDOM as a proxy for DOC, as real-time DOC monitoring is expensive (Griffin et al. 2018).

ATP Analysis

An ATP test was conducted on four samples; two from Cannonsville and two from Neversink, each collected on November 25, and December 9, 2019. All samples were analyzed on December 11, 2019. The ATP assay provides a sense of the microbial activity and possibly the quality of the organic matter. On average, Cannonsville has higher microbial activity, 104.205 ± 56.08 , while Neversink has a mean of 67.48 ± 28.45 (Table 3.2). This may reflect the characteristics of the Cannonsville watershed, as there is a greater population density, agricultural activity, and number of wastewater treatment plants compared to the Neversink watershed. However, it is important to recognize the restrictions of these results as there were only a few samples measured. Continued research with the ATP assay is necessary to have a more definitive result and analysis. This work may be compelling to conduct because the tests to gather information on the microbial activity and quality of the water samples are relatively quick to perform (~10 minutes) and inexpensive (\$12/sample) (Moore 2020).

Table 3.2. ATP tests results for each sample analyzed.

Matrix	Sample Date	Date Analyzed	ATP Results
Cannonsville	November 25, 2019	December 11, 2019	64.55
Cannonsville	December 9, 2019	December 11, 2019	143.86
Neversink	November 25, 2019	December 11, 2019	87.60
Neversink	December 9, 2019	December 11, 2019	47.36

Conclusions

Possible refinements to the temperature quenching evaluation

Limitations to this research during laboratory experiments include the fact that samples in the cuvette were not continuously agitated throughout the experiment. By including these components to the experiment, the added steps would give greater assurance that measurement error was reduced. However, given the logistics of handling small volumes of water that are temperature-controlled, measurement error is unavoidable. Furthermore, due to the limited time for this project, samples were only analyzed during the late fall/winter season. If this research could be continued into the spring, summer, and early fall, valuable information could be attained to gain a broader perspective on seasonal effects on temperature compensation.

Sample and site differences in the temperature coefficient

Current literature does not have clear recommendations on how often CDOM measurements should be made to establish suitable temperature correction factors. Watras et al. (2011) advises that temperature coefficient is site and fluorometer specific, while Ryder et al. (2012) and Saraceno et al. (2012) suggest that temperature coefficient varies over time and

throughout events, such as storms, in the same body of water. This study indicates that, within the same sites, there are variations based on sample collection with regards to the river hydrology (Figures 3.3 and 3.4). To further investigate this phenomenon, grab samples should be collected during storm events. In addition, site differences between Neversink and Cannonsville watersheds can be further investigated with intensive sampling throughout various seasons (Moore 2020).

Contrasts between fluorometers with different calibration standards

Turner Designs, the manufacturer of the Aquafluor Handheld fluorometers used in this study, advises the usage of quinine sulfate as the solution for instrument calibration for the CDOM channel (Henderson 2020). However, some researchers use rhodamine dye as the calibration standard and may be prompted to do so over quinine sulfate because quinine sulfate is not shelf stable. Rhodamine dye is only recommended as a calibration standard for the chlorophyll and phycocyanin channels. As previously stated, DEP's fluorometer was calibrated using quinine sulfate while Bard's fluorometer was calibrated with rhodamine dye. Interestingly, the average temperature coefficients of the two fluorometers had negligible differences, despite differences in calibrations. However, there are clear differences in the units of the fluorometer, as Bard's fluorometer is scaled from 0 to 1 RFU while DEP's fluorometer is scaled from 0 to 100 RFU. To compare samples on a different scale, samples were ranked from high to low fluorescence. This allowed comparable results from Bard's fluorometer, even though non-recommended calibrations standards were used. To further support these comparisons, supplementary sample testing over a wide range of organic matter concentration and composition would need to be conducted (Moore 2020).

Chapter 4: Recommendations for the Saw Kill Monitoring Program

Disinfection byproducts are a local, regional, and global issue. Although DBPs are of concern, the usage of disinfectants on the water supply cannot be compromised. Disinfectants like chlorine protect us from harmful pathogens, viruses, and bacterial diseases (CDC 2016). This study analyzes the precursors of DBPs in the Saw Kill, and then evaluates the measurement of CDOM, which is a proxy for DBPs. This paper will conclude by connecting the results of temperature effects on CDOM fluorescence emission intensity back to the Saw Kill Monitoring Program (SKMP). Thus, recommendations for the SKMP will be advised in efforts to improve the monitoring of CDOM via fluorometry of the Saw Kill.

To recap, the CDOM channel on the AquaFluor HandHeld Fluorometer from the Bard Water Lab should be calibrated using quinine sulfate instead of Rhodamine WT, as recommended by Turner Designs. The excitation and emission signals from Rhodamine WT (Ex: 530 +/- 25nm and Em: ≥ 570 nm) are not in alignment with the excitation and emission signals of the CDOM channel (Ex: 350 +/- 40nm and Em: ≥ 420 nm). Additionally, Watras et al. (2011) finds that as temperature increases, CDOM fluorescence emission intensity decreases, and recommends using the following equation to correct for temperature effects:

$$\text{CDOM}_r = \text{CDOM}_m / [1 + \rho(T_m - T_r)].$$

In this equation, T is temperature ($^{\circ}\text{C}$), ρ is the temperature-specific coefficient of fluorescence ($^{\circ}\text{C}^{-1}$), and the subscripts r and m are the reference and measured values (Watras et al. 2011).

Watras et al. (2011) explains that the temperature coefficient is calculated by “slope/intercept”

and it is site and fluorometer-specific. Furthermore, Downing et al. (2012) encourages the correction of CDOM for light attenuation due to suspended particles, in addition to correcting for temperature effects.

The SKMP does not correct for temperature effects on CDOM. For this reason, Chapter 2's explorations of the seasonal variability in Figure 2.4 may not be reflective of the true CDOM levels throughout the years as temperature is a confounding factor. When analyzing raw CDOM data of the Saw Kill over various seasons that have temperature changes, the data may be misleading (Downing et al. 2012). More specifically, there is uncertainty around determining the cause of the CDOM peak in fall 2018 as it could be derived from temperature or seasonal effects. In addition, perhaps CDOM concentration may have also peaked in summer 2018 but was not detected by the fluorometer given that higher temperature reduces CDOM emission signals.

In efforts to establish a more robust dataset of the Saw Kill, the monitoring program is recommended to correct CDOM for temperature effects using the equation provided by Watras et al. (2011). It may not be of great concern to allocate resources to correct for turbidity as well, accounting for the fact that the Saw Kill has low concentrations of turbidity. To achieve the goal of temperature compensation, temperature fluorescence quenching experiments should be run on samples from sites along the Saw Kill on a seasonal basis, following the protocol I created with the NYC DEP (see Appendix F). It is important to analyze sites across all seasons to gain an awareness of the seasonal effects on temperature compensation. When determining a suitable temperature coefficient for the Saw Kill, the monitoring program should be aware that extreme weather events, such as storms (Ryder et al. 2012; Saraceno et al. 2012), and sample collection in relation to river hydrology (Chapter 3) will have an impact on the temperature coefficient within the same water body. Some variables that should be contemplated are if temperature correction

should be applied on a seasonal scale (e.g. only during the fall) or on a monthly basis when samples are collected and processed. Ultimately, the goal is to figure out what is suitable for the Saw Kill.

Appendix

A. SKMP Sampling Protocol

Bard Water Lab

Water Sampling Protocol

TO BEGIN:

- YOU MUST WEAR GLOVES and use a new pair at each site.**
- During the process, maintain sterile conditions and use aseptic technique – do not leave caps off for any period of time, work quickly and carefully.**
- Never go sampling alone**

1. Fill out site sheet for the current site location.
2. Use aseptic technique. Wearing a new pair of gloves for each site. Take out the sampling bottle for the correlating site.
3. Rinse sampling bottle with site water 3 times. Fill the bottle 1/3 of the way with water. Recap and shake to rinse. Dump “used” water on side of stream or grass to avoid mixing sediment into the water column.
4. On the fourth time fill bottle, try to fill all the way leaving minimal air space.
5. If you are using a dipper or bucket they should be rinsed 3 times as well before collecting the sample.
6. Close the bottle tightly and place into the cooler backpack with icepacks. Keep it out of direct sunlight and high temperatures for the duration of the field work.
7. Use the YSI probe to measure dissolved oxygen content, conductivity, etc. of the water and record the results. The probe should be placed into the water up to the base where the cord is connected. After approximately 30 seconds, press Enter and record the data set number on the screen.
8. Return the water samples to the Bard Water Lab as soon as possible after collection. This is important for ensuring optimal data and reliable results.

B. SKMP Turbidity Protocol

Bard Water Lab

Turbidimeter Protocol

Materials

- Hach Turbidimeter 2100Q
- Glass Vessel
- Silicone Oil
- Lint Free Cloth

1. Invert your sample three times to be sure no settling has occurred.
2. Fill a clean sample cell halfway with sample cap it, shake and dump out. Repeat 3x.
3. Fill a clean sample cell to the line (~15mL) with sample and cap it.
4. Use a lint-free cloth to wipe down the cell and remove any water spots and fingerprints.
5. Apply one drop of silicone oil (as needed). Wipe with a soft cloth until there's an even film over the entire cell's surface.
6. Insert the cell into the turbidimeter compartment so that the triangular orientation mark aligns with the raised mark in front of the compartment.
7. Close the compartment, press **READ** and record the turbidity in NTU.
8. Empty the cell of the sample, carefully rinse the cell with tap water and return to step 1 for the next sample.

Quality Control Notes:

1. Blank: run one blank sample (using autoclaved DI water as "sample") during each sampling run. Record the turbidity reading.
2. Positive control: run a duplicate sample for Site #2 (2A, 2B) during each sampling run. Record the turbidity reading.
3. If the sample is highly turbid, you may need to perform a dilution and re-read the turbidity. First try a 1/10 dilution (2 ml sample + 18 ml DI water).

Updated May 2020

C. SKMP Turbidity Protocol

Bard Water Lab

Fluorometry Protocol

Materials

-Two Turner Aquafluor set to measure: Chlorophyll a, Phycocyanin, Optical Brighteners, and Color Dissolved Organic Materials

-Plastic Turner Cuvette, check that there are no marks or scratches

-Lab wipes

-DI Water for rinsing cuvette

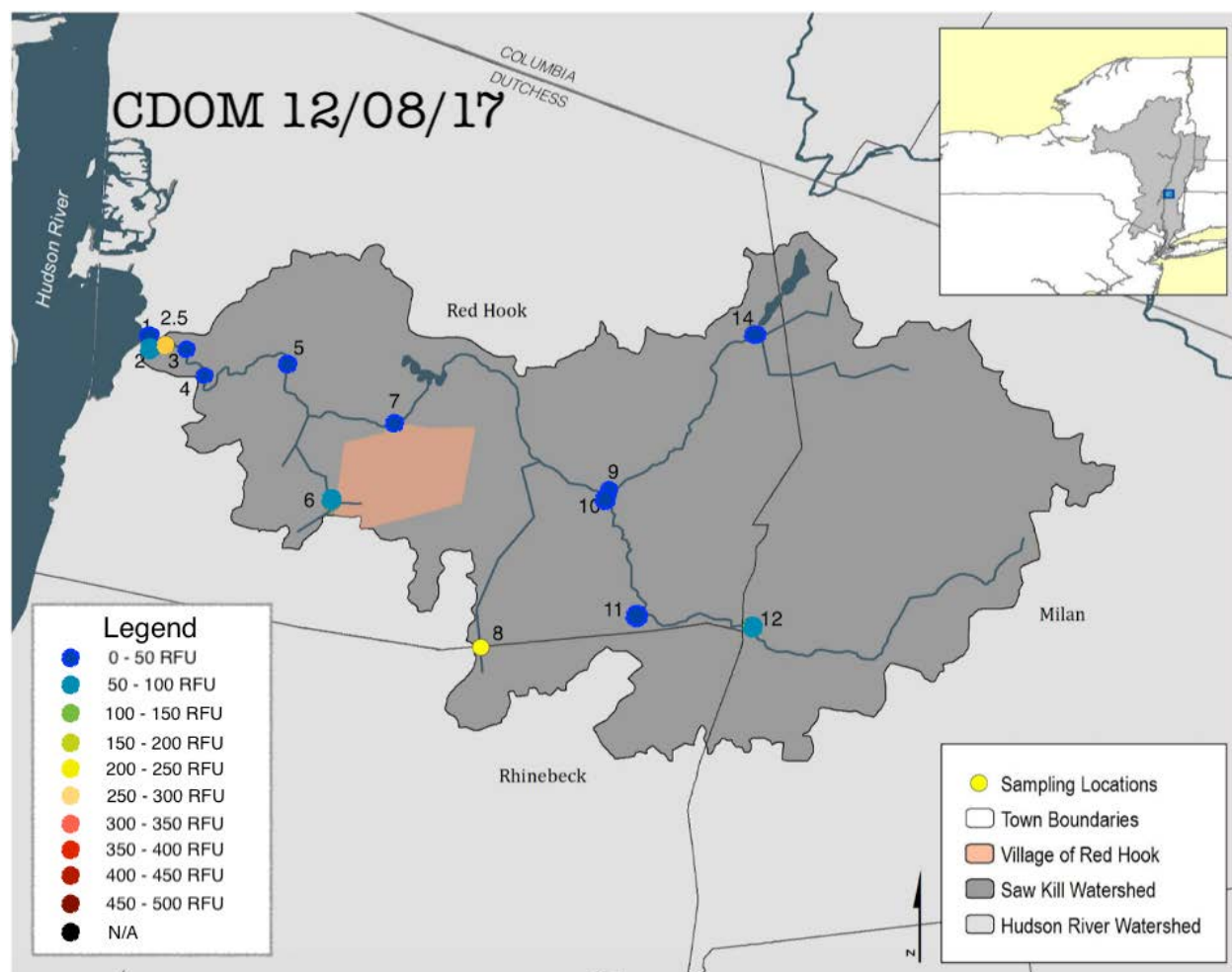
1. Select the correct Aquafluor fluorometer to measure your parameter; each fluorometer is only set up to measure 2 of 4 parameters. One Aquafluor measures Phycocyanin (channel A) and CDOM (channel B), while the other measures optical brighteners (channel A) and Chlorophyll (channel B). Check this by turning on the device and pressing the <A/B> button, which will show you the parameters it measures.
2. Turn on the fluorometers by pressing the <ON/OFF> button, and wait at least 5 seconds for the instruments to boot up.
3. Using gloves, obtain a plastic cuvette (**NO GLASS CUVETTES**), making sure that the outer surfaces are clean and free of noticeable scratches or marks. **Check for the sharpie mark on the rim of the cuvette; make sure to insert the cuvette with this side facing you for every reading.**
4. **Run one blank sample FIRST (using DI water) for all 4 channels before measuring the other samples.**
Follow the instructions below and repeat steps 5 -14 for each sample.
5. Rinse the cuvette with DI water **3 times**.
6. Gently agitate your water sample to re-suspend any particles that have settled to the bottom.
7. Rinse the cuvette with your sample **3 times**, then fill the cuvette until it is $\frac{3}{4}$ full (DO NOT fill the cuvette to its maximum volume).
8. Gently clean off any smudges or liquid droplets from the outside of the cuvette with a lab wipe.
9. After opening the small hatch to the sample bay, place your sample into the fluorometer, **making sure not to spill any of the contents of the sample into the interior of the device. If a spill occurs, quickly invert the device and immediately let a member of the BWL know.**
10. Select your desired parameter to measure using the <A/B> button.
11. Press either of the two <READ> buttons, and record the measured parameter in RFU.
Make sure to measure all 4 parameters (Chla, PC, OB, and CDOM) for each sample.
12. Empty the cuvette and start at step 5 to measure the next sample.
13. **Finally, read one more blank sample after all of the other samples have been measured.**

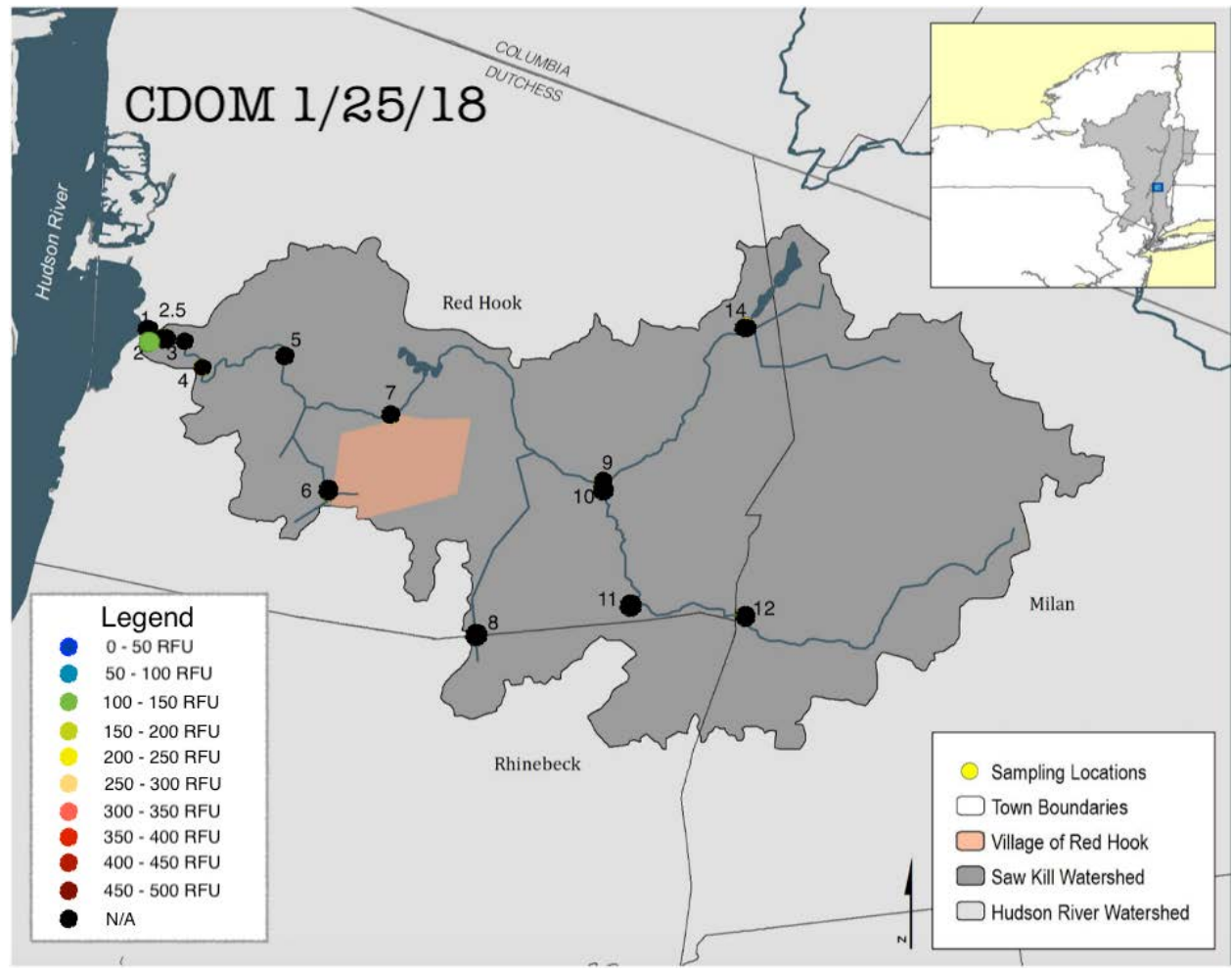
IMPORTANT NOTES:

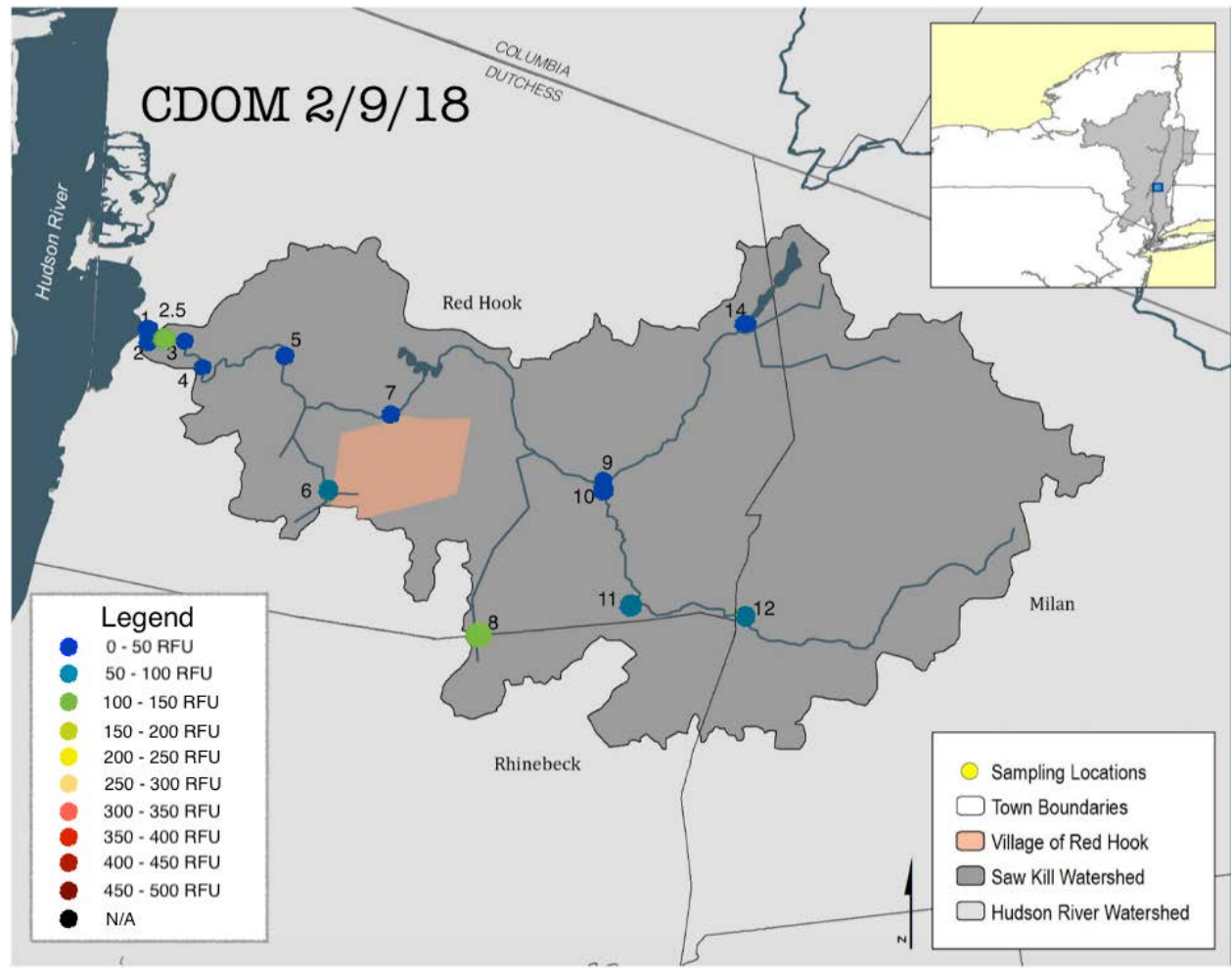
- Positive control: Measure the Site 2 sample twice (2A, 2B) for each parameter to provide an indication of instrument variation.
- If your cuvette becomes too dirty or scratched, you may discard it and take a new one. However, you **MUST run another blank for all 4 parameters before proceeding to the next sample**. This allows us to account for variability between cuvettes.
- Follow this same protocol for running filtered fluorometry samples.

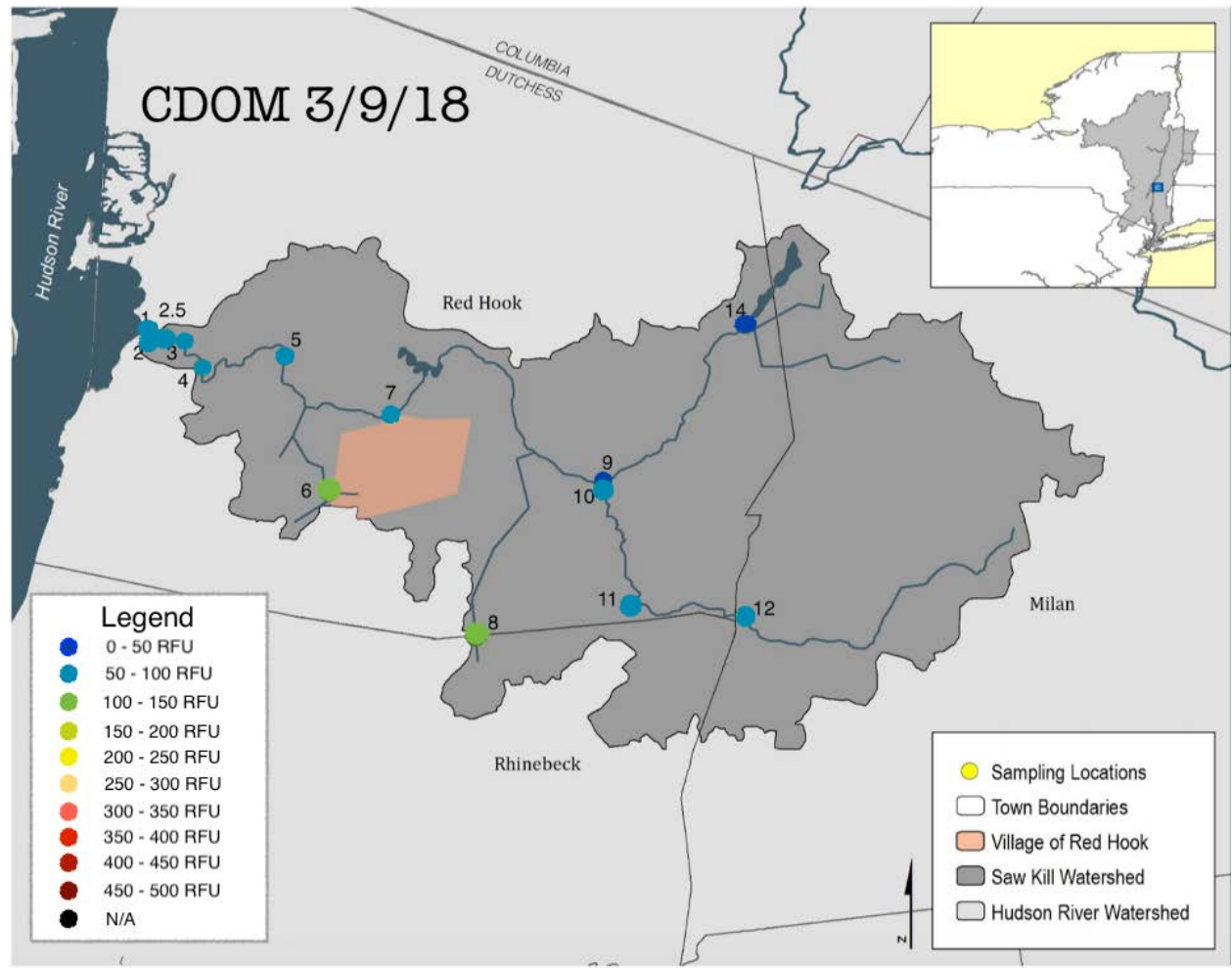
D. Flipbook of CDOM concentrations in the Saw Kill from 2017 to 2019

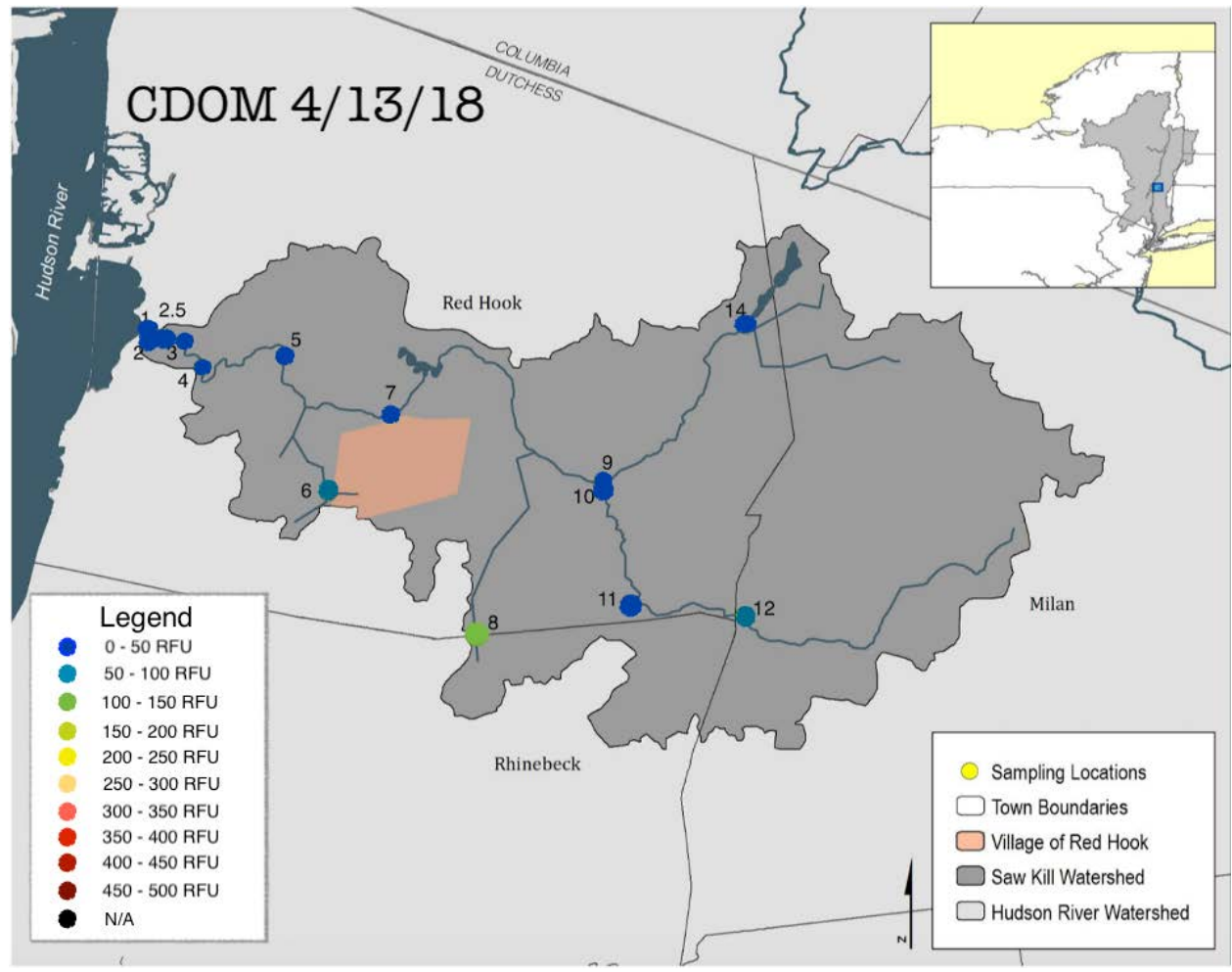
All maps in this flipbook are modified from (Riverkeeper, n.d.).

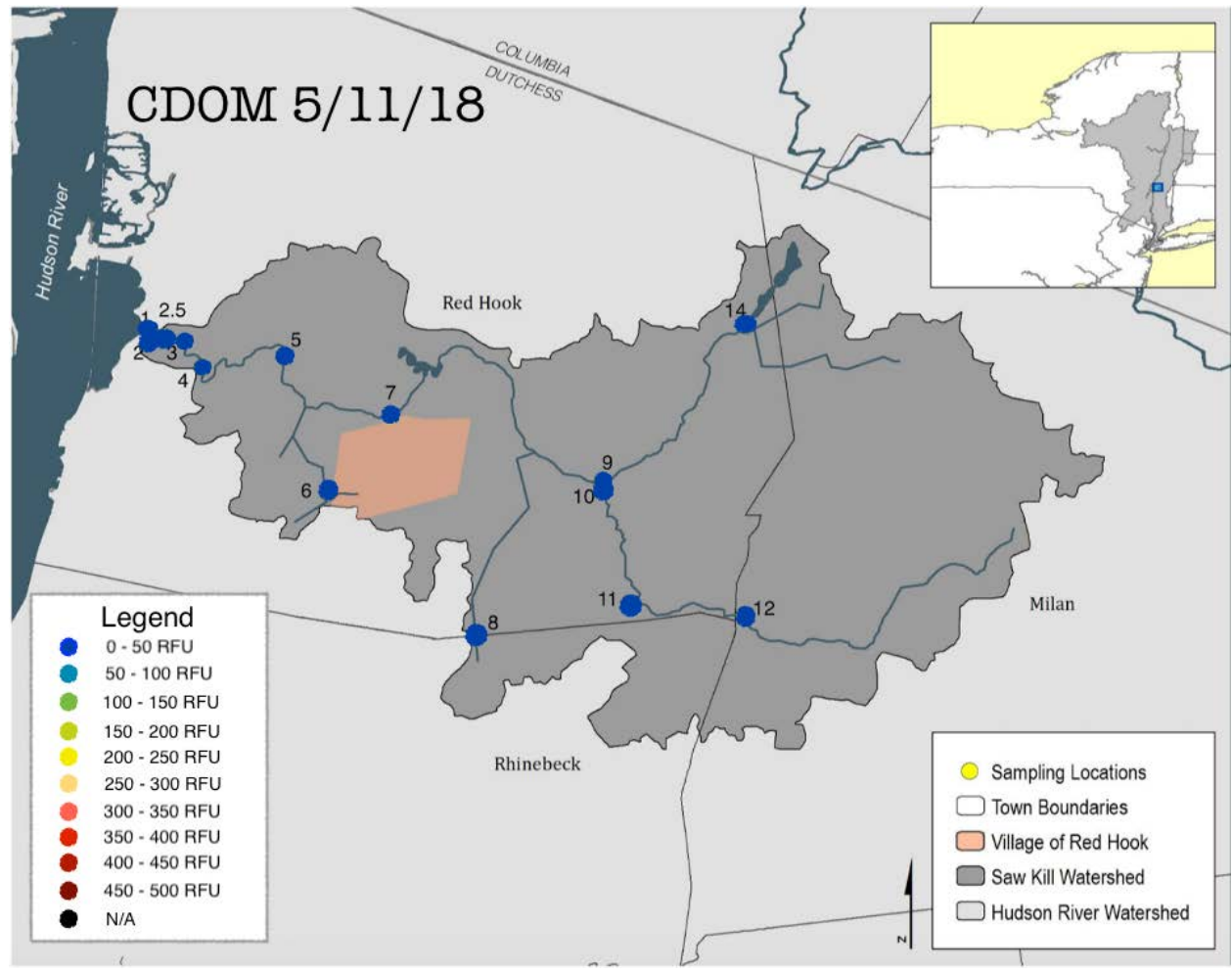


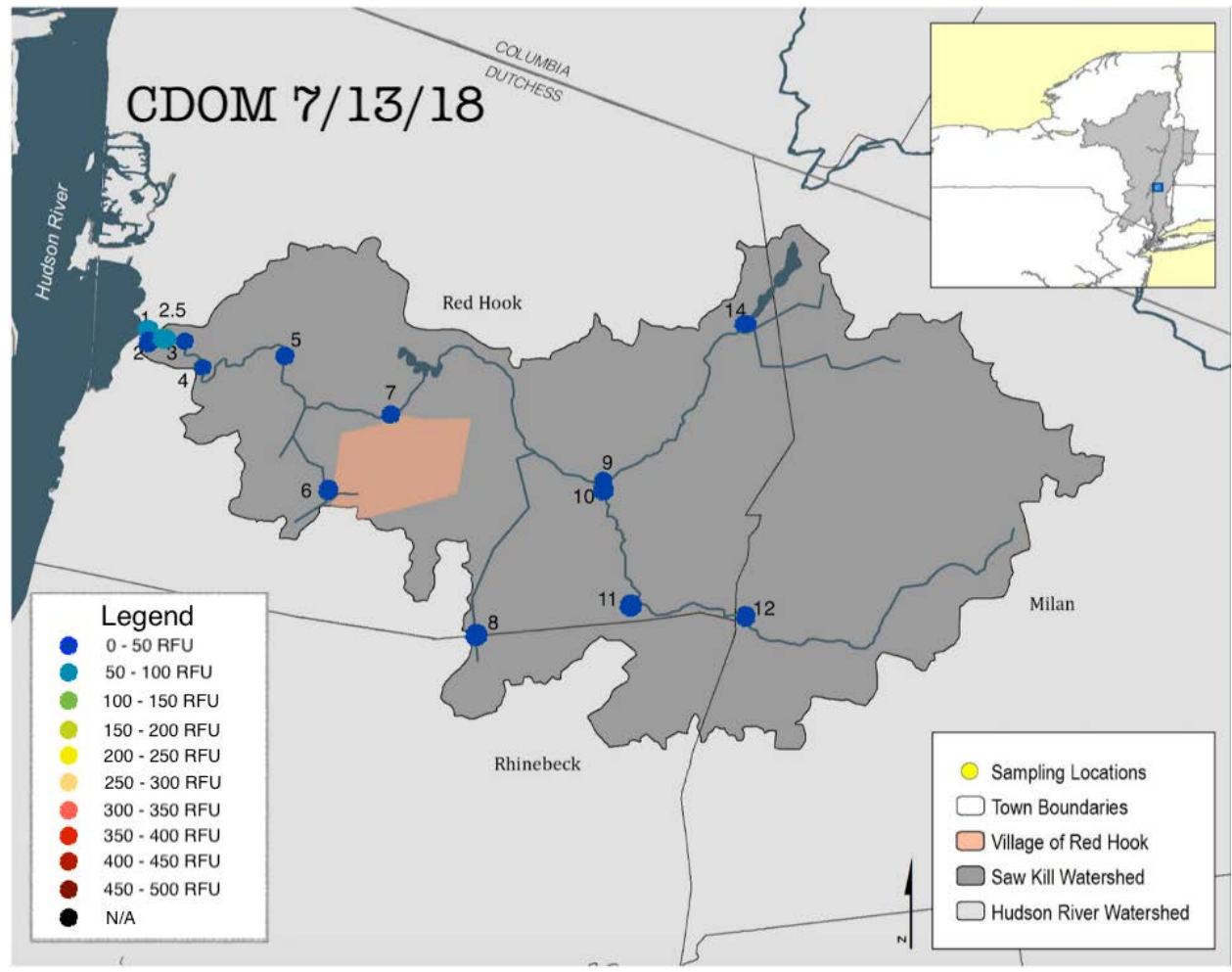


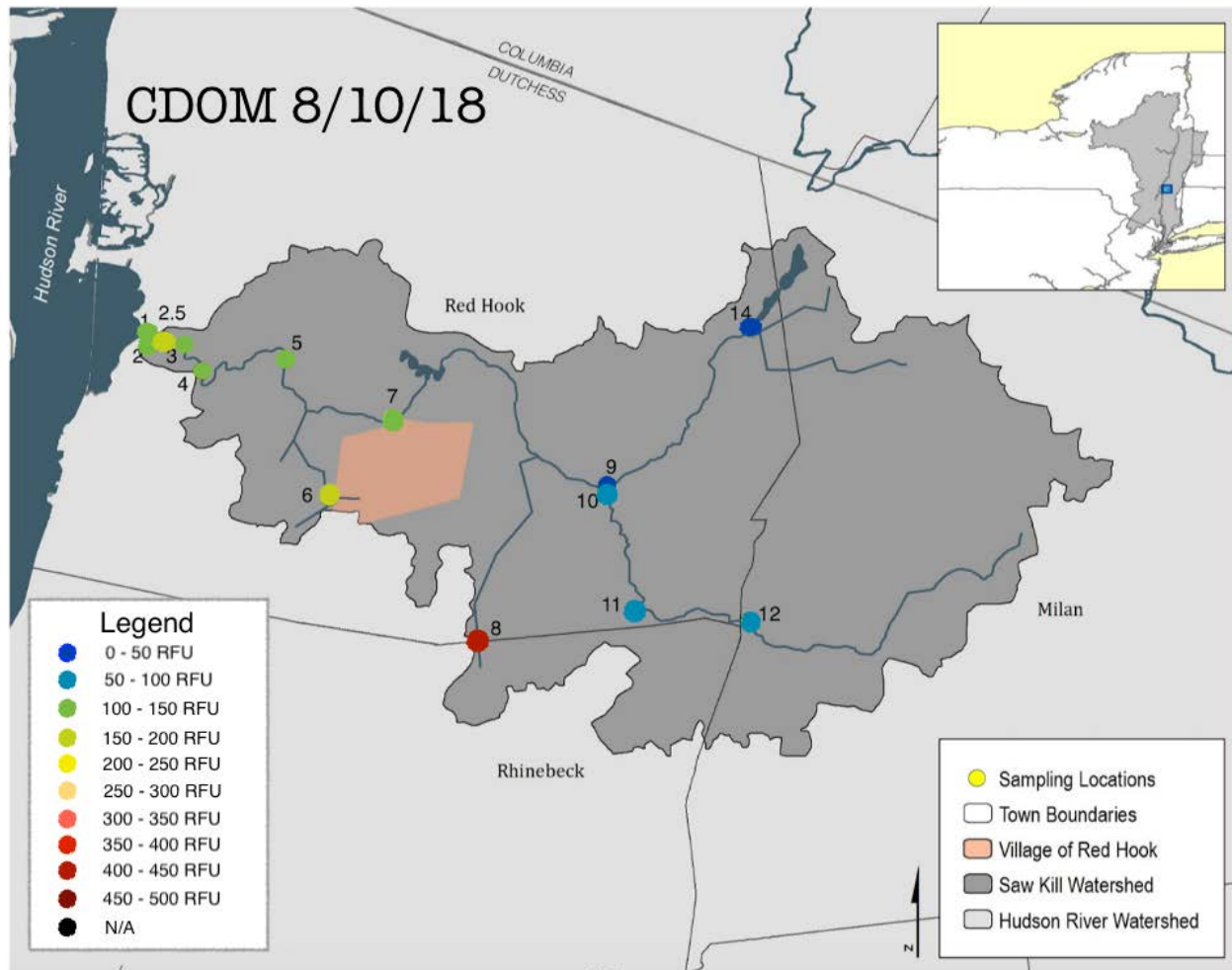


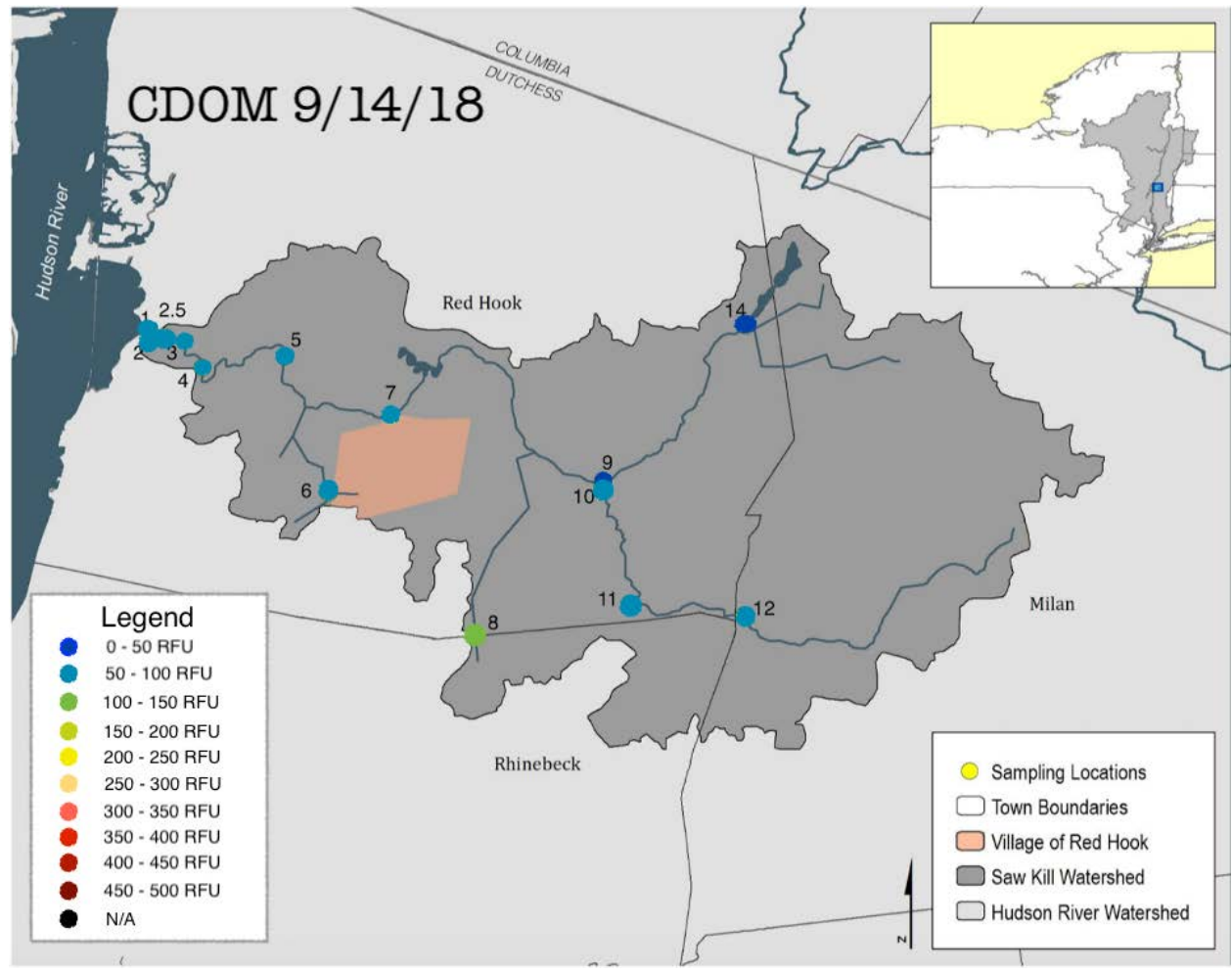


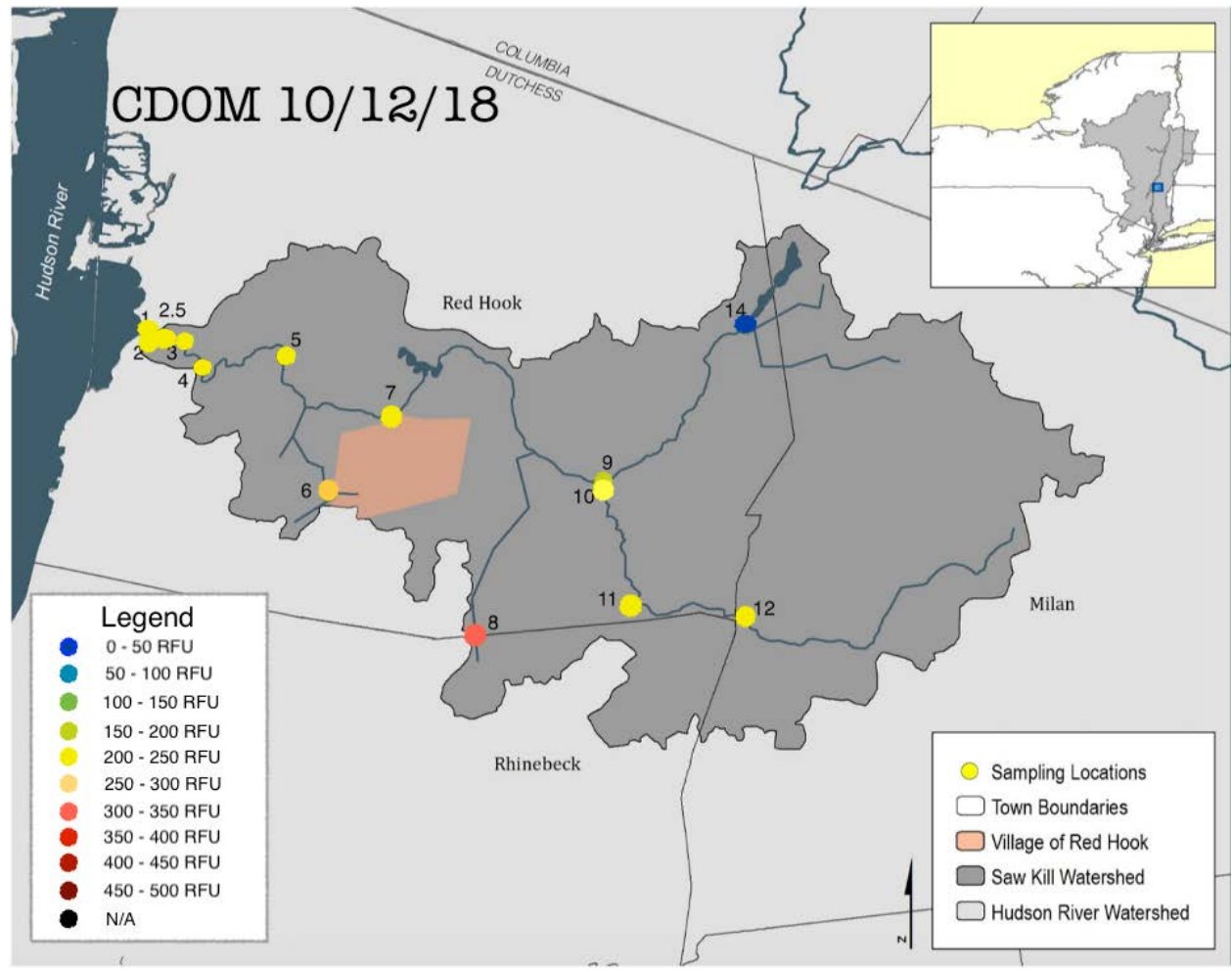


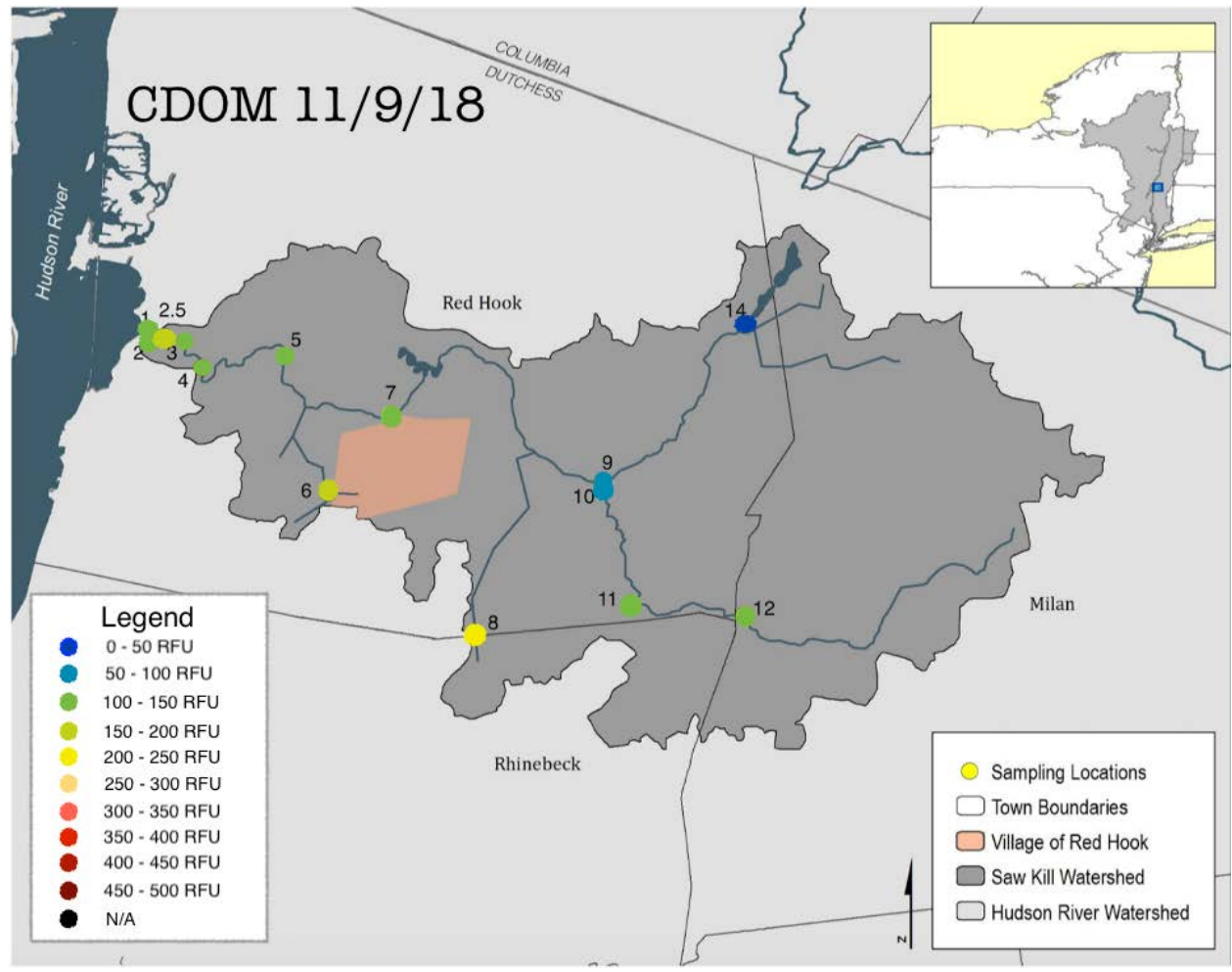


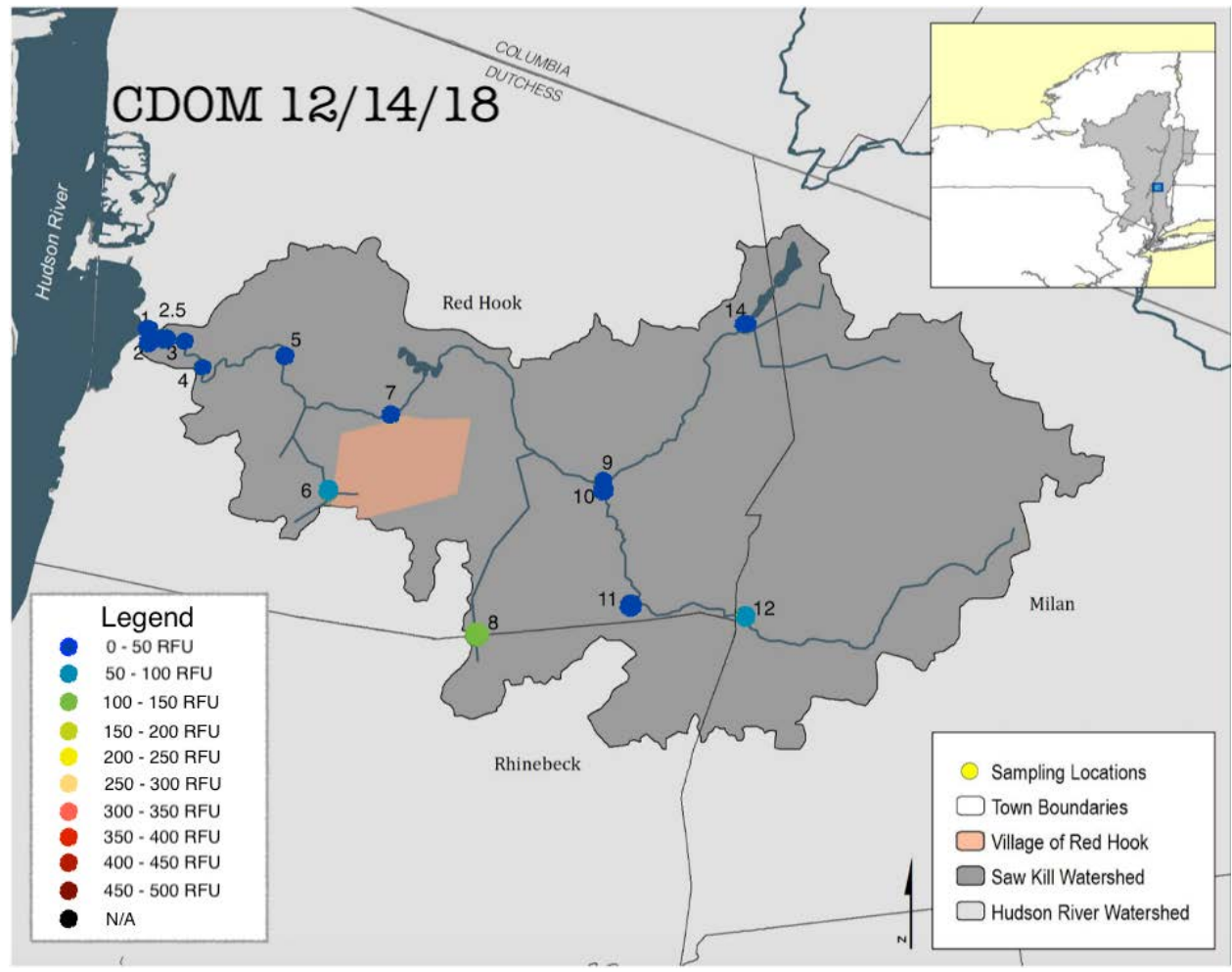


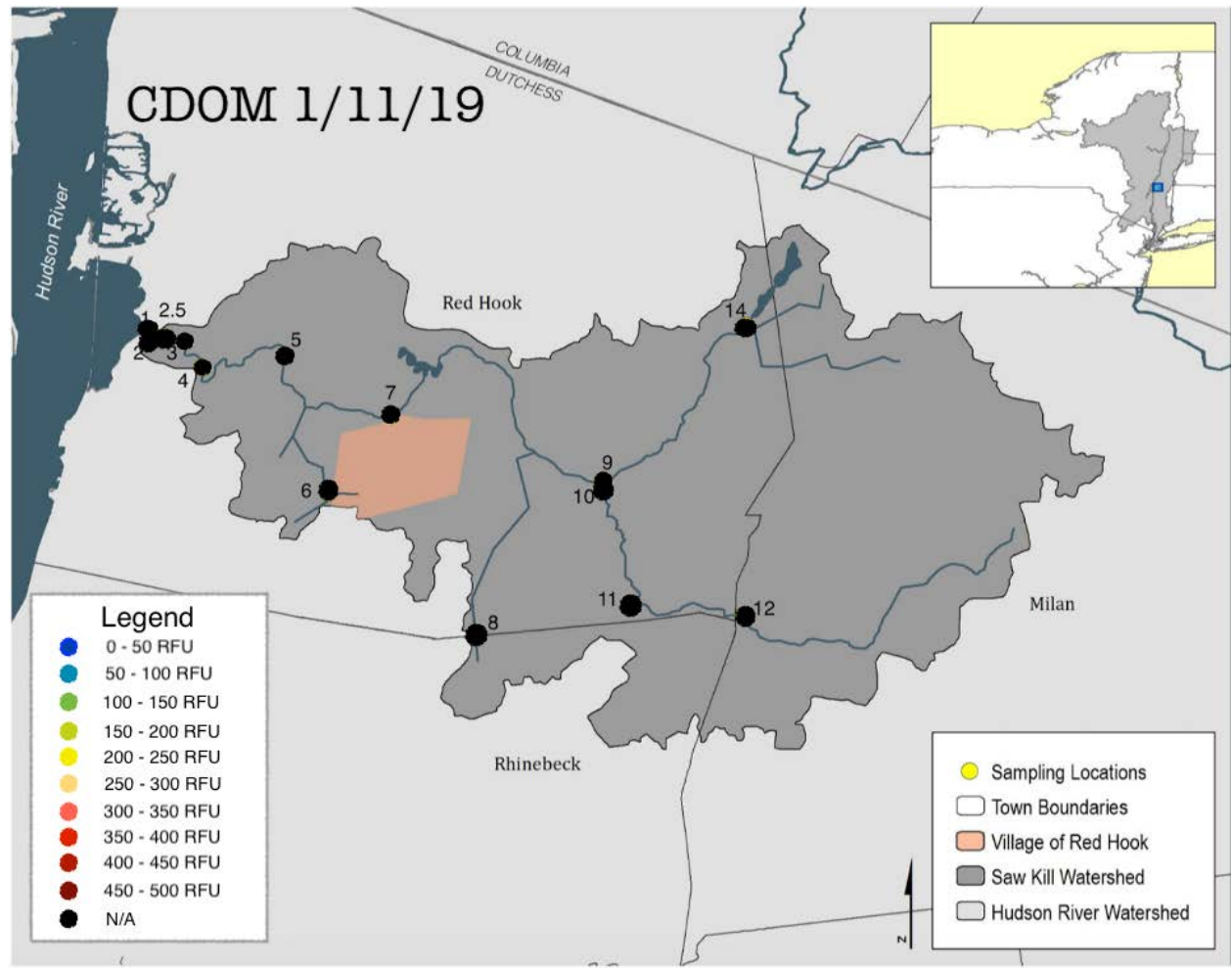


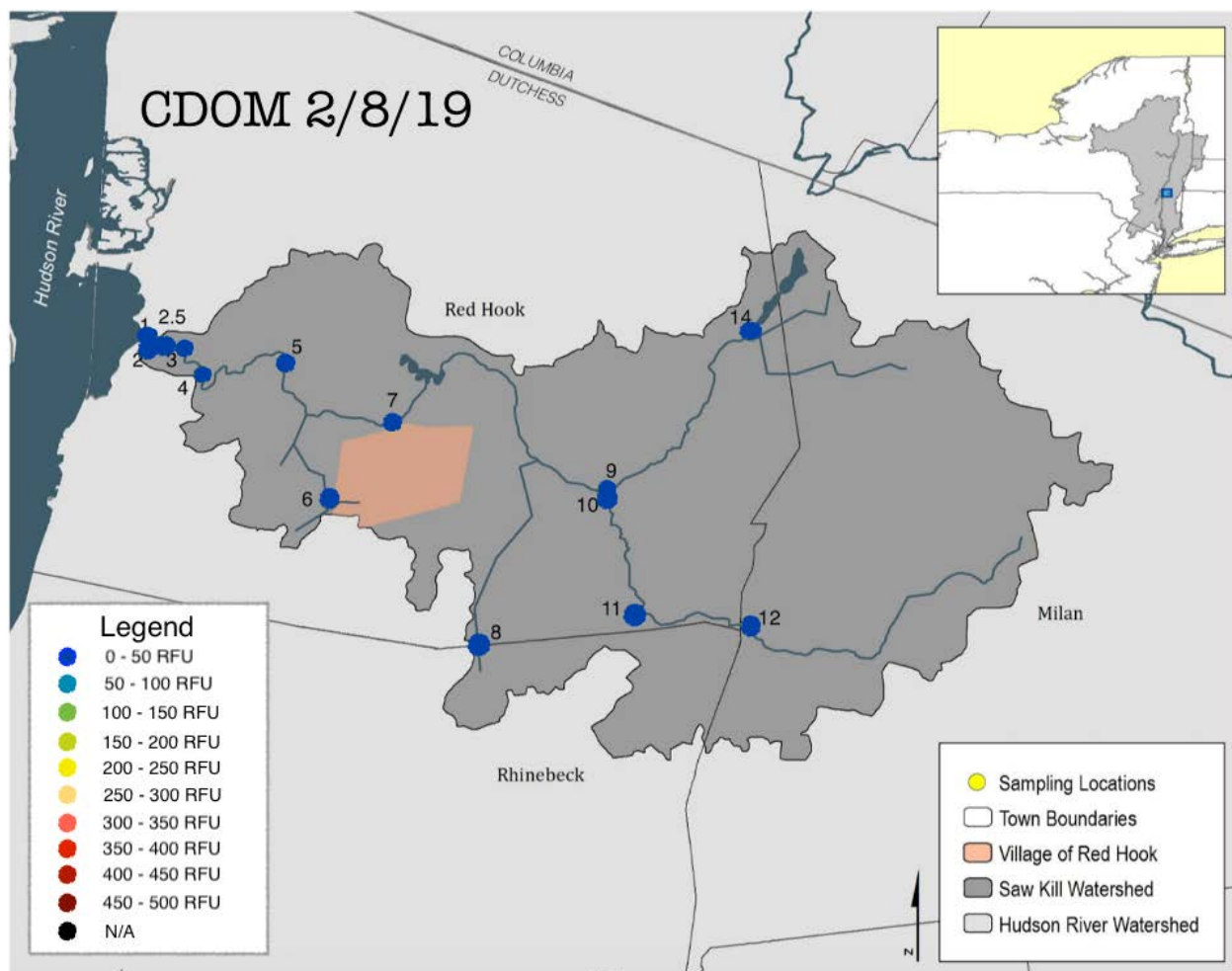


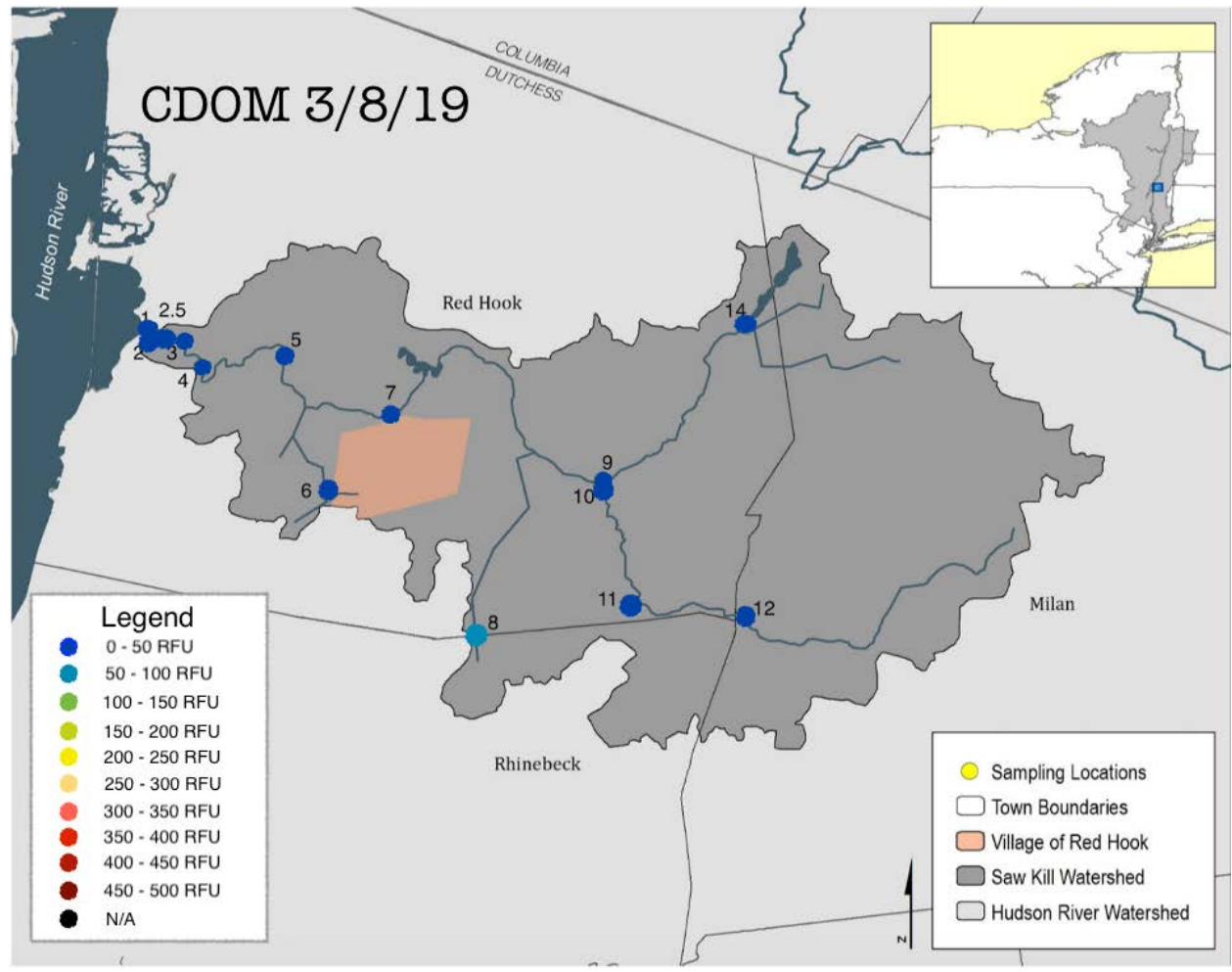


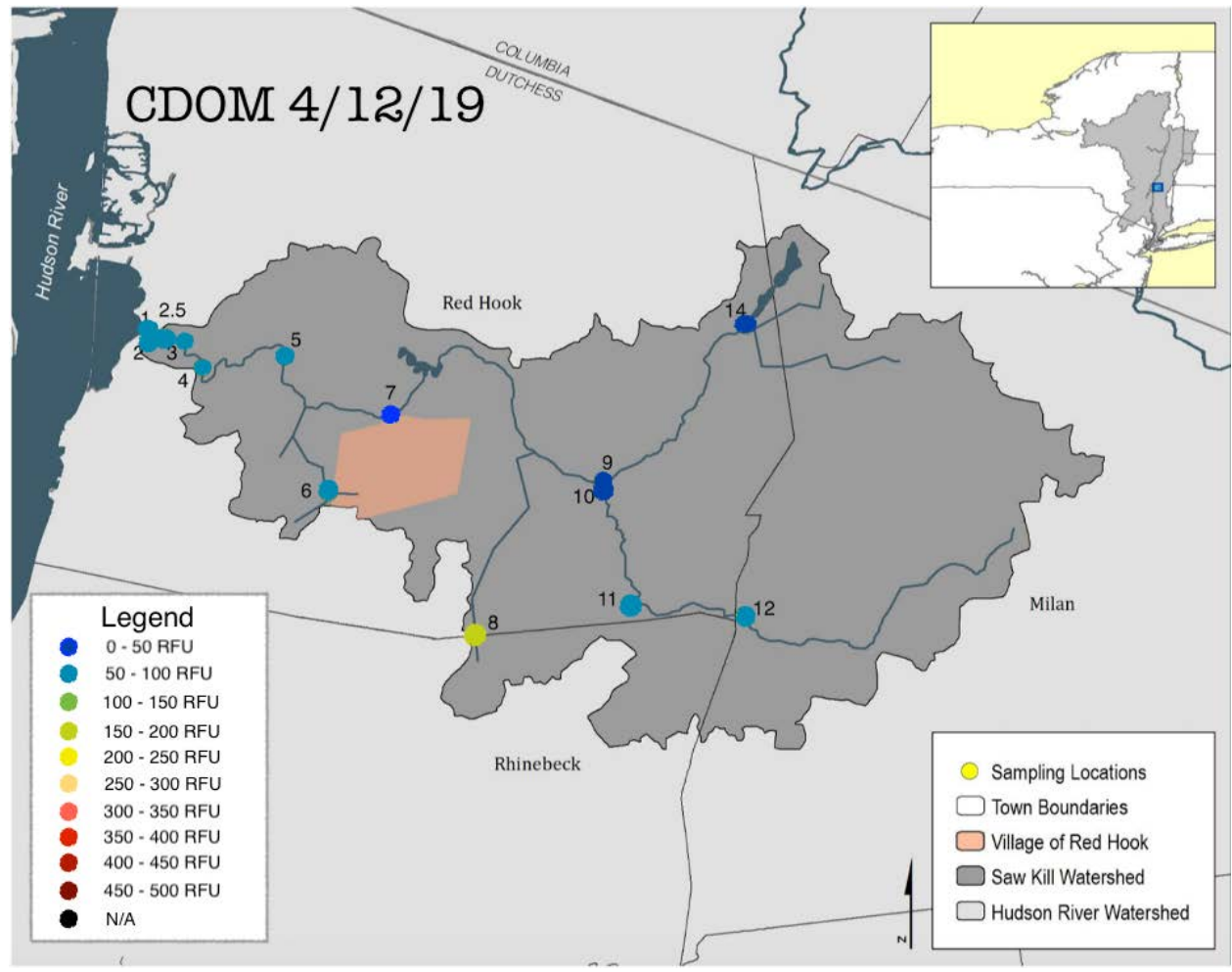


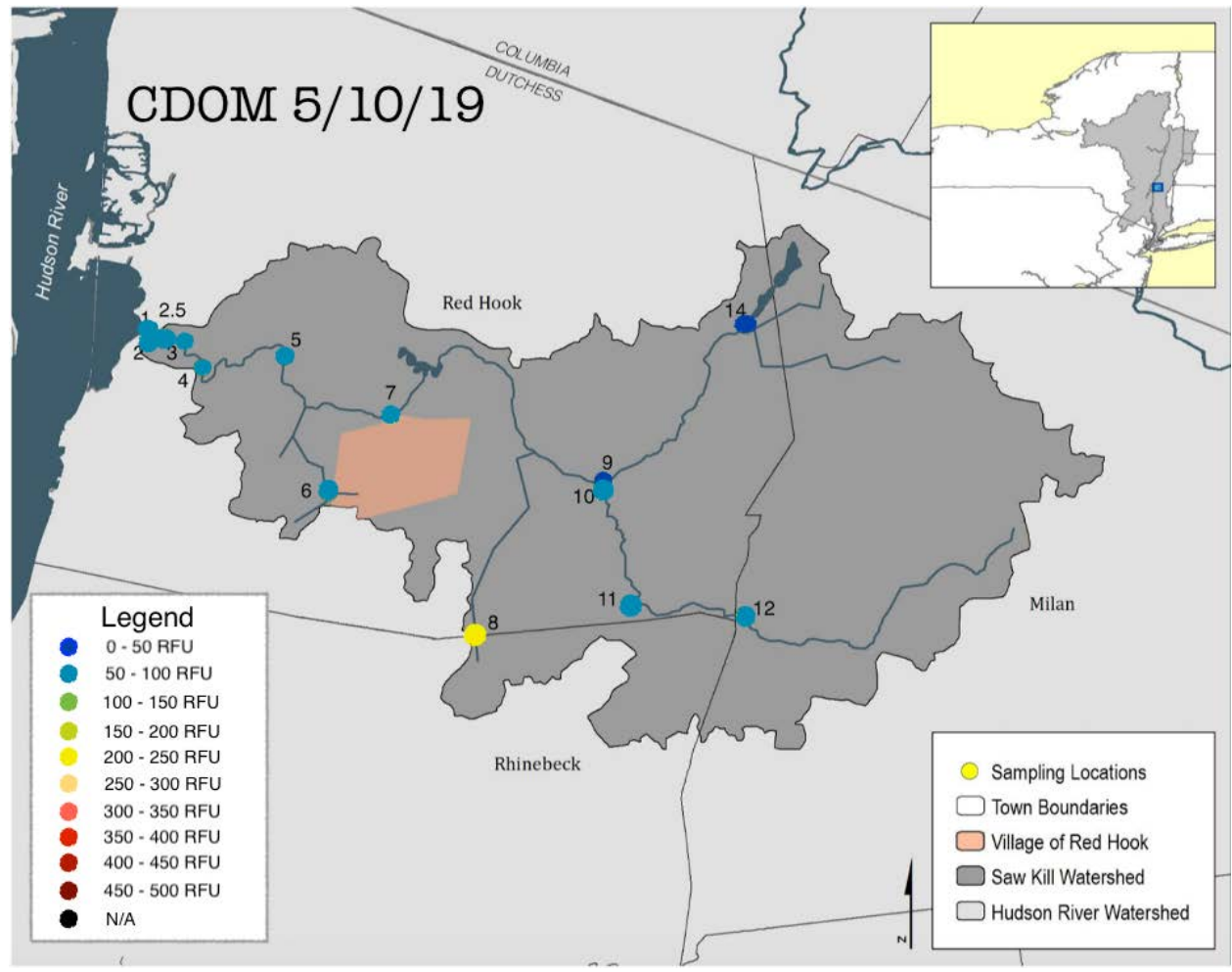


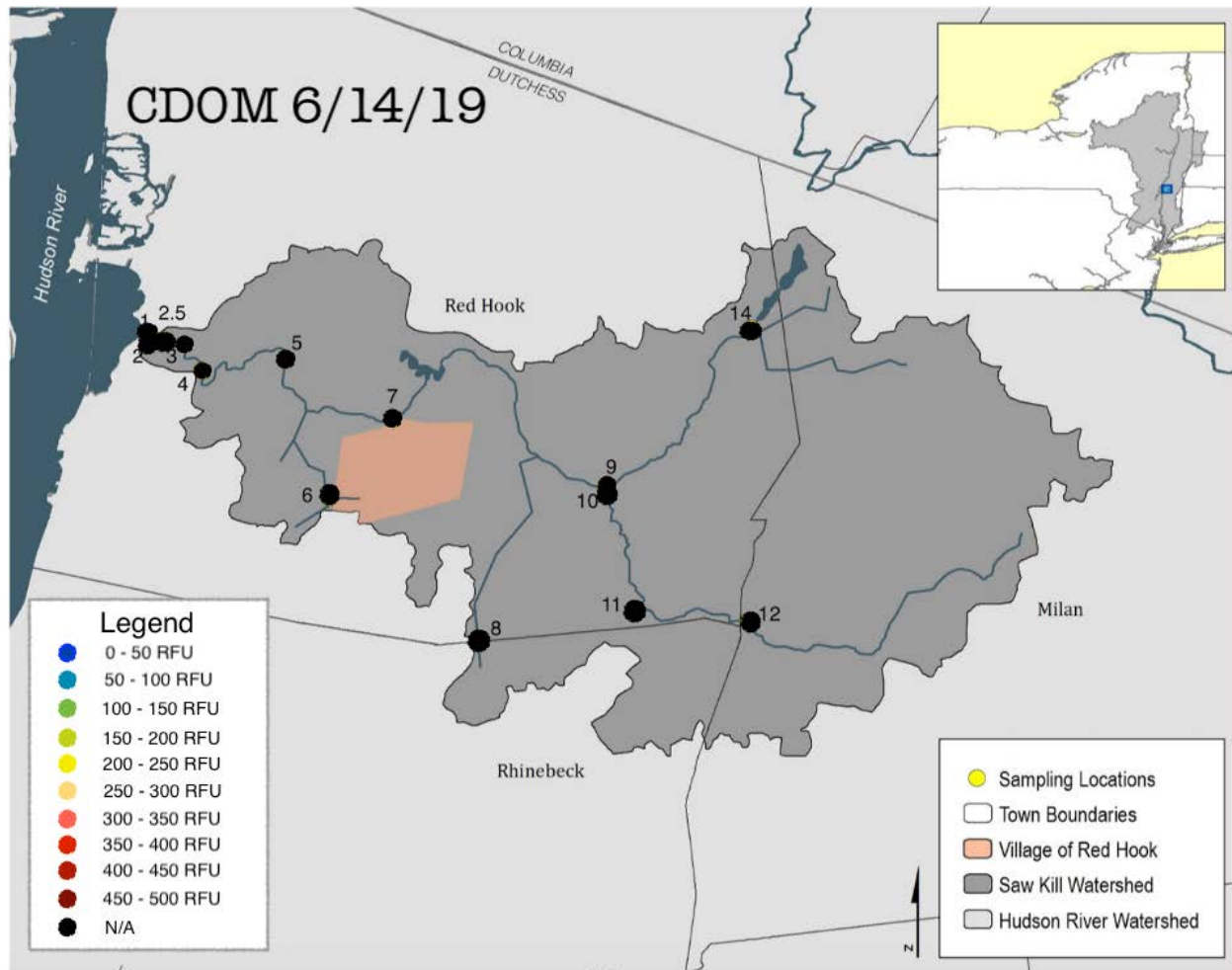


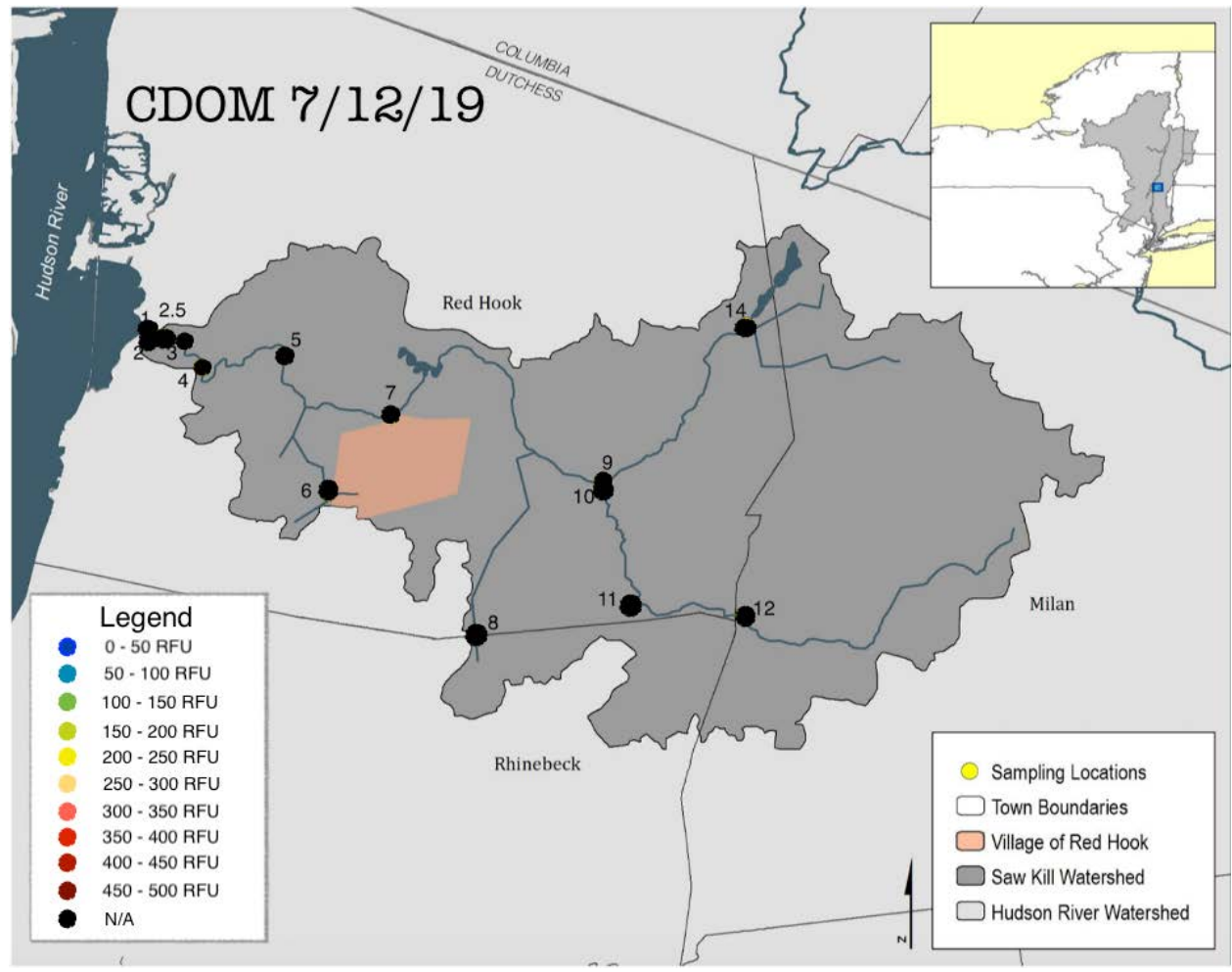


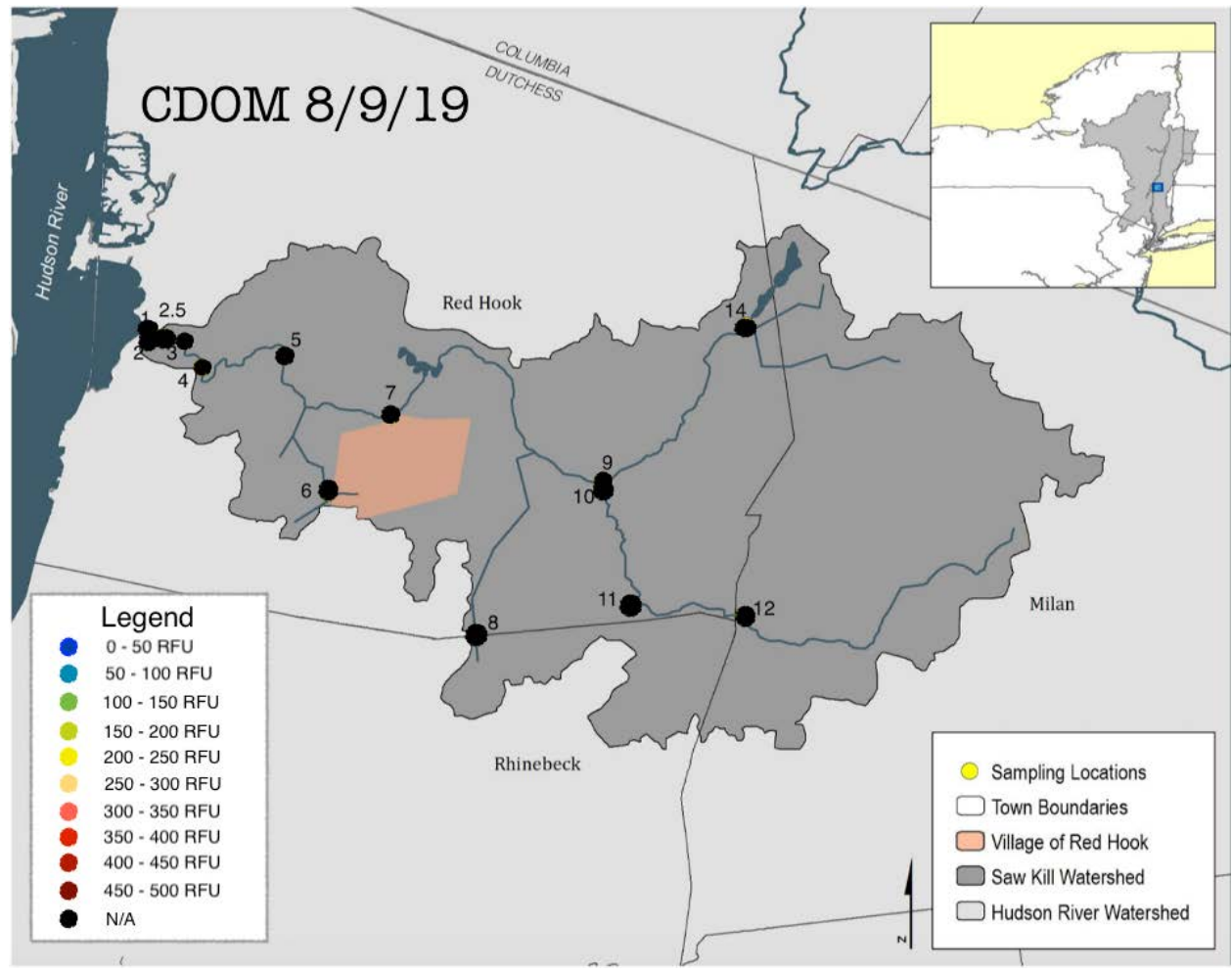


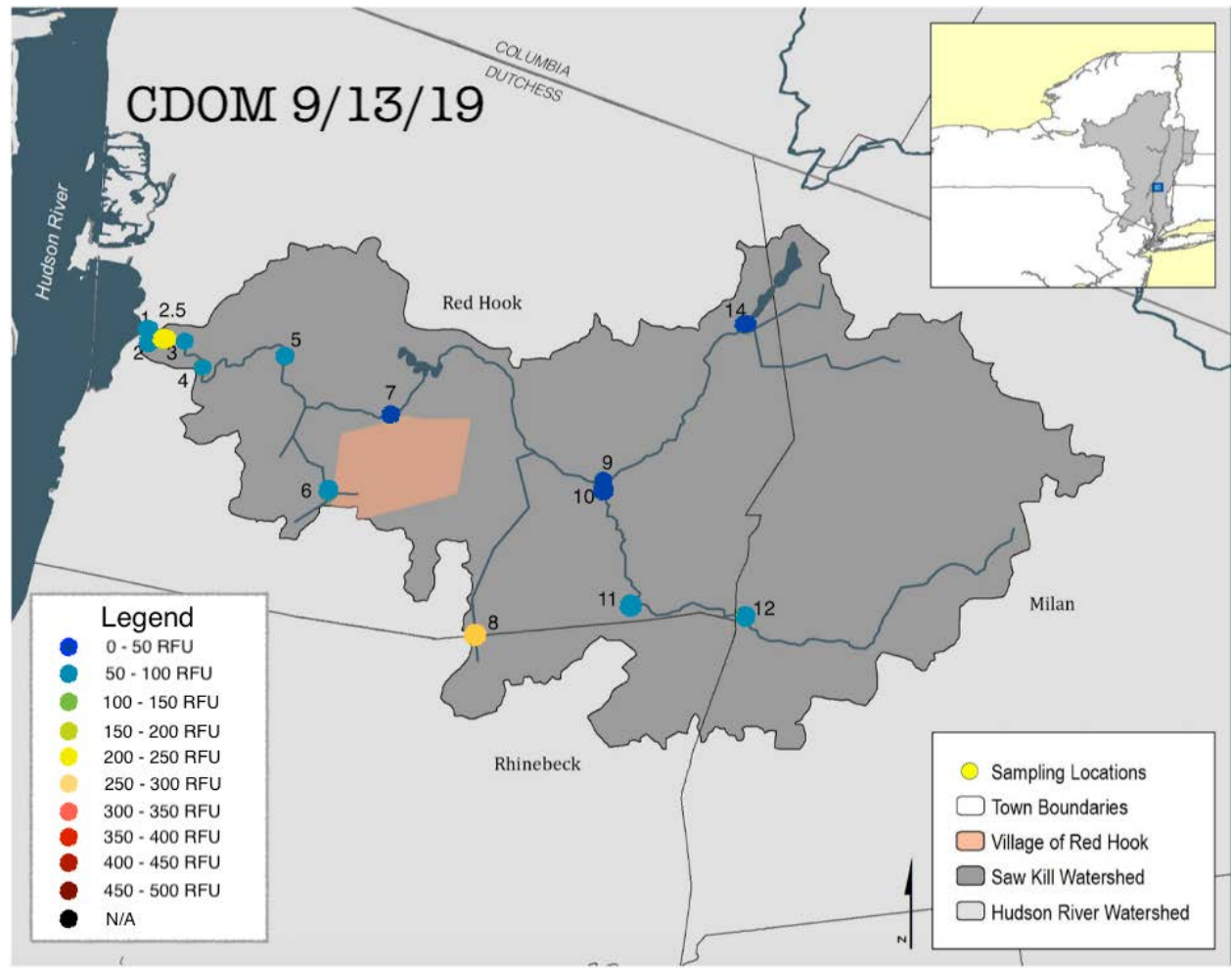


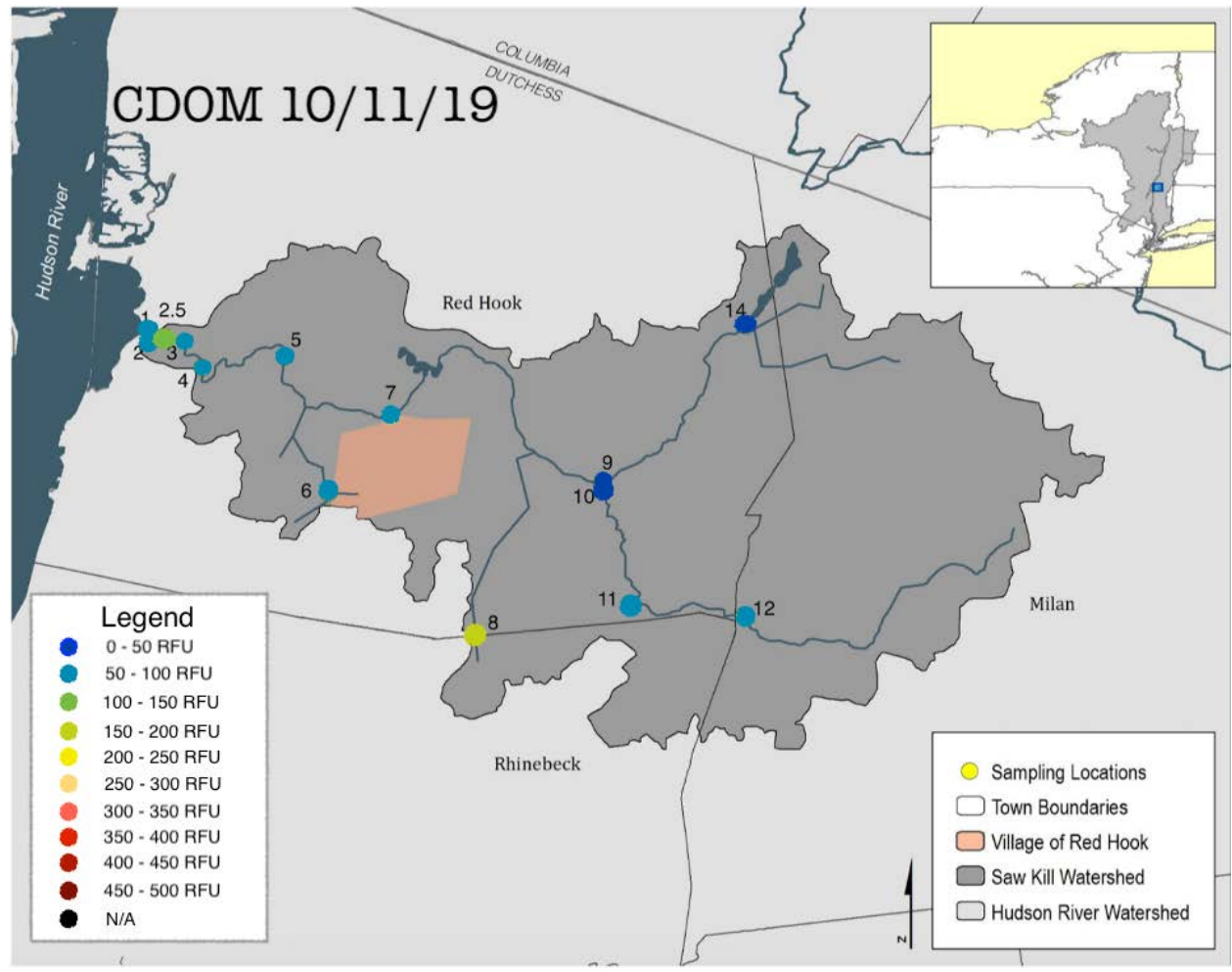


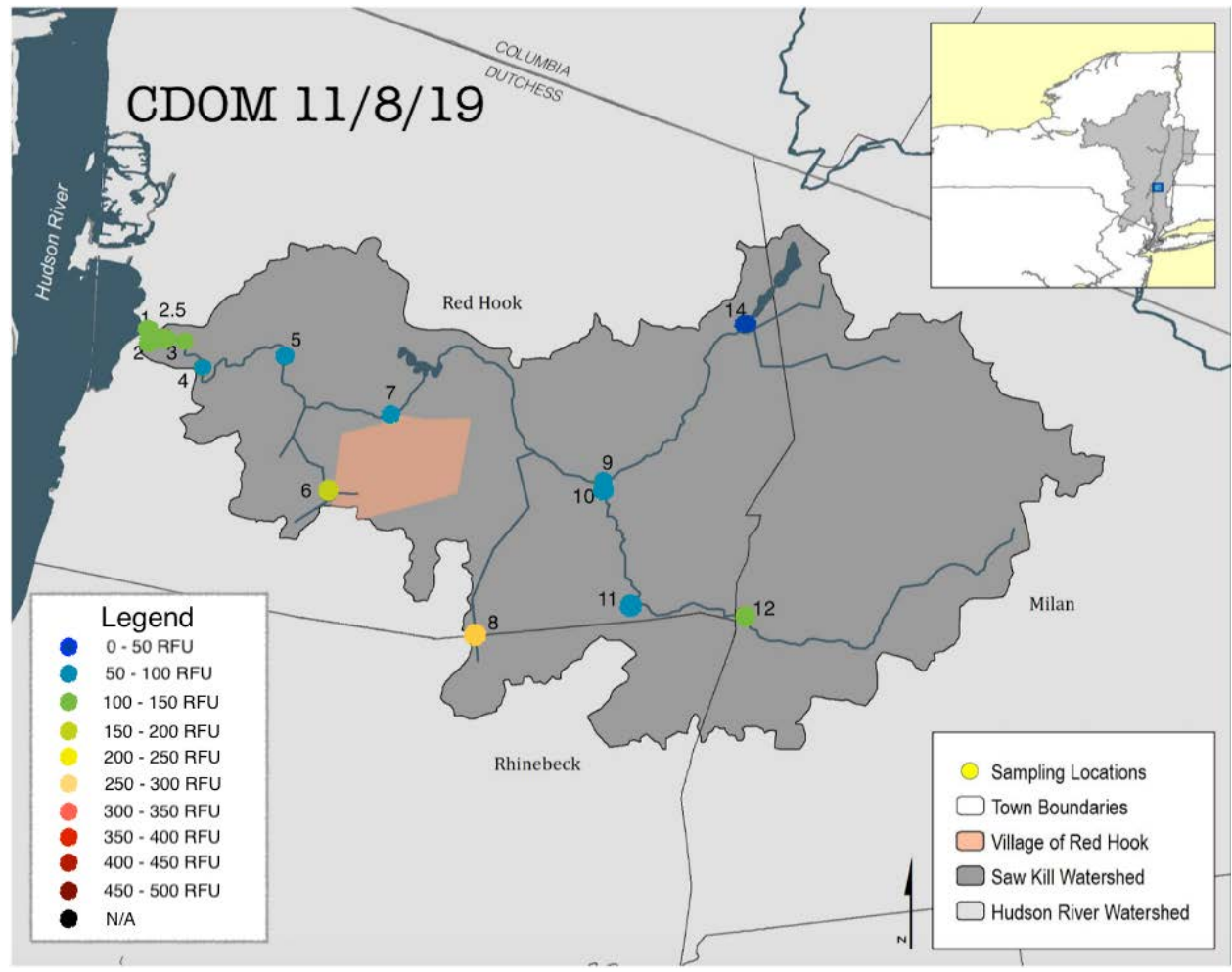


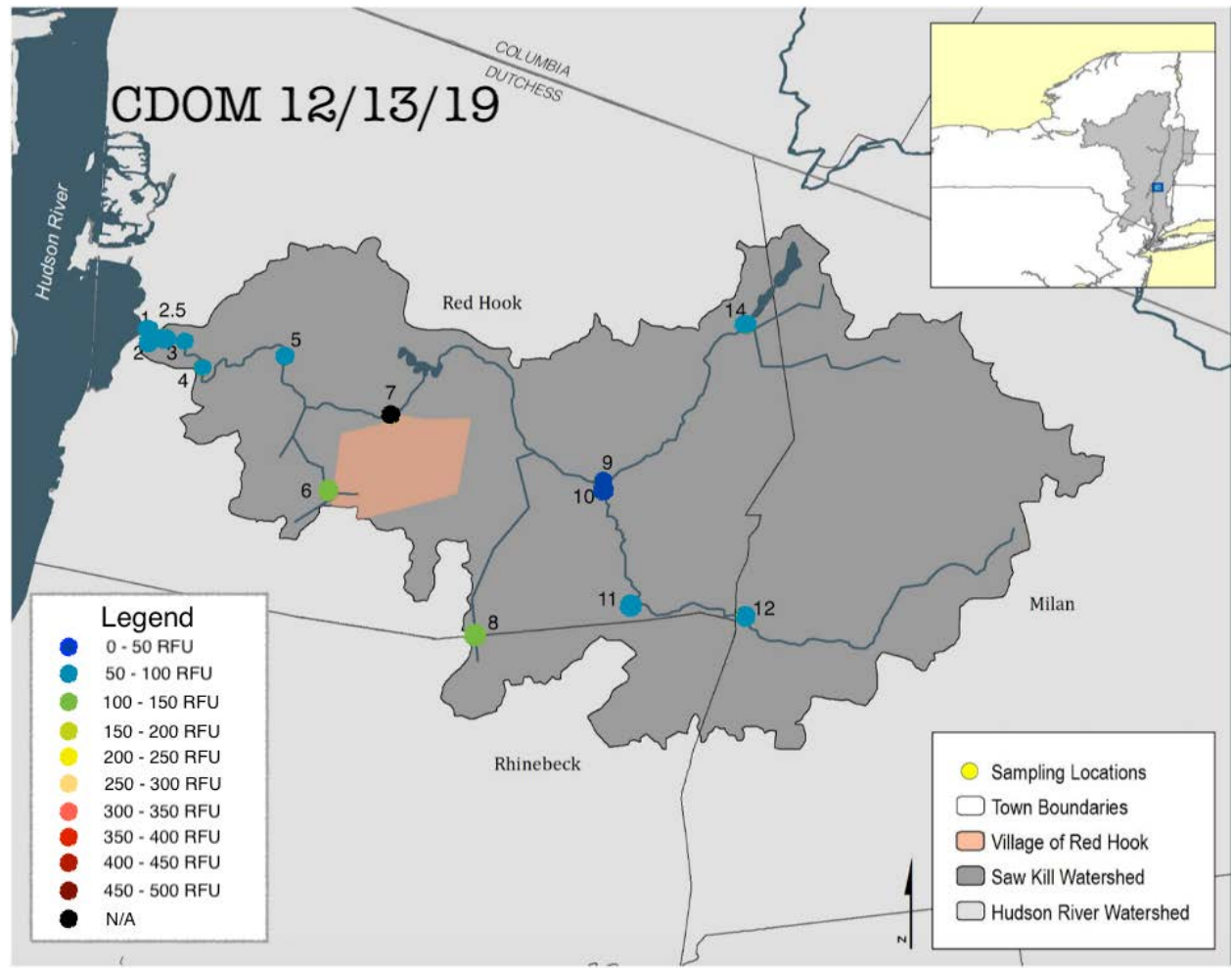




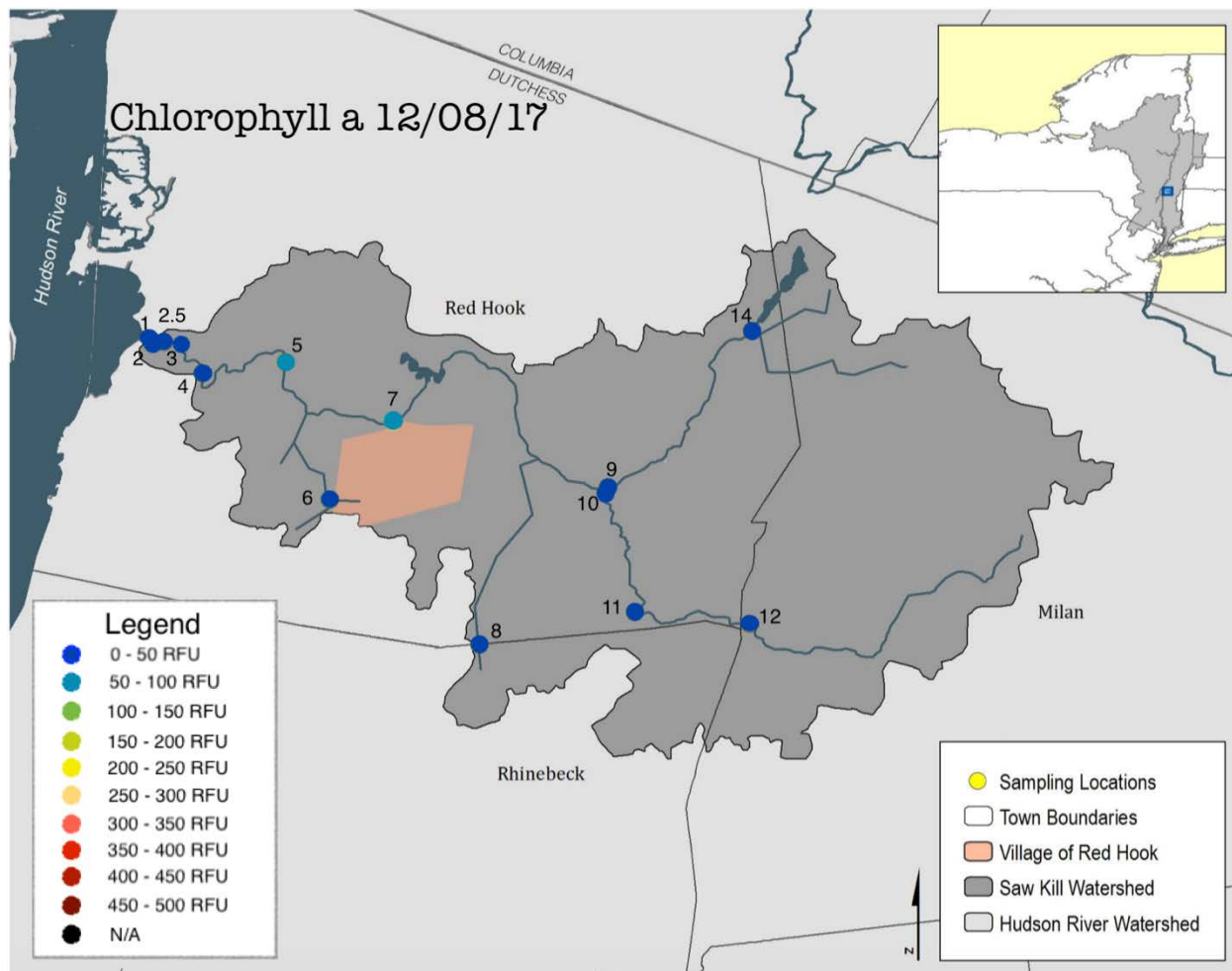


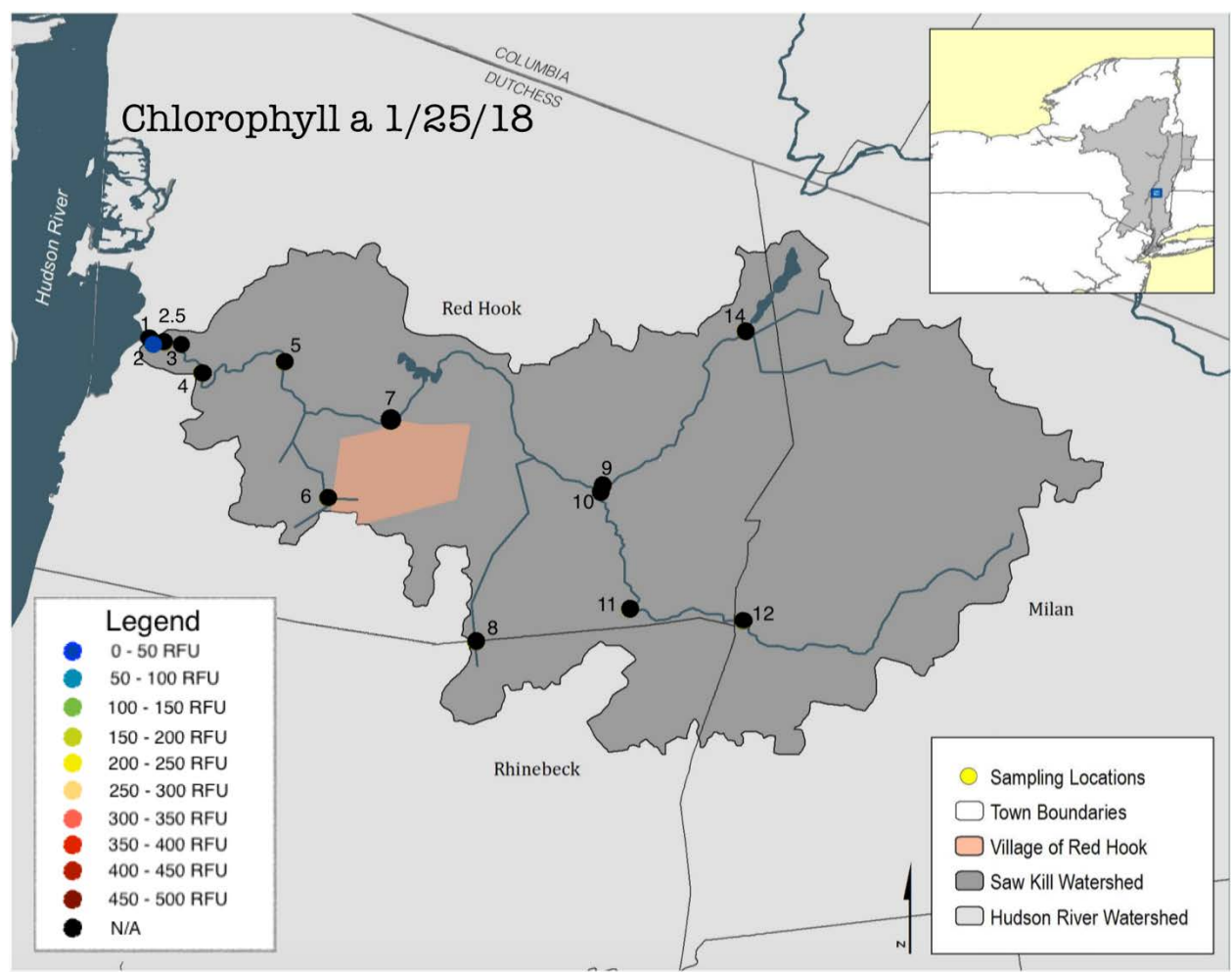


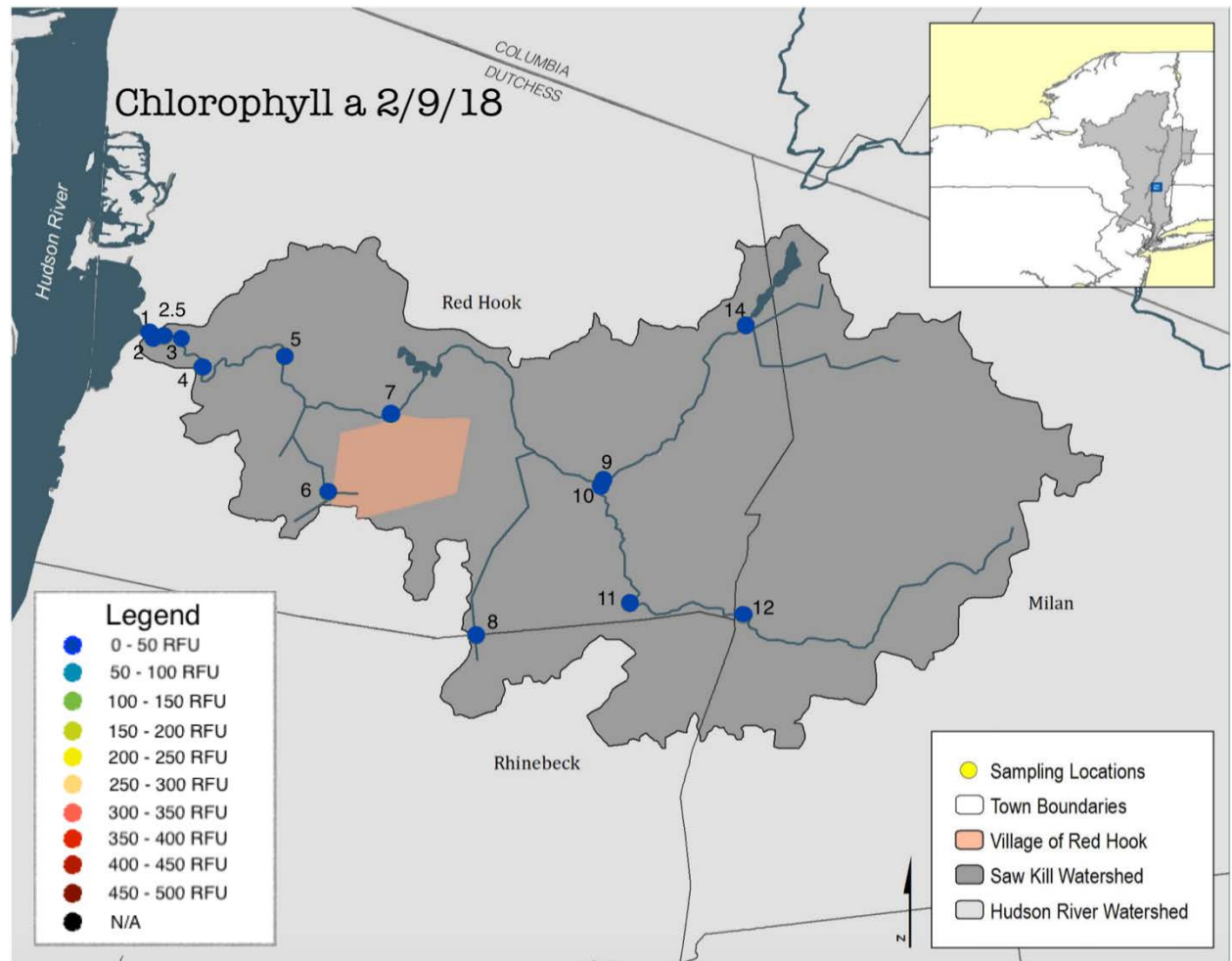


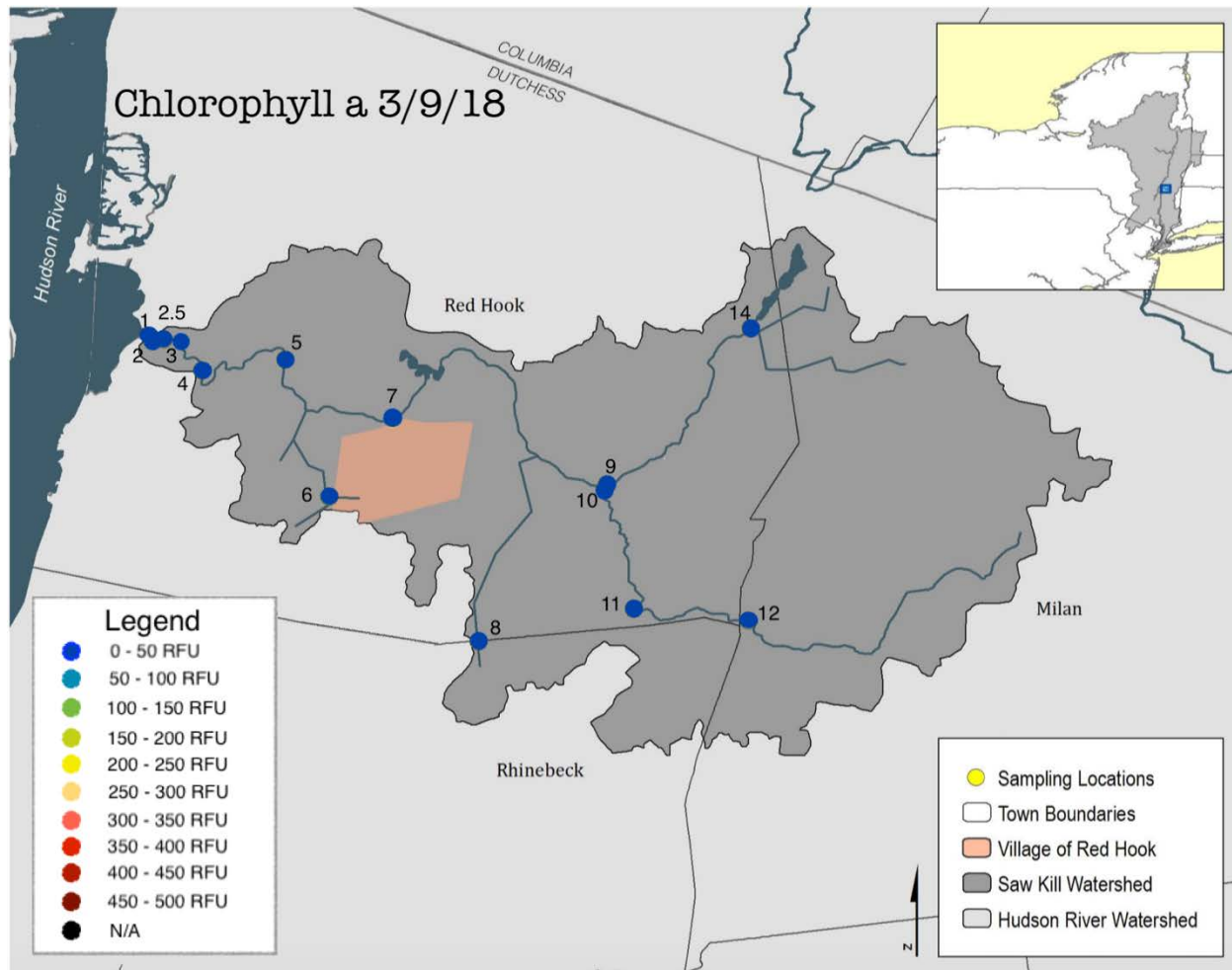


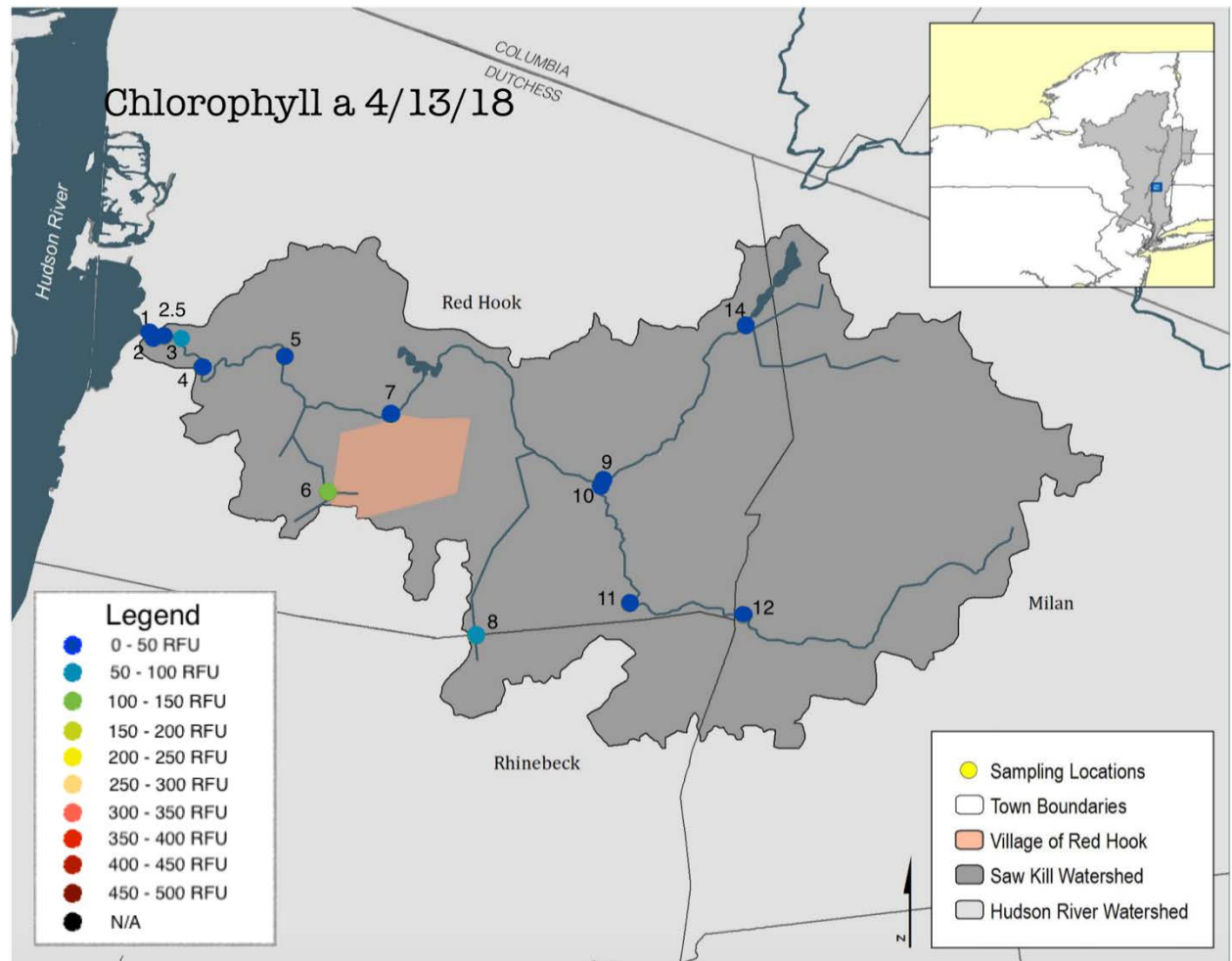
E. Flipbook of chlorophyll a concentrations in the Saw Kill from 2017 to 2019
 All maps in this flipbook are modified from (Riverkeeper, n.d.).

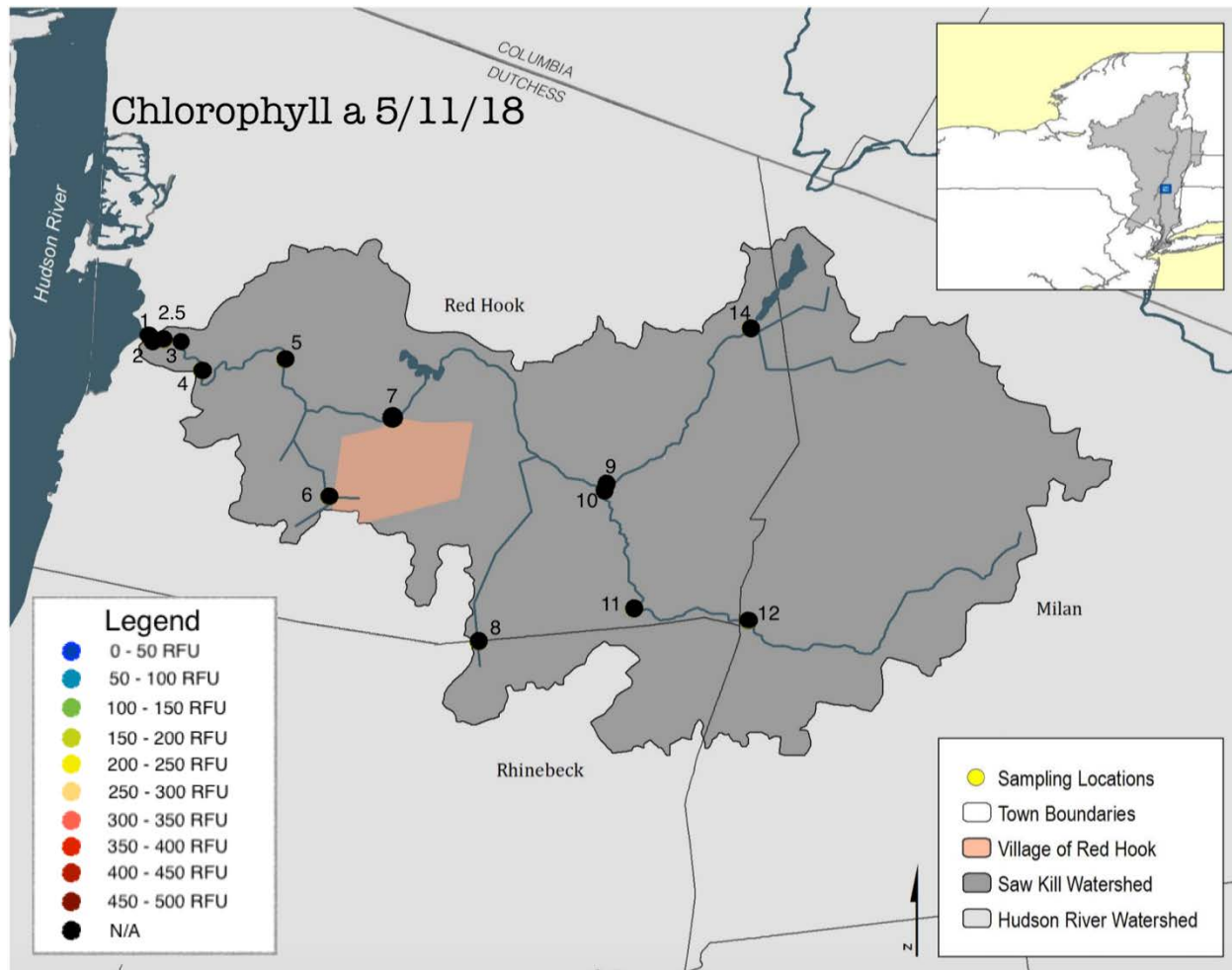


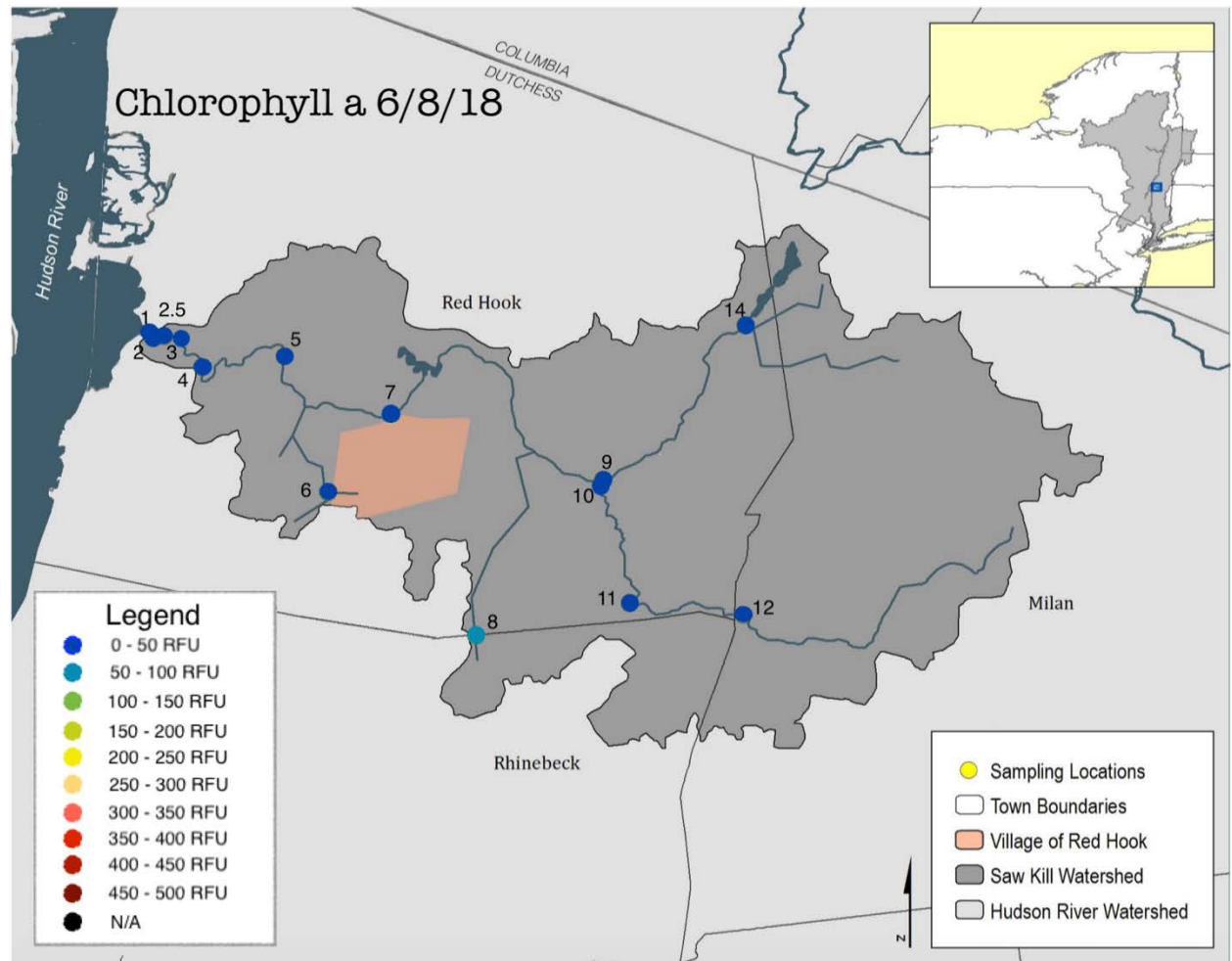


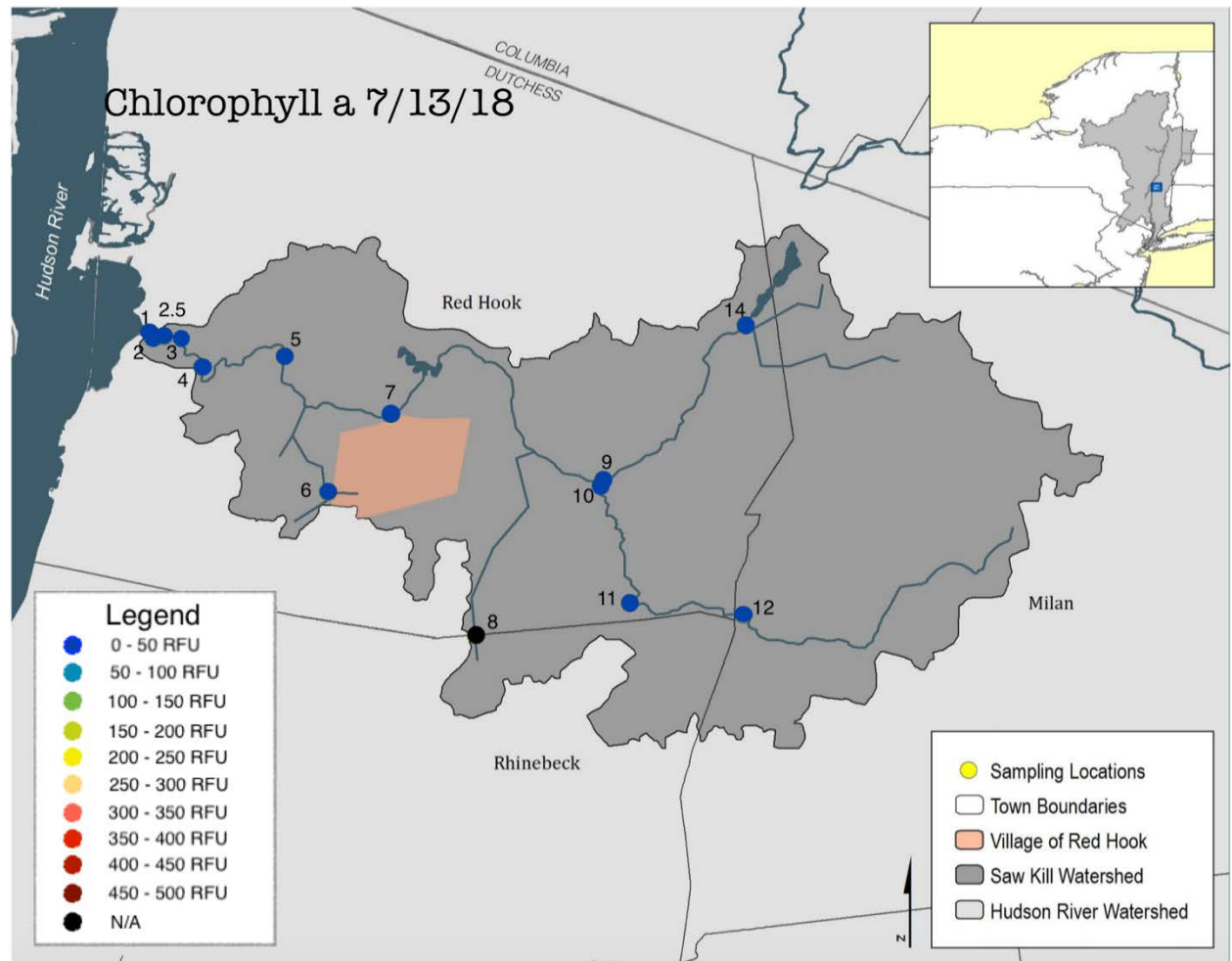


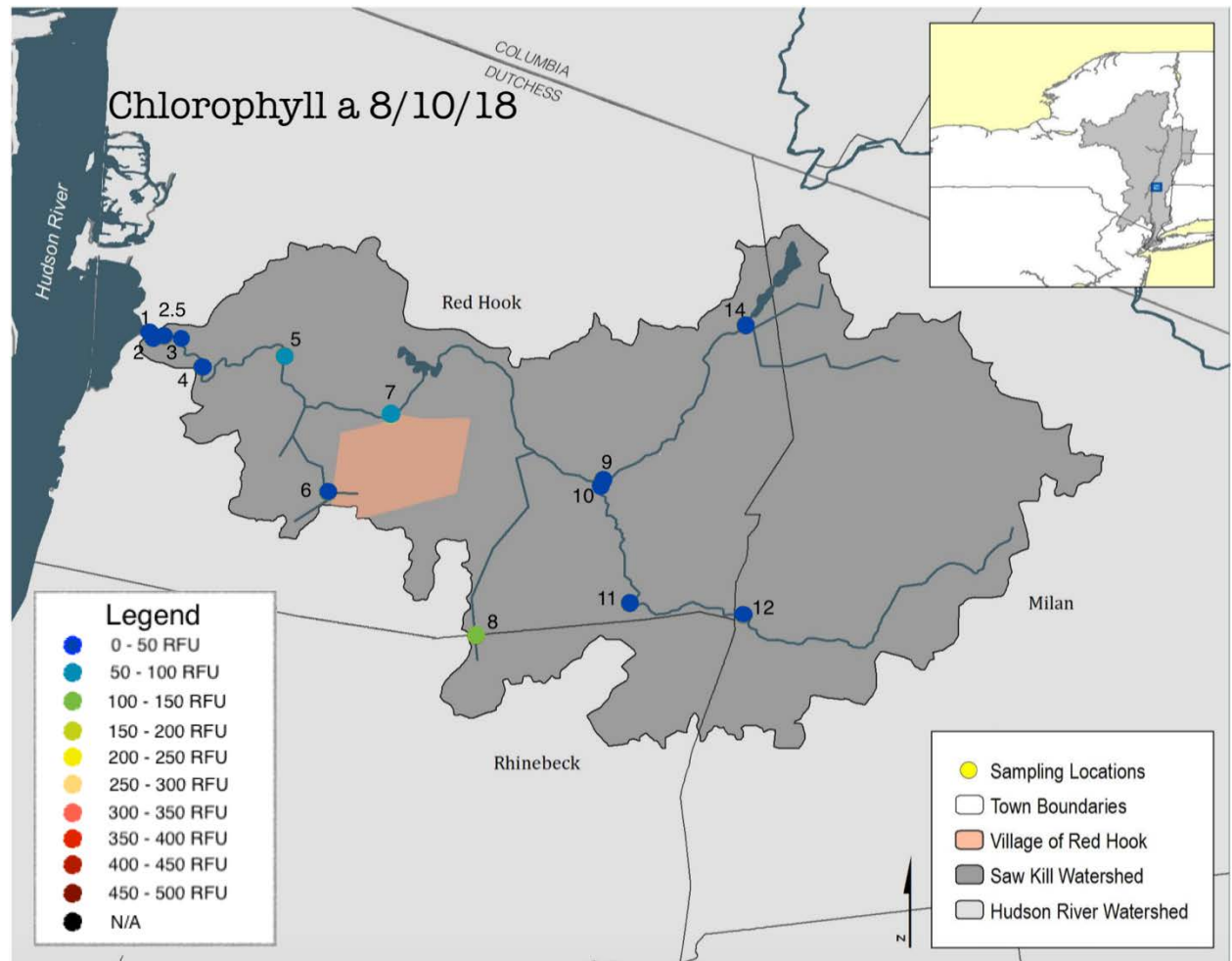


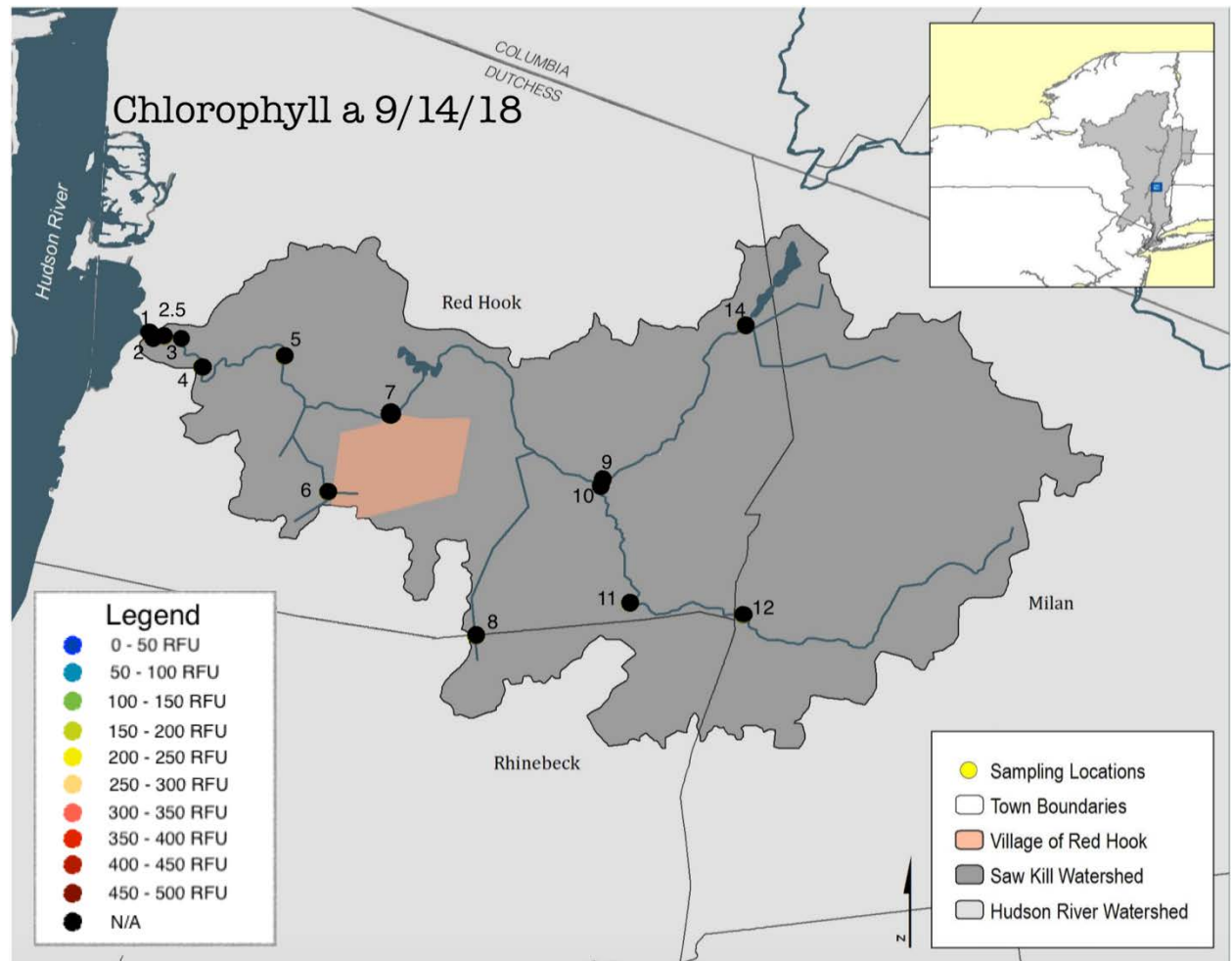


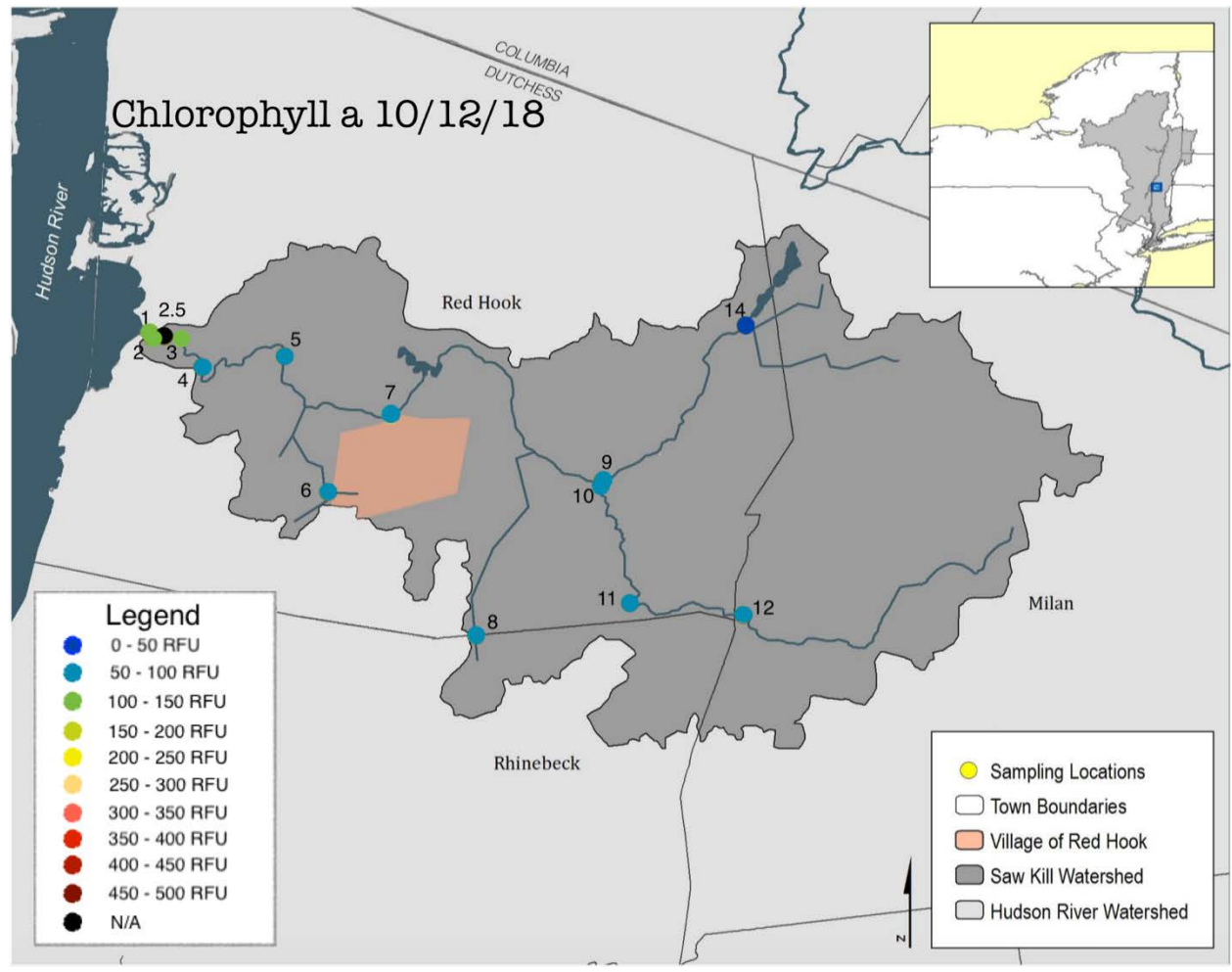


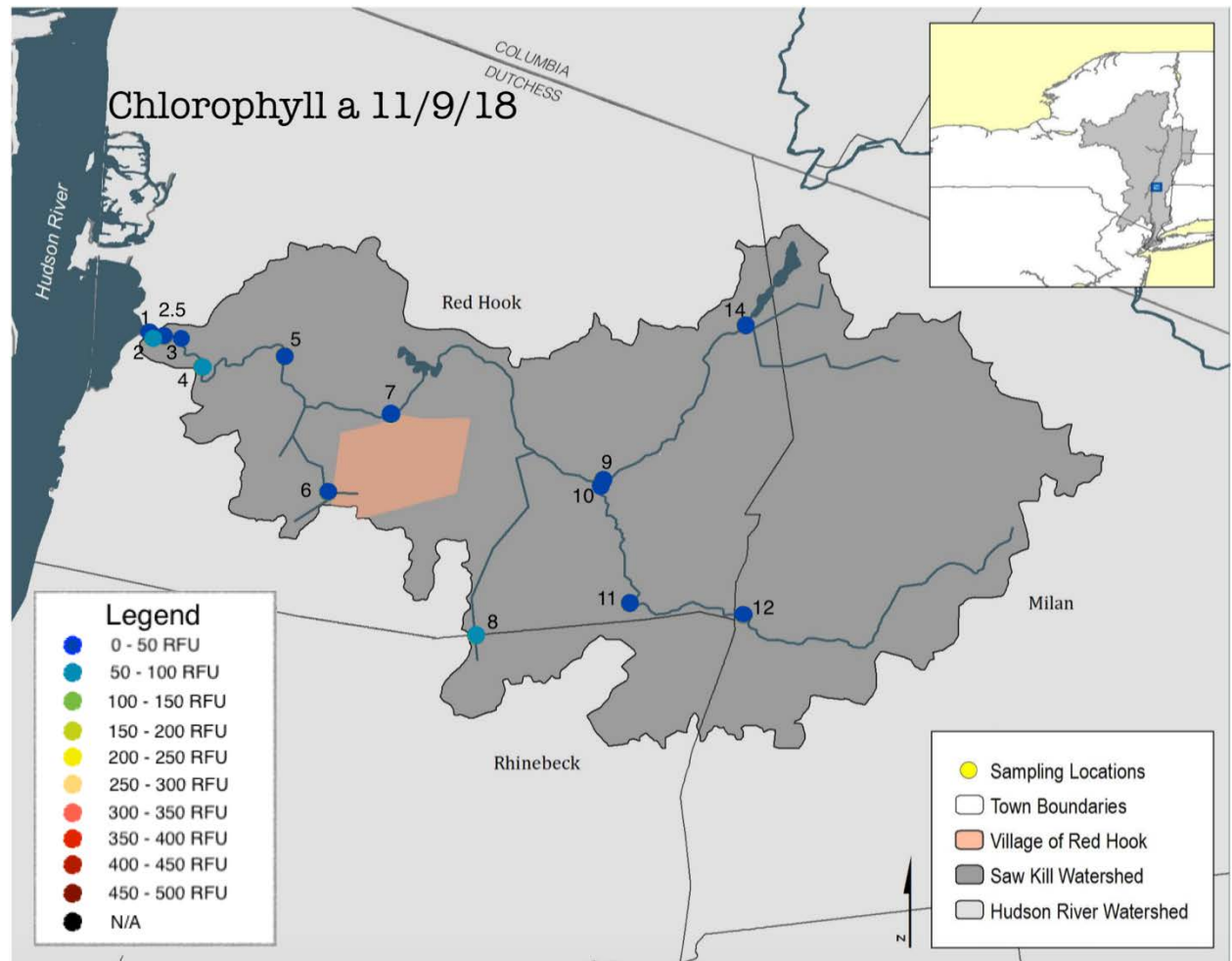


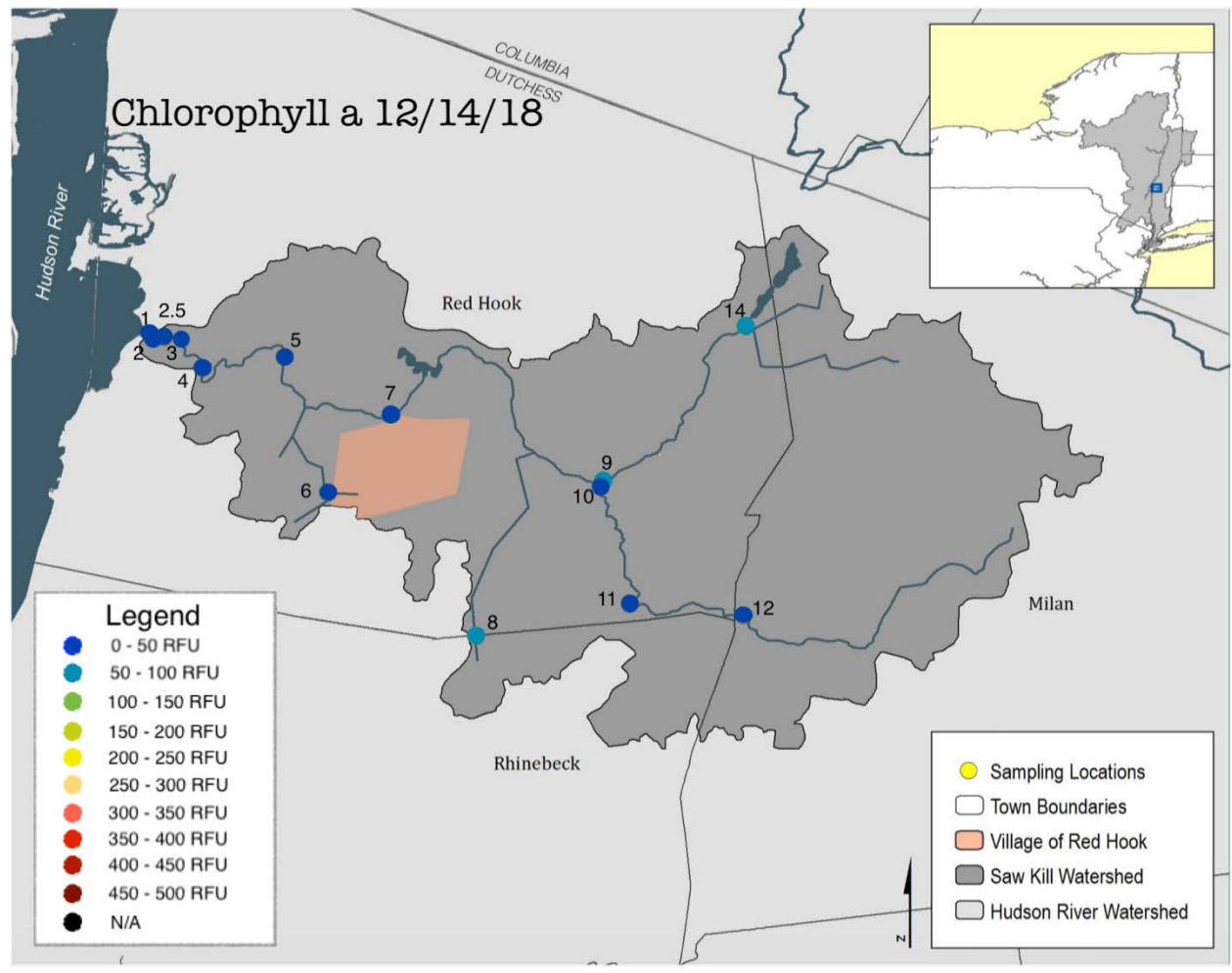


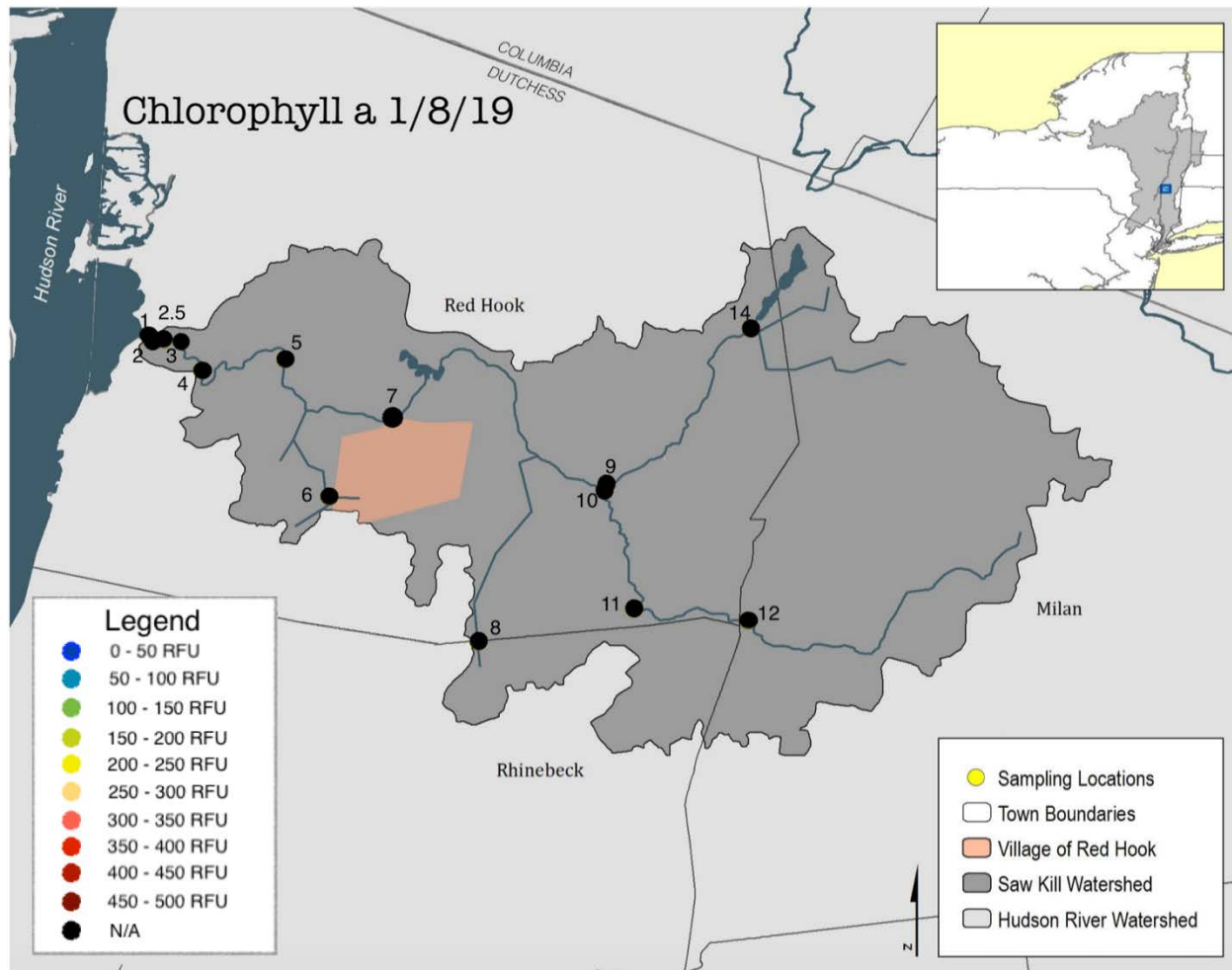


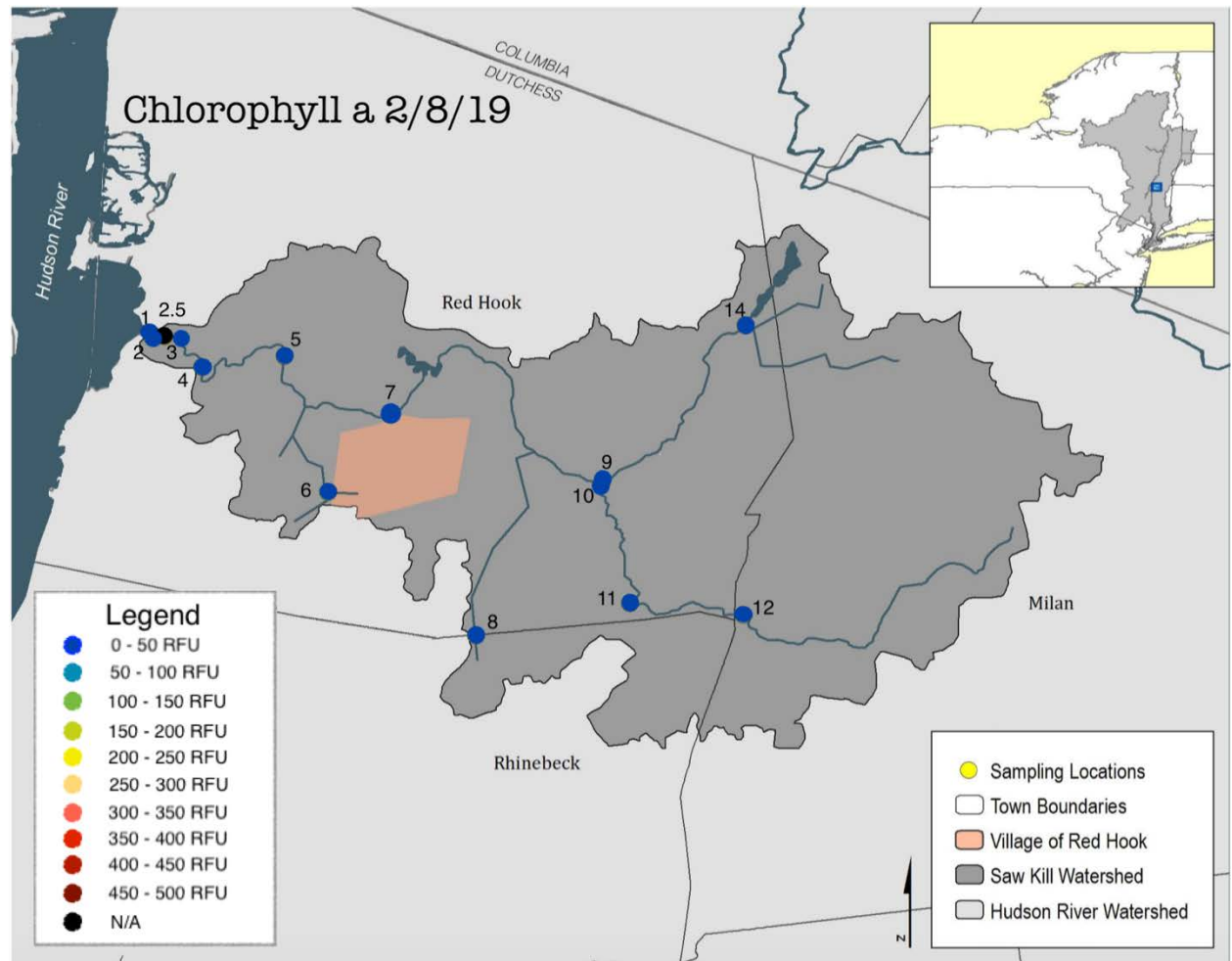


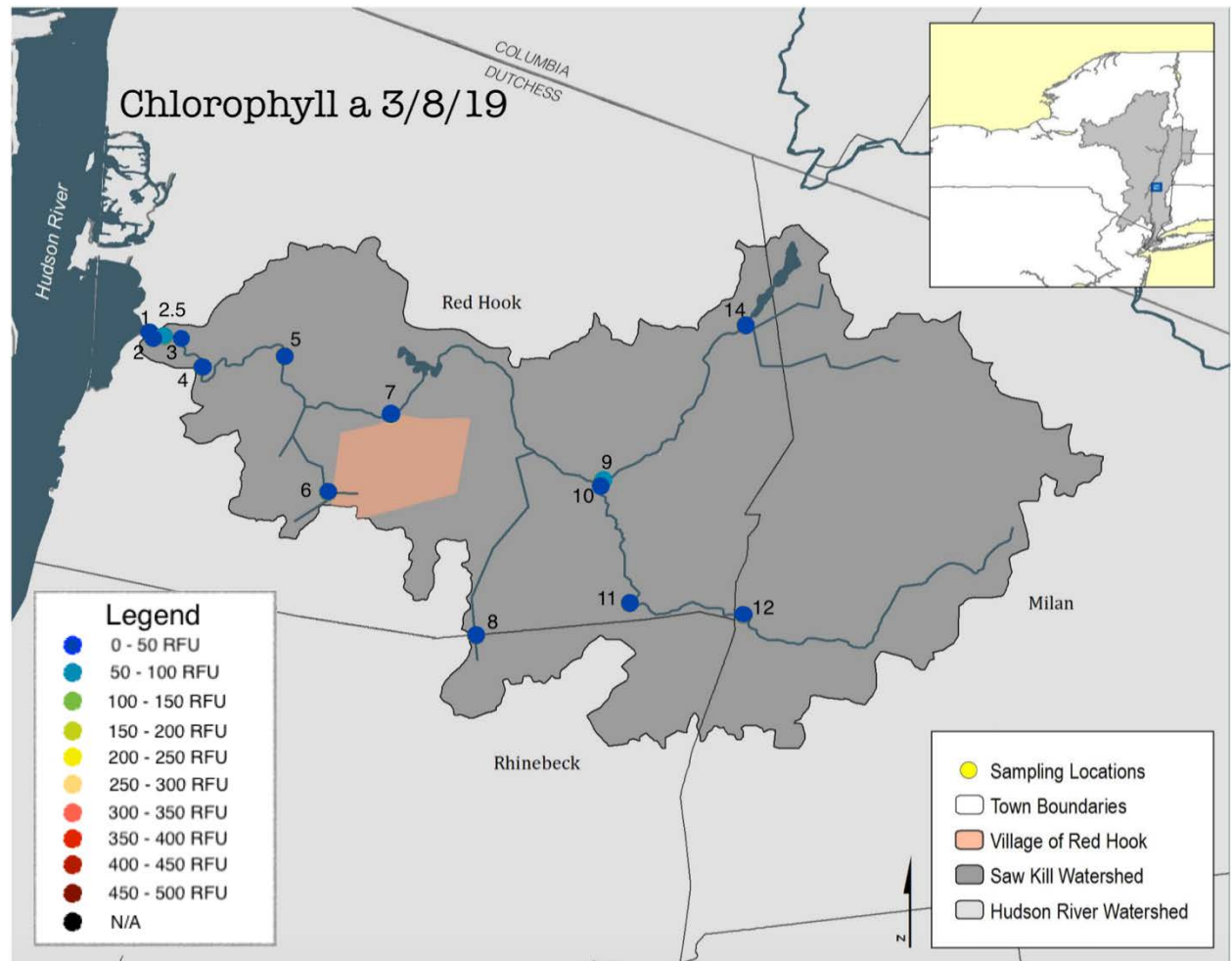


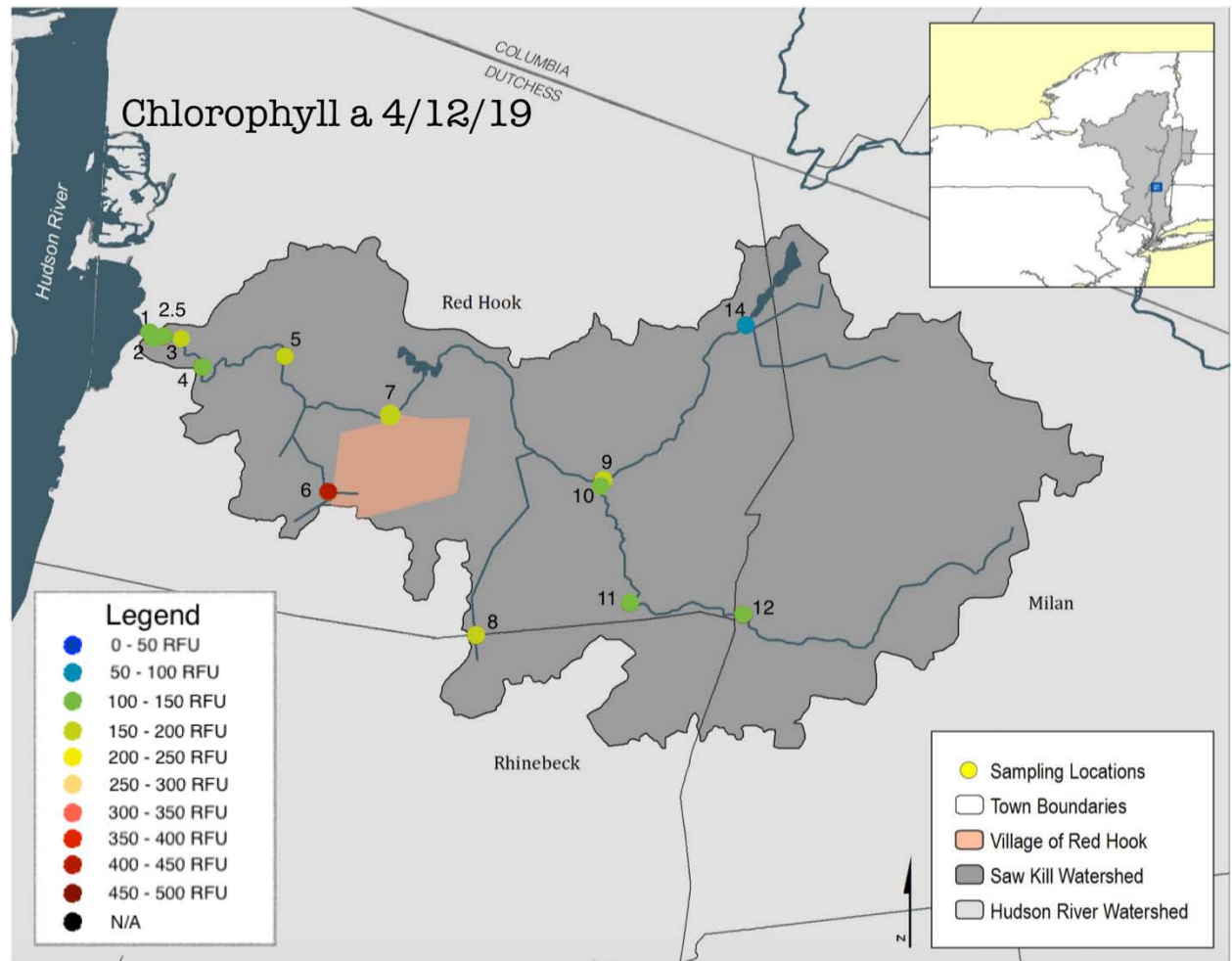


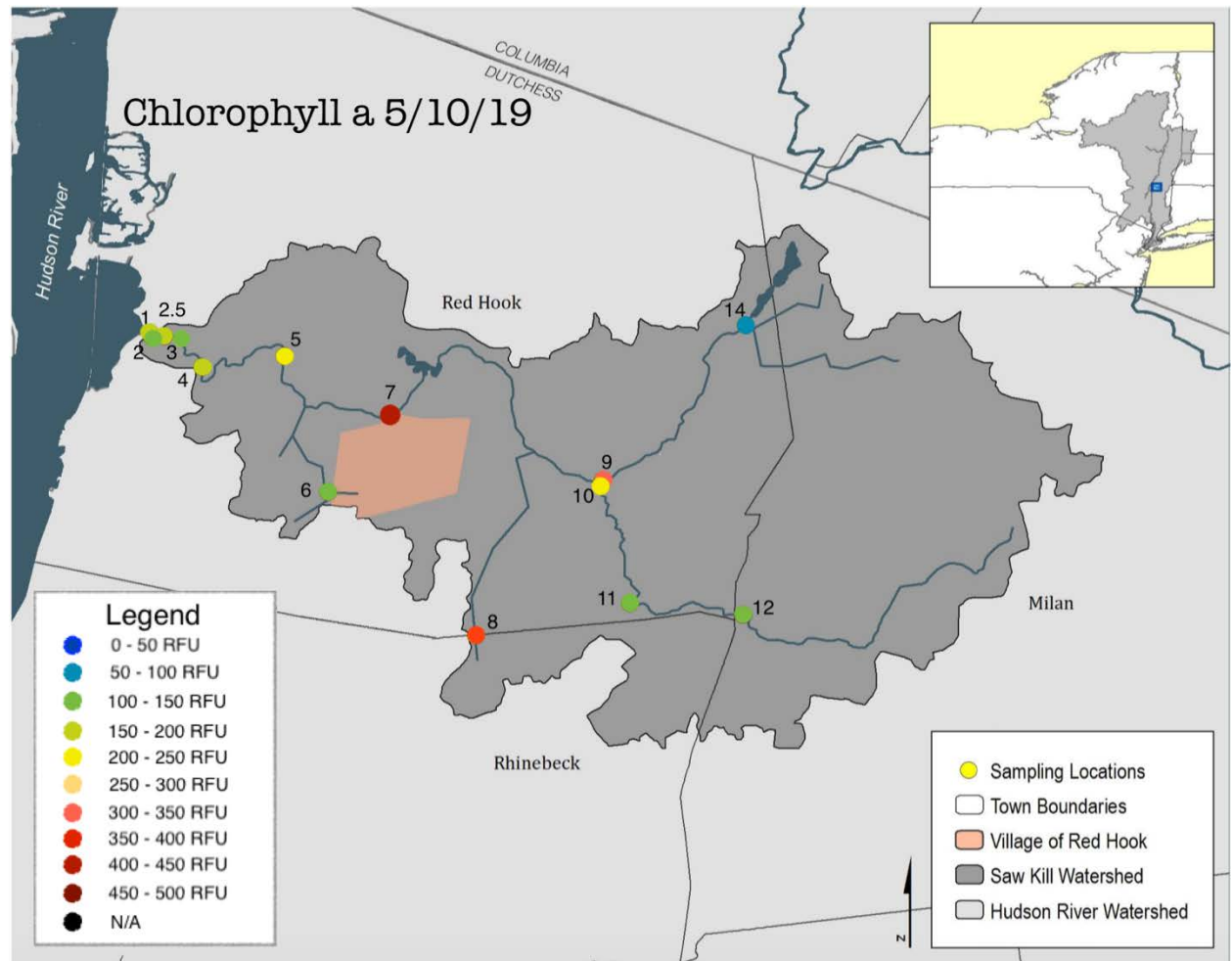


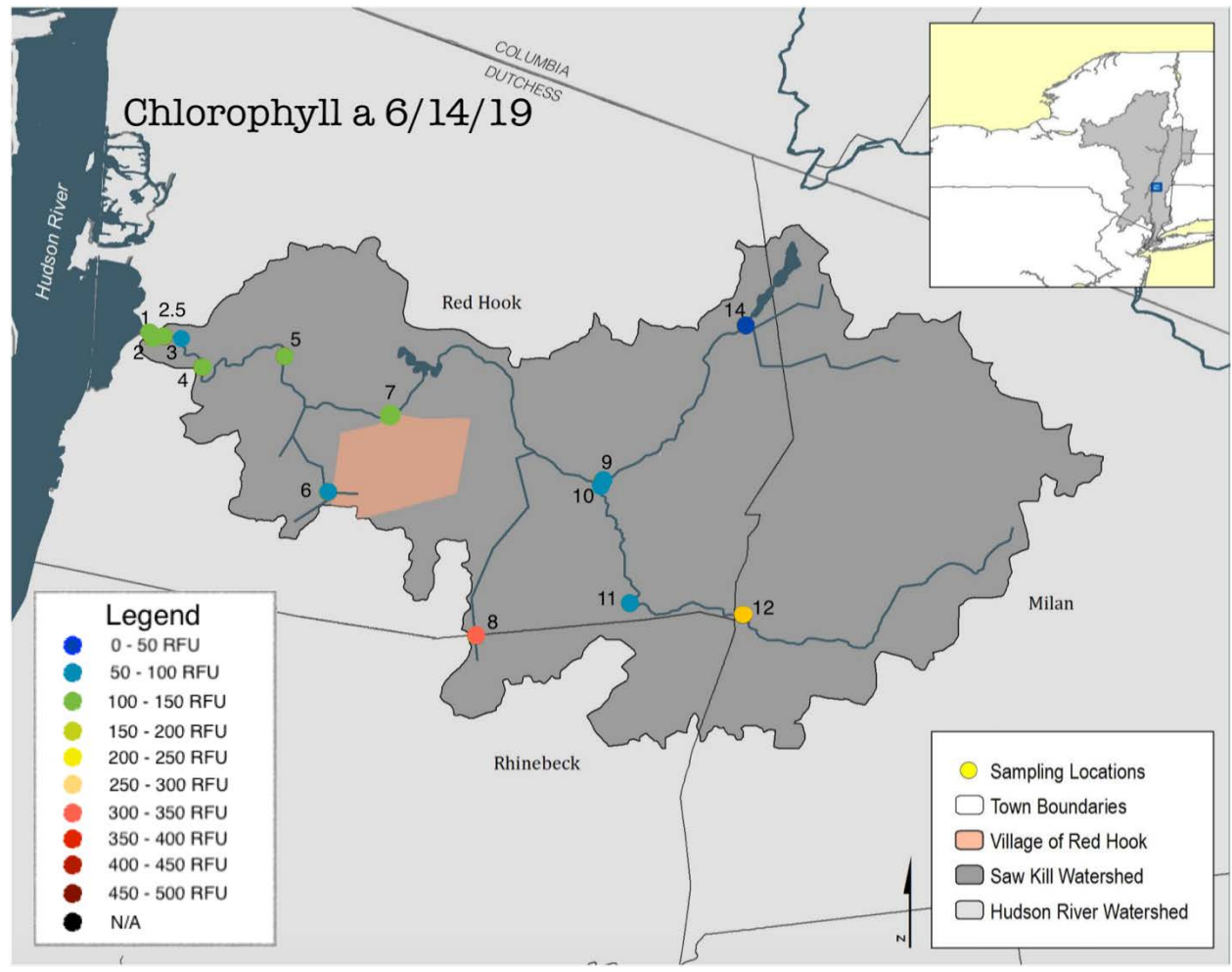


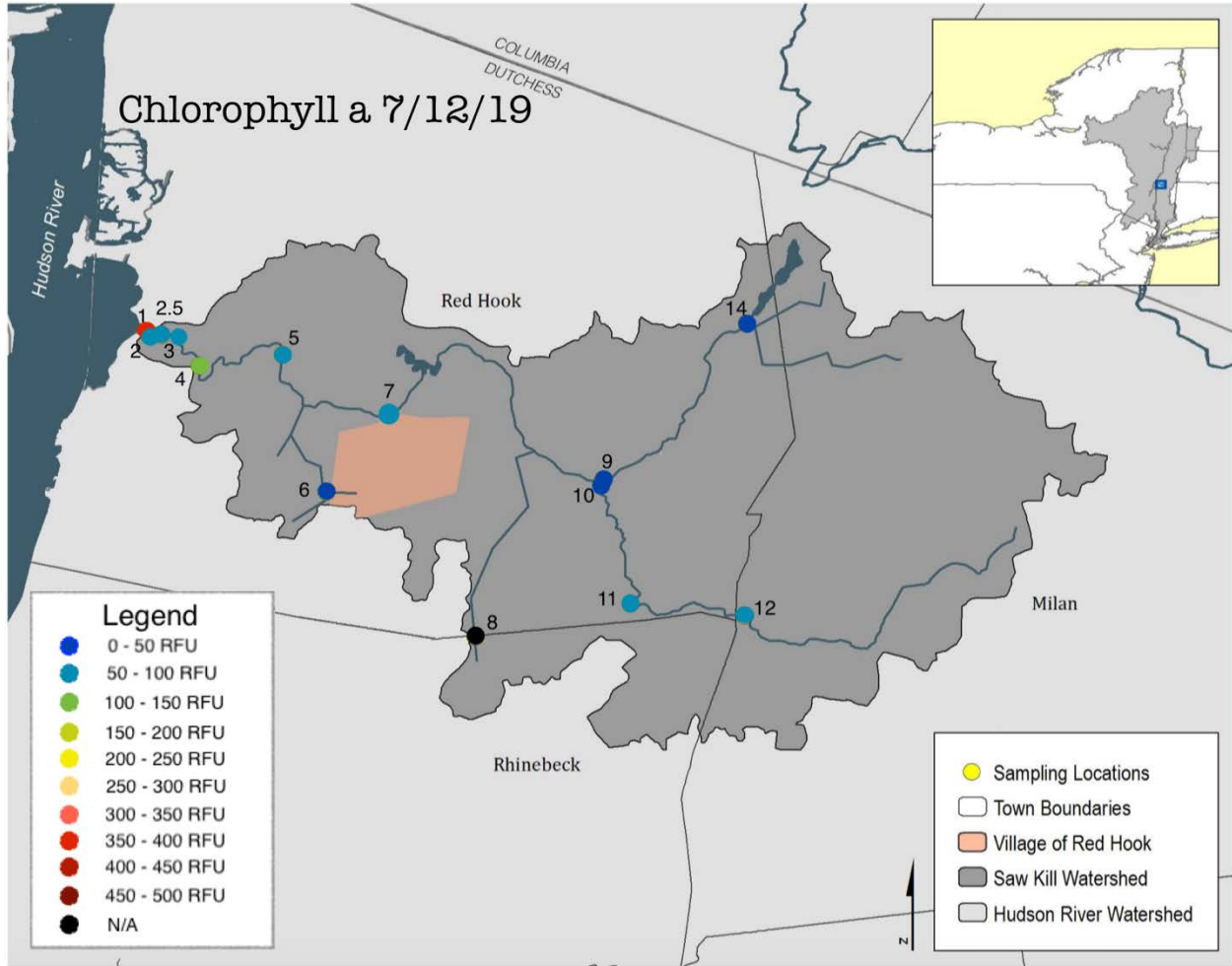


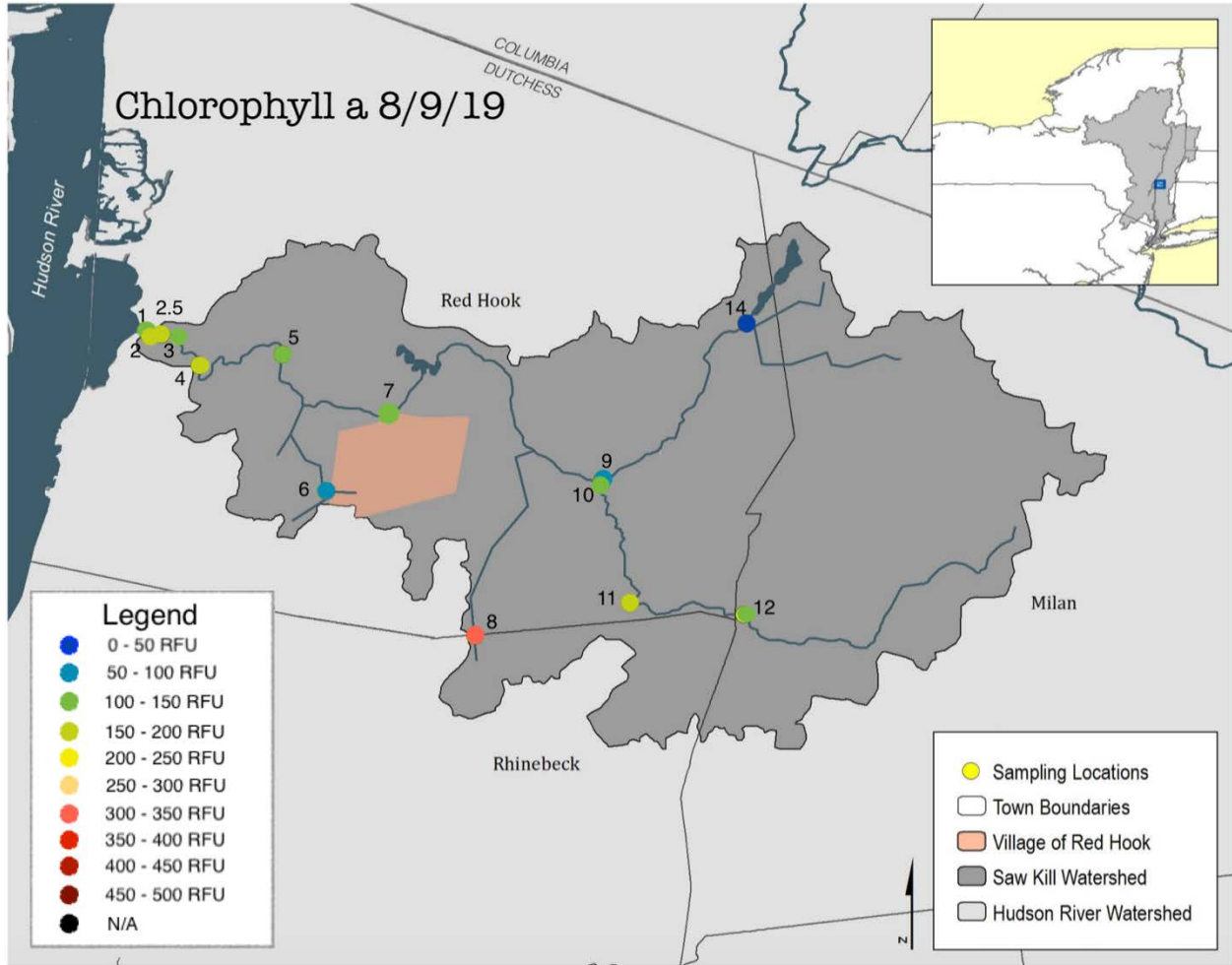


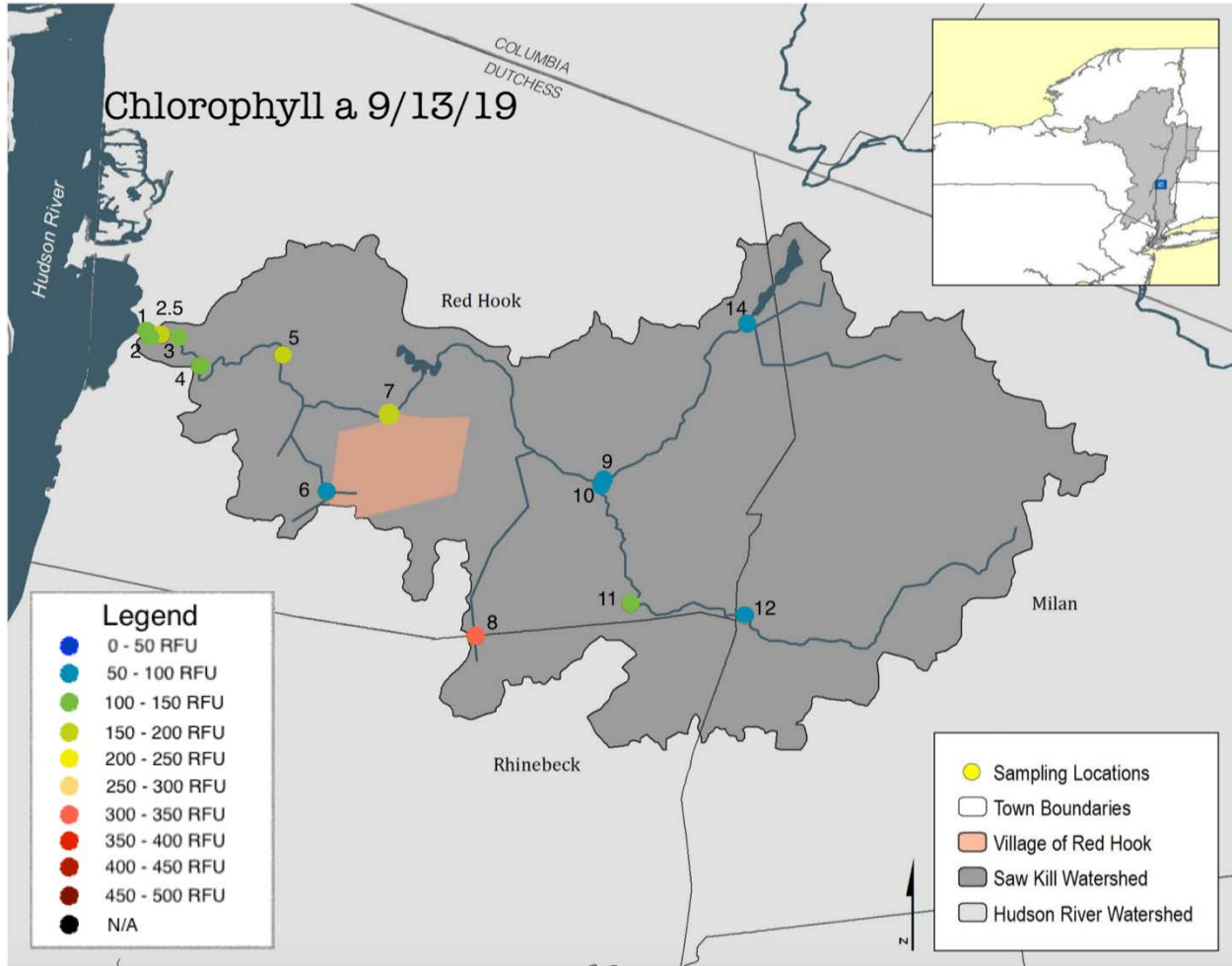


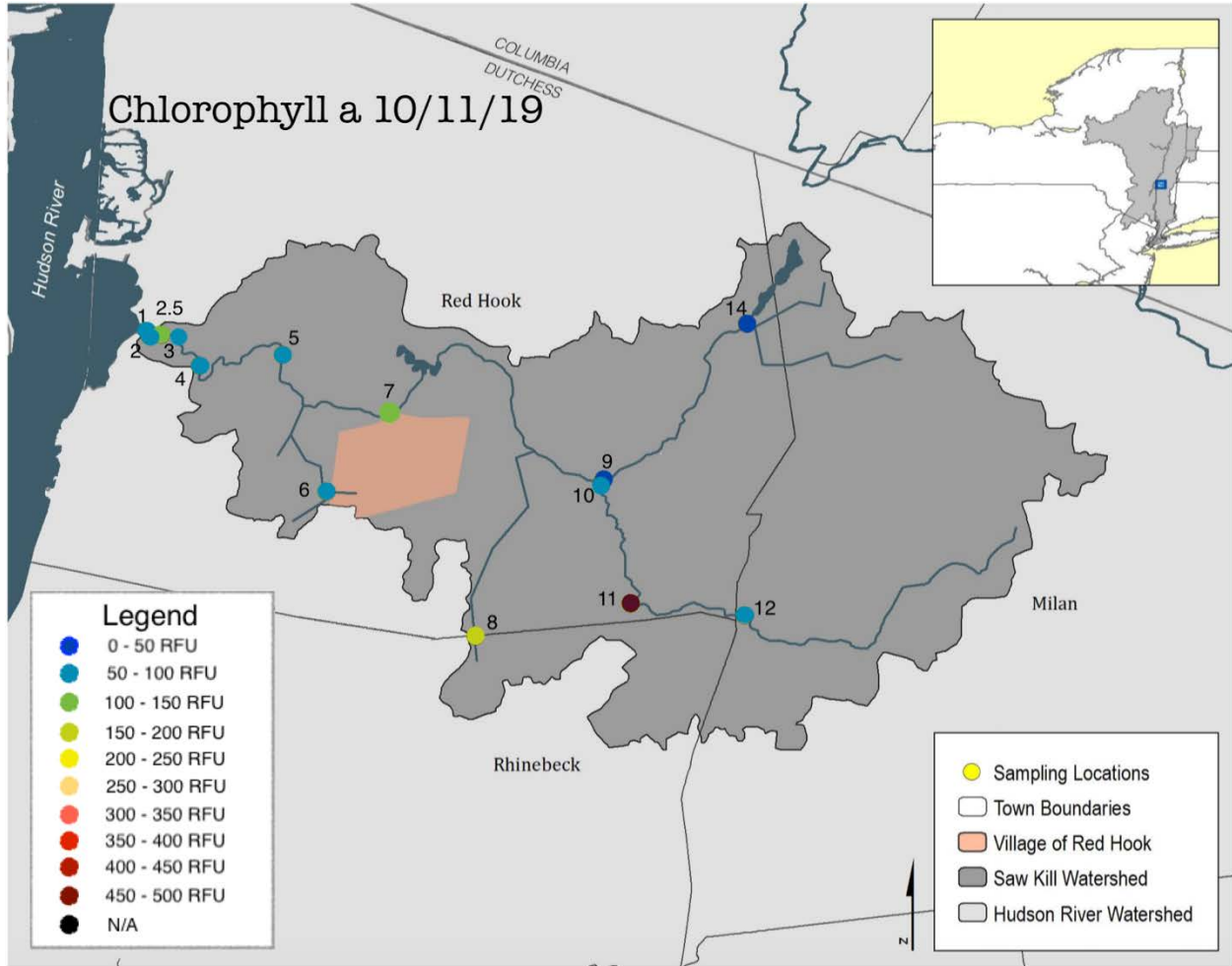


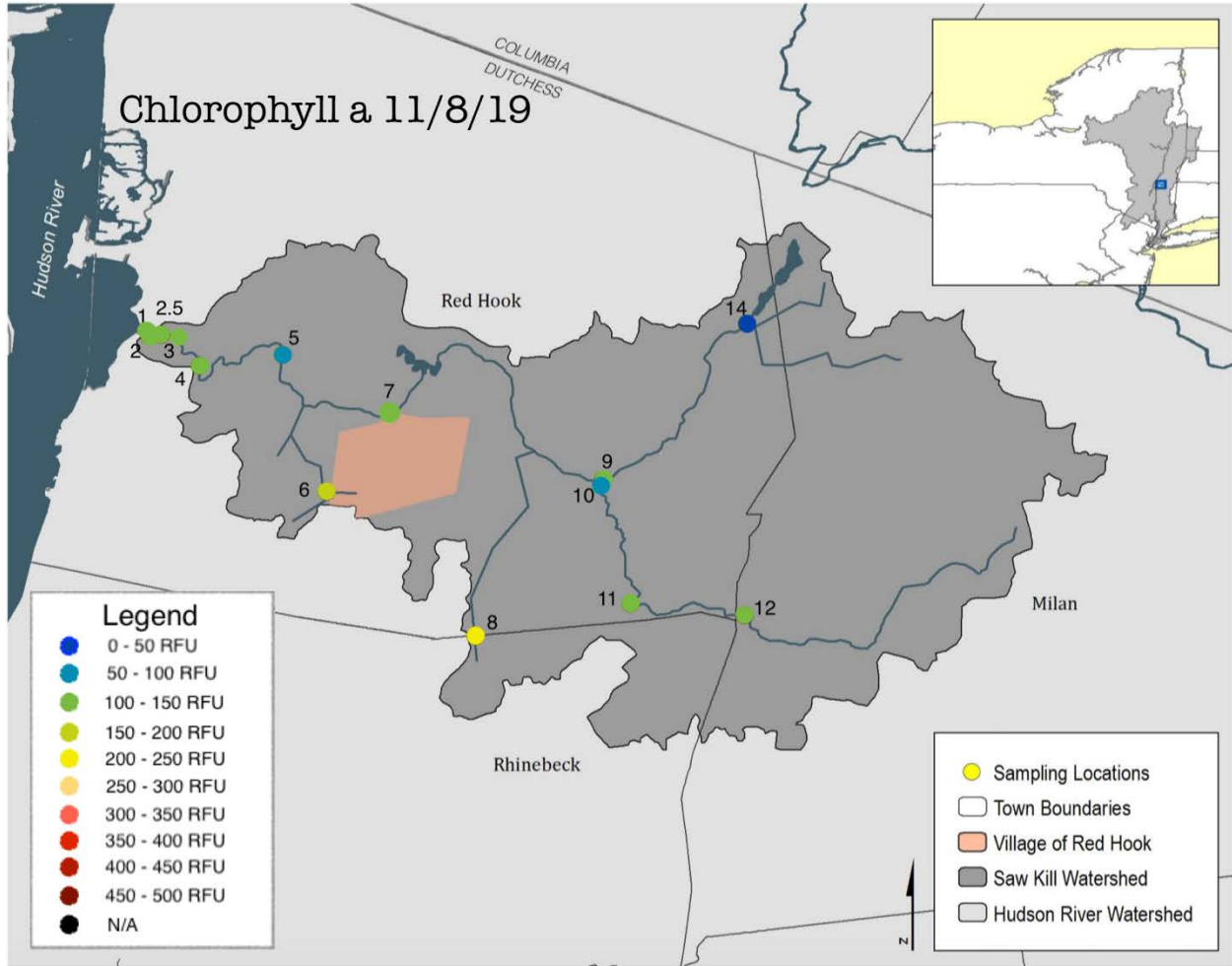


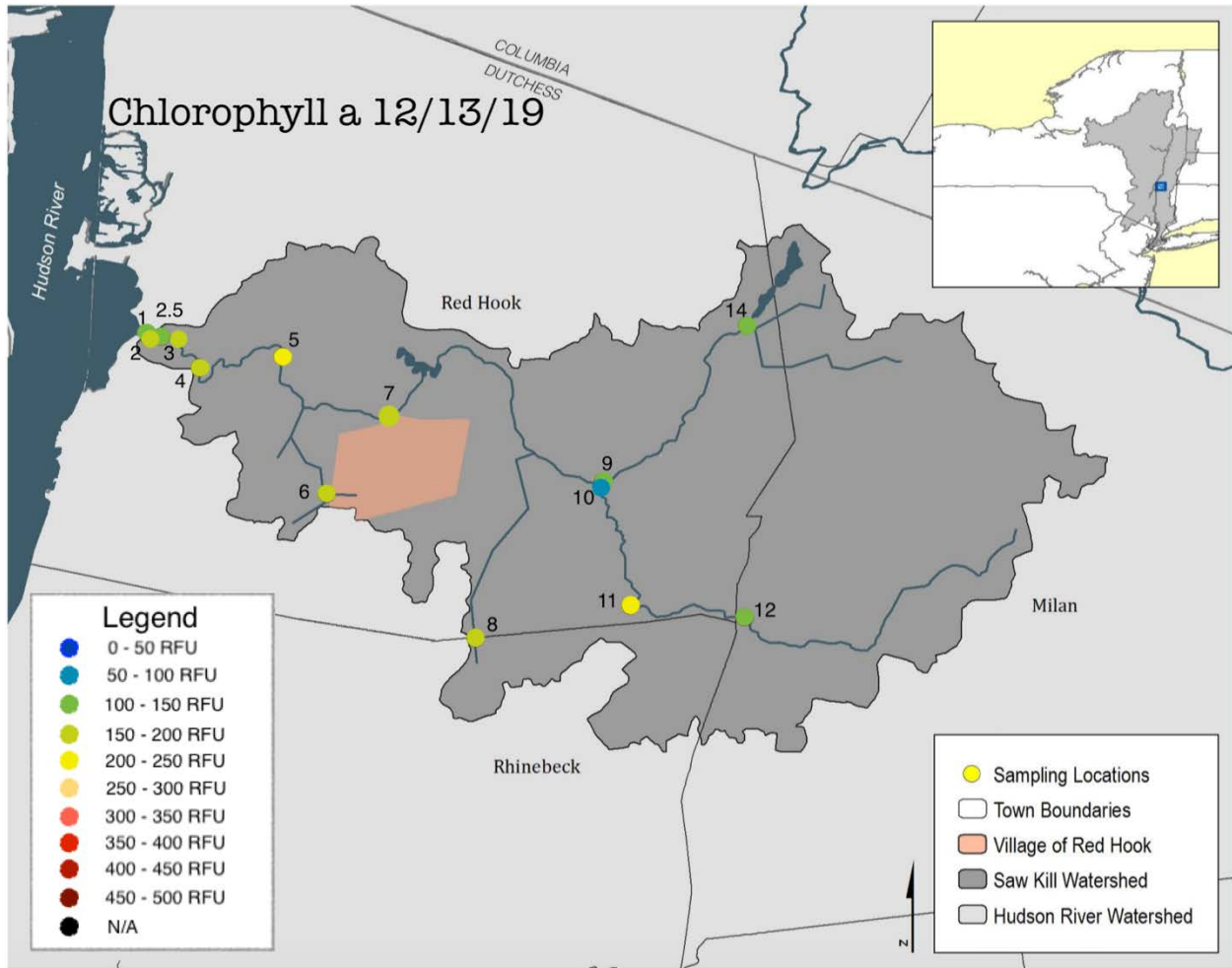












F. Temperature Quenching Protocol

Document Title: Evaluating the Effects of Temperature on CDOM Fluorescence Quenching on Water Samples

1 Introduction

- 1.1 Fluorescence quenching is the decrease in fluorescence intensity of a substance, which can result from a variety of processes such as temperature, turbidity, and molecular interactions. This protocol describes an approach to determine the effects of temperature on quenching of the CDOM (colored dissolved organic matter) fluorescence signal (also known as fDOM, or fluorescent dissolved organic matter) from the AquaFluor Handheld Fluorometer by Turner Designs. It also serves as a basis to correct for temperature in fluorescence and examine the variability in the temperature correction factor between diverse water samples.

2 Summary of Test Method

- 2.1 This protocol provides an explanation on how to set up and run a temperature fluorescence quenching experiment. The goal is to measure colored dissolved organic matter (CDOM) in water samples at a temperature range of approximately 3°C to 30°C to derive a quenching factor that is site-specific.
- 2.2 Ideally, 5-8 CDOM measurements should be taken using the fluorometer at the following temperature ranges:
 - <5°C
 - 5°C - 10°C
 - 10°C - 15°C
 - 15°C - 20°C
 - 20°C - 25°C
 - 25°C - 30°C.

3 Safety

- 3.1 Safety glasses must be worn.
- 3.2 A portion of the procedures will be conducted in a cold room. Dress appropriately.

4 Equipment and Supplies

- 4.1 Ice
- 4.2 Ice Bucket
- 4.3 Four 250 mL Beakers
- 4.4 Dial thermometer
- 4.5 NIST Digital thermometer
- 4.6 Two bottles of Deionized (D.I.) Water
- 4.7 Two boxes of Kimtech Wipes
- 4.8 Fluorometers
 - 4.8.1 Turner Designs, Model: 8000-010 (Bard College's fluorometer)
 - 4.8.2 Turner Designs, Model: 8000-010 (NYCDEP's fluorometer)
- 4.9 Steel Cart
- 4.10 Hot Plate

- 4.11 1 L Glass Basin
- 4.12 Methacrylate Cuvettes (Turner Designs, P/N 7000-959) or another suitable substitute
- 4.13 Safety Glasses
- 4.14 Water Samples
- 4.15 Waterproof pen (e.g., Sharpie®)

5 Set Up

- 5.1 Keep the samples in the walk-in cooler (cold room with a temperature around 4°C).
- 5.2 Fill the ice bucket with ice.
- 5.3 Fill two 250 mL beakers with ice and water to create an ice bath.
 - 5.3.1 Place one in the cold room.
 - 5.3.2 Place the second in the laboratory.
 - 5.3.3 Note: Refill the ice bath with ice as needed.
- 5.4 For the walk-in Cooler
 - 5.4.1 Place the following items on the Steel Cart and into the cold room to equilibrate the items to the cold room's temperature:
 - Bottled Water Samples
 - Kimtech Wipes
 - Fluorometer
 - 1 - bottle of D.I. Water
 - 1 - ice bath in beaker
 - 1 - waste beaker
 - NIST Digital thermometer

5.4.2 Notes

- 5.4.2.1 When borrowing the NIST Digital Thermometer, ensure that the sign out sheet is completed.
 - 5.4.2.2 Allow sufficient time for the fluorometer and NIST Digital Thermometer to cool down and equilibrate to the cold room's temperature (about 4 °C). The instruments need to be in equilibrium with the cold room to minimize the thermal impact on the samples because the fluorometer's internal electronics continuously generate heat.
- 5.5 For the benchtop workspace
 - 5.5.1 Place the following items on the benchtop space:
 - Hot Plate
 - 1 L glass basin
 - Kimtech Wipes
 - Ice bucket
 - 1 - waste beaker
 - 1 - ice bath in beaker

- Cuvettes
- Sharpie
- Dial Thermometer
- Waterproof pen (Sharpie®)

5.5.2 Fill the glass basin halfway with water and place it on the hot plate. Set the temperature of the hot plate to approximately 40°C to create a hot water bath. Place the Dial Thermometer in the glass basin.

5.5.3 Note: Continuously monitor the temperature of the water in the glass basin by turning the hot plate off when the temperature becomes warmer than 40°C, and turning the hot plate on when the temperature becomes cooler than 40°C.

5.6 Select a cuvette for use with the fluorometer.

5.6.1 Select a cuvette by inspecting cuvettes for scratches or damages. Choose one with little to no scratches.

5.6.2 Use a waterproof pen to mark the top of the lip of the cuvette with a dot.

5.6.3 Note: The mark on the cuvette serves as a guide for consistency purposes, allowing the orientation of the cuvette to be the same for each reading. Every time the cuvette is placed into the fluorometer, the dot should be towards the display.

6 Procedures

6.1 Record information on the table in Section 6.

6.2 Analysis in the cold room.

6.2.1 Note: The analysis in the cold room should be able to measure the first and possibly second temperature ranges.

6.2.2 Turn the fluorometer on and ensure that it is on the correct channel by checking the back of the fluorometer.

6.2.2.1 The correct channel for DEP and Bard's fluorometer is Channel B.

6.2.2.2 Note: Continually check the fluorometer to confirm that it is on.

6.2.3 In the cold room, rinse the cuvette and the NIST Digital Thermometer with D.I. water once.

6.2.3.1 Note: The experiment begins in the cold room, because it is extremely difficult to get the temperature of the cuvette and instruments to about 4°C in the laboratory.

6.2.4 Gently invert the bottled water sample three times. Rinse the cuvette with the sample three times and pour the water into the waste beaker.

6.2.5 Fill up the cuvette 3/4 with the sample.

6.2.5.1 Notes: This aliquot of sample will be continuously used throughout this experiment until all temperature ranges are achieved. If the aliquot of sample is poured out before the entire experiment is finished, the experiment must be restarted with a new aliquot.

- 6.2.6 Place the cuvette in the ice bath for about a minute to cool the cuvette and sample, to the cold room's temperature.
 - 6.2.7 Wipe off water and condensation from the outside of the cuvette with a Kimtech Wipe. Place the cuvette into the fluorometer with the dot towards the display.
 - 6.2.7.1 Note: When wiping the cuvette, hold it by the edge of the top to prevent additional smudges.
 - 6.2.8 Measure the temperature of the sample in the cuvette.
 - 6.2.8.1 Place the NIST Digital thermometer into the cuvette while it is in the fluorometer.
 - 6.2.8.2 Temperature stabilization is extremely difficult to achieve because of body heat, and heat from the thermometer and fluorometer. Due to this natural state of temperature fluctuation, it is acceptable to record the temperature when it is slowly changing by the 10th of a degree (0.1°C).
 - 6.2.8.3 Record the temperature in Celsius and to the nearest 10th of the degree with intentions of achieving the first temperature range (about 4°C).
 - 6.2.9 After recording the temperature, remove the digital thermometer.
 - 6.2.9.1 Check to make sure the fluorometer is still on. If the fluorometer is off, turn it on, and wait for it to completely start up before recording the temperature.
 - 6.2.9.2 Quickly take the digital thermometer out of the cuvette by pulling it against an edge of the cuvette in efforts to minimize the amount of water droplets leaving the cuvette.
 - 6.2.9.3 Once the thermometer is removed, keep it at a distance from all objects to prevent contamination and the generation of additional heat.
 - 6.2.10 Quickly press "Read" on the fluorometer and record the CDOM values in the table.
 - 6.2.11 Record any observations in the note column.
 - 6.2.12 Repeat steps 6.2.8 to 6.2.11 when the sample in the cuvette has reached the next target temperature (about 8°C).
- 6.3 Analysis at the benchtop.
- 6.3.1 Take the fluorometer with the cuvette inside, and the digital thermometer into the laboratory.
 - 6.3.1.1 Note: Verify that the fluorometer is held right side up so that the sample in the cuvette won't spill.
 - 6.3.2 Dip the cuvette into the hot water bath for about 30 seconds so the temperature can increase to the next target range (10°C-15°C).
 - 6.3.2.1 In instances where the sample overshoots to the next temperature target range, record the temperature and CDOM values. Then, dip the cuvette into the ice bath for about 30 seconds to cool the sample in order to achieve the original target

- range.
- 6.3.2.2 In instances where the temperature of sample does not meet the next target range, place the sample into the hot water bath again to heat up the sample.
- 6.3.3 Wipe off water and condensation from the outside of the cuvette with a Kimtech Wipe. Place the cuvette into the fluorometer with the dot towards the display.
- 6.3.3.1 Note: When wiping the cuvette, hold it by the edge of the top to prevent additional smudges.
- 6.3.4 Measure the temperature of the sample in the cuvette with intentions of achieving the third target range (10°C-15°C).
- 6.3.4.1 Place the NIST Digital thermometer into the cuvette while it is in the fluorometer.
- 6.3.4.2 Temperature stabilization is extremely difficult to achieve because the sample is consistently trying to equilibrate with the laboratory's temperature. Due to this natural state of temperature fluctuation, it is acceptable to record the temperature when it is slowly changing by the 10th of a degree.
- 6.3.4.3 Record the temperature in Celsius and to the nearest 10th of the degree.
- 6.3.5 Repeat steps 5.3.2 to 5.3.4 with the intentions of increasing the temperature to the next target range.
- 6.3.6 Repeat steps 5.3.2-5.3.4 until all temperature ranges between 4°C and 30°C have been achieved.
- 6.3.7 Pour out the sample into the waste beaker.
- 6.4 Repeat Steps 5.1-6.3 for each additional sample.
- 6.5 Clean up
- 6.5.1 There are no special disposal requirements.
- 6.5.2 When all the analysis with the samples are finished, return the NIST digital thermometer and record when the NIST thermometer is returned on the sign out sheet. Pour the ice, ice baths, water from the glass basin, and water samples from the waste beaker into the sink. Return dirty glassware so they can be washed. Return all other equipment and make sure the bench space is cleaned.

Bibliography

- Abildtrup, Jens, Serge Garcia, and Anne Stenger. 2013. "The Effect of Forest Land Use on the Cost of Drinking Water Supply: A Spatial Econometric Analysis." *Ecological Economics, Land Use*, 92 (August): 126–36.
<https://doi.org/10.1016/j.ecolecon.2013.01.004>.
- Avantes BV. 2019. "An Introduction to the Theory Behind Fluorescence Spectrometers." *AZO Materials* (blog). <https://www.azom.com/article.aspx?ArticleID=17998>.
- Bard Water Lab. n.d. "Saw Kill Program." Accessed April 28, 2020.
<https://waterlab.bard.edu/sawkill/>
- Bove, Gerald E, Jr, Peter A Rogerson, and John E Vena. 2007. "Case Control Study of the Geographic Variability of Exposure to Disinfectant Byproducts and Risk for Rectal Cancer." *International Journal of Health Geographics* 6 (May): 18.
- Camara, Moriken, Nor Rohaizah Jamil, and Ahmad Fikri Bin Abdullah. 2019. "Impact of Land Uses on Water Quality in Malaysia: A Review." *Ecological Processes* 8 (1): 10.
<https://doi.org/10.1186/s13717-019-0164-x>.
- CDC. 2009. "Disinfection By-products (DBPs)." Centers for Disease Control and Prevention. Accessed April 28, 2020. https://www.cdc.gov/biomonitoring/pdf/THM-DBP_FactSheet.pdf.
- CDC. 2016. "Disinfection By-Products." Centers for Disease Control and Prevention. Last modified December 2, 2016. <https://www.cdc.gov/safewater/chlorination-byproducts.html#four>.
- Cedergren, Marie I., Anders J. Selbing, Owe Löfman, and Bengt A.J. Källén. 2002. "Chlorination Byproducts and Nitrate in Drinking Water and Risk for Congenital Cardiac

Defects.” *Environmental Research* 89 (2): 124–30.

<https://doi.org/10.1006/enrs.2001.4362>.

Chaves, Raquel S., Catarina S. Guerreiro, Vítor V. Cardoso, Maria J. Benoliel, and Miguel M. Santos. 2019. “Hazard and Mode of Action of Disinfection by-Products (DBPs) in Water for Human Consumption: Evidences and Research Priorities.” *Comparative Biochemistry and Physiology Part C: Toxicology & Pharmacology* 223: 53–61.
<https://doi.org/10.1016/j.cbpc.2019.05.015>.

Chen, Chao, Xiao-Jian Zhang, Ling-Xia Zhu, Jing Liu, Wen-Jie He, and Hong-Da Han. 2008. “Disinfection by-Products and Their Precursors in a Water Treatment Plant in North China: Seasonal Changes and Fraction Analysis.” *Science of The Total Environment* 397 (1-3): 140–47. <https://doi.org/10.1016/j.scitotenv.2008.02.032>.

Cunha, Davi Gasparini Fernandes, Lyda Patricia Sabogal-Paz, and Walter Kennedy Dodds. 2016. “Land Use Influence on Raw Surface Water Quality and Treatment Costs for Drinking Supply in São Paulo State (Brazil).” *Ecological Engineering* 94: 516–24.
<https://doi.org/10.1016/j.ecoleng.2016.06.063>.

Downing, Bryan D., Brian A. Pellerin, Brian A. Bergamaschi, John Franco Saraceno, and Tamara E.C. Kraus. 2012. “Seeing the Light: The Effects of Particles, Dissolved Materials, and Temperature on in Situ Measurements of DOM Fluorescence in Rivers and Streams: Effects and Compensation for in Situ DOM Fluorescence.” *Limnology and Oceanography: Methods* 10 (10): 767–75. <https://doi.org/10.4319/lom.2012.10.767>.

Emily White, email message to author, April 21, 2020.

EPA. 2014. “Cyanobacteria and Cyanotoxins: Information for Drinking Water Systems.” Environmental Protection Agency. Accessed April 28, 2020.

https://www.epa.gov/sites/production/files/201408/documents/cyanobacteria_factsheet.pdf.

EPA. 2019. “Climate Change and Harmful Algal Blooms.” Environmental Protection Agency.

Last modified December 17, 2019. <https://www.epa.gov/nutrientpollution/climate-change-and-harmful-algal-blooms>.

Ernst, Caryn, Richard Gullick, and Kirk Nixon. 2004. “Conserving Forests to Protect Water.”

Opflow 30 (5): 1–7. <https://doi.org/10.1002/j.1551-8701.2004.tb01752.x>.

Freeman, Laura E. Beane, Kenneth P. Cantor, Dalsu Baris, John R. Nuckols, Alison Johnson,

Joanne S. Colt, Molly Schwenn, et al. 2017. “Bladder Cancer and Water Disinfection By-Product Exposures through Multiple Routes: A Population-Based Case–Control Study (New England, USA).” *Environmental Health Perspectives* 125 (6): 1–9.

<https://doi.org/10.1289/EHP89>.

Griffin, Claire G., Jacques C. Finlay, Patrick L. Brezonik, Leif Olmanson, and Raymond M.

Hozalski. 2018. “Limitations on Using CDOM as a Proxy for DOC in Temperate Lakes.” *Water Research* 144 (November): 719–27. <https://doi.org/10.1016/j.watres.2018.08.007>.

Higgins, Patrick. 2014. “The Basics of Chlorophyll Measurement in Surface Water.” YSI. Last

modified June 27, 2014. <https://www.ysi.com/ysi-blog/water-blogged-blog/2014/06/the-basics-of-chlorophyll-measurement-in-surface-water>.

Hung, Yen-Con, Brian W. Waters, Veerachandra K. Yemmireddy, and Ching-Hua Huang. 2017.

“PH Effect on the Formation of THM and HAA Disinfection Byproducts and Potential Control Strategies for Food Processing.” *Journal of Integrative Agriculture* 16 (12):

2914–23. [https://doi.org/10.1016/s2095-3119\(17\)61798-2](https://doi.org/10.1016/s2095-3119(17)61798-2).

Ivan Hascic, and JunJie Wu. 2006. "Land Use and Watershed Health in the United States." *Land Economics* 82 (2): 214.

Jones, Rena R., Curt T. DellaValle, Peter J. Weyer, Kim Robien, Kenneth P. Cantor, Stuart Krasner, Laura E. Beane Freeman, and Mary H. Ward. 2019. "Ingested Nitrate, Disinfection by-Products, and Risk of Colon and Rectal Cancers in the Iowa Women's Health Study Cohort." *Environment International* 126 (May): 242–51.
<https://doi.org/10.1016/j.envint.2019.02.010>.

Kathleen Henderson, email message to Karen Moore, March 23, 2020.

Kramer, Michael D., Charles F. Lynch, Peter Isacson, and James W. Hanson. 1992. "The Association of Waterborne Chloroform with Intrauterine Growth Retardation." *Epidemiology* 3 (5): 407–413.

Latitude. n.d. Accessed April 26, 2020. <https://latitude.to/articles-by-country/us/united-states/114428/cannonsville-reservoir>

Levallois, Patrick, Suzanne Gingras, Sylvie Marcoux, Christelle Legay, Cyril Catto, Manuel Rodriguez, and Robert Tardif. 2012. "Maternal Exposure to Drinking-Water Chlorination By-Products and Small-for-Gestational-Age Neonates." *Epidemiology* 23 (2): 267–276.
<https://doi.org/10.1097/EDE.0b013e3182468569>.

Lindsey, Rebecca and Michon Scott. 2010. "What are Phytoplankton?" NASA Earth Observatory (blog). <https://earthobservatory.nasa.gov/features/Phytoplankton>

Matilainen, Anu, Egil T. Gjessing, Tanja Lahtinen, Leif Hed, Amit Bhatnagar, and Mika Sillanpää. 2011. "An Overview of the Methods Used in the Characterisation of Natural Organic Matter (NOM) in Relation to Drinking Water Treatment." *Chemosphere* 83 (11): 1431–42. <https://doi.org/10.1016/j.chemosphere.2011.01.018>.

- Matilainen, Anu, Mikko Vepsäläinen, and Mika Sillanpää. 2010. “Natural Organic Matter Removal by Coagulation during Drinking Water Treatment: A Review.” *Advances in Colloid and Interface Science* 159 (2): 189–97. <https://doi.org/10.1016/j.cis.2010.06.007>.
- Moore, Karen, Elias Munthali, Emmets Owens, Theo Kpodonu, and Dave V. Valkenburg. “Before the Pipe: Monitoring and Modeling Disinfection Byproduct Precursors in Drinking Water Sources.” Presented at GLEON, 2019a.
- Moore, Karen and Watershed Science & Research Program Evaluation and Planning Group. “Summary of Current Research on Disinfection By-Product Precursors.” Presented at the NYC Environmental Protection, Kingston, NY, May 2019b.
- Moore, Karen, email message to author, April 14, 2020.
- Moreno-Andrés, Javier, and Louis Peperzak. 2019. “Operational and Environmental Factors Affecting Disinfection Byproducts Formation in Ballast Water Treatment Systems.” *Chemosphere* 232 (October): 496–505. <https://doi.org/10.1016/j.chemosphere.2019.05.152>.
- Nieuwenhuijsen, Mark J., Mireille B. Toledano, Naomi E. Eaton, John Fawell, and Paul Elliott. 2000. “Chlorination Disinfection Byproducts in Water and Their Association with Adverse Reproductive Outcomes: A Review.” *Occupational and Environmental Medicine* 57 (2): 73–85. <https://doi.org/10.1136/oem.57.2.73>.
- NYC Department of Environmental Conservation. n.d. “Cannonsville Reservoir.” Accessed April 26, 2020. <https://www.dec.ny.gov/outdoor/84906.html>.
- NYC Environmental Protection. n.d. “Cannonsville Reservoir.” Accessed April 26, 2020. <https://www1.nyc.gov/site/dep/water/cannonsville-reservoir.page>

- NYC Environmental Protection. n.d. "Neversink Reservoir." NYC Environmental Protection. Accessed April 26, 2020. <https://www1.nyc.gov/site/dep/water/neversink-reservoir.page>.
- Pires, Mark. 2004. "Watershed Protection for a World City: The Case of New York." *Land Use Policy* 21 (2): 161–75. <https://doi.org/10.1016/j.landusepol.2003.08.001>.
- Regli, Stig, Jimmy Chen, Michael Messner, Michael S. Elovitz, Frank J. Letkiewicz, Rex A. Pegram, T.J. Pepping, Susan D. Richardson, and J. Michael Wright. 2015. "Estimating Potential Increased Bladder Cancer Risk Due to Increased Bromide Concentrations in Sources of Disinfected Drinking Waters." *Environmental Science & Technology* 49 (22): 13094–102. <https://doi.org/10.1021/acs.est.5b03547>.
- Riverkeeper. n.d. "Community Water Quality Monitoring Results 2016-2018." Riverkeeper. Accessed April 2018, 2020. <https://www.riverkeeper.org/wp-content/uploads/2019/04/2018-Entero-Report-SAW-KILL-Final.pdf>
- Ryder, Elizabeth, Eleanor Jennings, Elvira de Eyto, Mary Dillane, Caitriona NicAonghusa, Donald C. Pierson, Karen Moore, Martin Rouen, and Russell Poole. 2012. "Temperature Quenching of CDOM Fluorescence Sensors: Temporal and Spatial Variability in the Temperature Response and a Recommended Temperature Correction Equation: CDOM: Temperature Correction." *Limnology and Oceanography: Methods* 10 (12): 1004–10. <https://doi.org/10.4319/lom.2012.10.1004>.
- Saraceno, John Franco, James B. Shanley, Bryan D. Downing, and Brian A. Pellerin. 2017. "Clearing the Waters: Evaluating the Need for Site-Specific Field Fluorescence Corrections Based on Turbidity Measurements: Site-Specific FDOM Correction." *Limnology and Oceanography: Methods* 15 (4): 408–16. <https://doi.org/10.1002/lom3.10175>.

- Saw Kill Watershed Community. n.d. "About the Community." Saw Kill Watershed Community (blog). Accessed April 28, 2020. <https://sawkillwatershed.wordpress.com/about/>.
- Saw Kill Watershed Community. n.d. "Science." Saw Kill Watershed Community (blog). Accessed April 28, 2020. <https://sawkillwatershed.wordpress.com/science/>.
- Serrano, Maria, Isabel Montesinos, M. J. Cardador, Manuel Silva, and Mercedes Gallego. 2015. "Seasonal Evaluation of the Presence of 46 Disinfection By-Products throughout a Drinking Water Treatment Plant." *Science of The Total Environment* 517 (June): 246–58. <https://doi.org/10.1016/j.scitotenv.2015.02.070>.
- Sillanpää, Mika, Mohamed Chaker Ncibi, Anu Matilainen, and Mikko Vepsäläinen. 2018. "Removal of Natural Organic Matter in Drinking Water Treatment by Coagulation: A Comprehensive Review." *Chemosphere* 190 (January): 54–71. <https://doi.org/10.1016/j.chemosphere.2017.09.113>.
- Spencer, Robert G. M., Kenna D. Butler, and George R. Aiken. 2012. "Dissolved Organic Carbon and Chromophoric Dissolved Organic Matter Properties of Rivers in the USA." *Journal of Geophysical Research: Biogeosciences* 117 (G3). <https://doi.org/10.1029/2011JG001928>.
- Spodek, Marco Sebastian, "Nitrate Loading in the Saw Kill Watershed: small watershed nutrient dynamics, answering a community question, and assessing methodological approaches" (2017). Senior Projects Spring 2017. 18. http://digitalcommons.bard.edu/senproj_s2017/18
- Tang, Wang-Wang, Guang-Ming Zeng, Ji-Lai Gong, Jie Liang, Piao Xu, Chang Zhang, and Bin-Bin Huang. 2014. "Impact of Humic/Fulvic Acid on the Removal of Heavy Metals from

- Aqueous Solutions Using Nanomaterials: A Review.” *Science of The Total Environment* 468–469 (January): 1014–27. <https://doi.org/10.1016/j.scitotenv.2013.09.044>.
- Turner Designs. n.d. "Optical Specification Guide." Accessed April 27, 2020.
<http://docs.turnerdesigns.com/t2/doc/spec-guides/998-8081.pdf>.
- US EPA. 2020. “National Primary Drinking Water Regulations.” Ground Water and Drinking Water. Last modified February 14, 2020. <https://www.epa.gov/ground-water-and-drinking-water/national-primary-drinking-water-regulations#six>.
- USGS. 2020. “Turbidity and Water.” USGS. Accessed April 28, 2020.
https://www.usgs.gov/special-topic/water-science-school/science/turbidity-and-water?qt-science_center_objects=0#qt-science_center_objects.
- USGS. n.d. “Feature Detail Report for: Neversink Reservoir.” Accessed April 26, 2020.
https://geonames.usgs.gov/apex/f?p=gnispq:3:0::NO::P3_FID:958385.
- Vannote, Robin L., G. Wayne Minshall, Kenneth W. Cummins, James R. Sedell and Colbert E. Gushing. 1980. “The River Continuum Concept.” DOI:10.1139/f80-017.
- Watras, C.J., P.C. Hanson, T.L. Stacy, K.M. Morrison, J. Mather, Y.-H. Hu, and P. Milewski. 2011. “A Temperature Compensation Method for CDOM Fluorescence Sensors in Freshwater: CDOM Temperature Compensation.” *Limnology and Oceanography: Methods* 9 (7): 296–301. <https://doi.org/10.4319/lom.2011.9.296>.